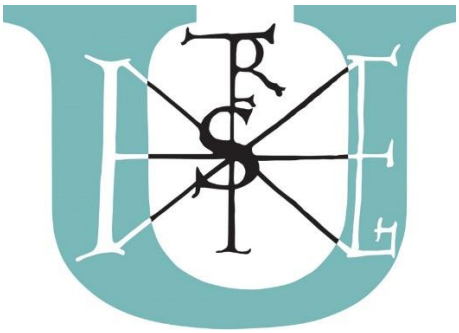

Szent István University

COMPREHENSIVE SELENIUM SPECIATION OF A SELENIUM ACCUMULATOR PLANT, *CARDAMINE VIOLIFOLIA*

DOI: 10.54598/000340

Doctoral (Ph.D.) thesis of

ESZTER BORBÁLA BOTH

Budapest

2020

Doctoral School/Program

Name: Doctoral School of Food Sciences

Field: Food Science

Head: **Prof. Livia Simonné Sarkadi, DSc**
Professor
SZIU, Faculty of Food Science
Institute of Food Quality, Safety and Nutrition
Department of Food Chemistry and Nutrition

Supervisors: **Mihály Dernovics, habil. PhD**
Senior researcher
Centre for Agricultural Research
Agricultural Institute, Martonvásár
Department of Plant Physiology

Zsuzsanna Jókainé Szatura, PhD
Associate professor
SZIU, Faculty of Food Science
Institute of Food Quality, Safety and Nutrition
Department of Applied Chemistry

……. …….....
……..

Signature of Head of Doctoral School Signatures of Supervisors

TABLE OF CONTENTS

LIST OF ABBREVIATONS

1D	One Dimensional
2D	Two Dimensional
AdoSeHCys	*Se*-adenosyl-homoselenocysteine
AdoSeMet	Selenoadenosylmethionine
AED	Atomic Emission Detection
AES	Atomic Emission Spectroscopy
APR	Adenosine 5’ Phosphosulphate Reductase
APSe	Adenosine 5’-Phosphoselenate
ATP	Adenosine Triphosphate
ATPS	Adenosine Triphosphate Sulphurylase
CEC	Capillary Electrochromatography
CGS	Cystathionine- γ-synthase
Chl	Chlorophyll
CID	Collision Induced Dissociation
CoQ10	Coenzyme Q10
Cys	Cysteine
CZE	Capillary Zone Electrophoresis
DAD	Diode-Array Detector
DHAA	Dehydroascorbic Acid
DMDSe	Dimethyldiselenide
DMSe	Dimethylselenide
DMSeP	Dimethylselenopropionate
DNA	Deoxyribonucleic Acid
DW	Dry Weight
EC	Enzyme Commission
EFSA	European Food Safety Authority
ESI	Electrospray Ionisation
FLD	Fluorescence Detection
FT ICR	Fourier-Transform Ion Cyclotron Resonance
GAE	Gallic Acid Equivalent
GC	Gas Chromatography
GPS	Global Positioning System
GSH	Glutathione

HA	Hyperaccumulator
HFBA	Heptafluorobutyric Acid
HG-AFS	Hydride Generation Atomic Fluorescence Spectrometry
HILIC	Hydrophilic Interaction Chromatography
HMT	Homocysteine *S*-Methyltransferase
HPLC	High Performance Liquid Chromatography
HR	High Resolution
ICP	Inductively Coupled Plasma
IDA	Isotope Dilution Analysis
IEF	Isoelectric Focusing Electrophoresis
IP-RP	Ion Pairing Reversed Phase (Chromatography)
IUPAC	International Union for Pure and Applied Chemistry
KEGG	Kyoto Encyclopedia of Genes and Genoms
LA	Laser Ablation
Lan	Lanthionine
LC	Liquid Chromatography
LSF	Least-Squares Fitting
m/z	Mass to Charge ratio
MALDI	Matrix Assisted Laser Desorption Ionisation
MC	Multicollector
MEKC	Micellar Electrokinetic Chromatography
MeSeCys	*Se*-(Methyl)Selenocysteine
Met	Methionine
MMT	Methylmethionine Methyltransferase, *S*-adenosyl-L-methionine:L-methionine *S*-methyltransferase
MS agar	Murashige and Skoog agar
MS	Mass Spectrometry
NMR	Nuclear Magnetic Resonance
OAS	*O*-acetylserine
OAS-TL	*O*-acetylserine (Thiol)-Lyase
OPH	*O*-Phosphohomoserine
PAGE	Poliacrylamide Gel Electrophoresis
ppm	Parts per Million
PTFE	Polytetrafluorethylene
Q	Quadrupole

RGB	Red-Green-Blue
RP	Reversed Phase (Chromatography)
S/N	Signal-to-noise
SAT	Serine Acetyltransferase
SAX	Strong Anion Exchange (Chromatography)
SCX	Strong Cation Exchange (Chromatography)
SDS	Sodium Dodecyl Sulphate
SEC	Size Exclusion Chromatography
SeCys	Selenocysteine
$SeCys_2$	Selenocystine
SeCysta	Selenocystathionine
SeHCys	Selenohomocysteine
SeHLan	Selenohomolanthionine
SeLan	Selenolanthionine
SEM	Standard Error of the Mean
SeMet	Selenomethionine
SeMetO	Selenomethionine-selenoxide
SeMM	*Se*-methyl-selenomethionine
SF	Sector Field
SiR	Sulphite Reductase
SMT	Selenocysteine Methyltransferase
SULTR	Sulphate Transporters
TEAC	Trolox-Equivalent Antioxidant Capacity
THF	Tetrahydrofolate
TOF	Time of Flight
tRNA	Transfer Ribonucleic Acid
USA	United States of America
UV	Ultraviolet
XANES	X-ray Absorption Near-Edge Structure
XAS	X-ray Absorption Spectroscopy
XRF	X-ray Fluorescence
γ-glu	γ-glutamyl

1. INTRODUCTION

Trace elements possess important roles in complex biological systems, such as active centres of enzymes or as structural components of bioactive substances. Besides essential or beneficial elements there are some notorious metals causing acute (*e.g.*, Hg) or chronic (*e.g.*, Pb) toxicity. However, several elements cannot be unambiguously classified due to their dual characteristics, that is, essential in one oxidation state and toxic in the other state or toxic in most forms, but essential or harmless in a particular organic form (Szpunar *et al.* 2003). Besides quality aspects, the quantity of a particular element can also define its effect on the biological system.

Among essential trace elements selenium (Se) shows one of the narrowest optimal daily intake, therefore both selenium deficiency and toxicity are global issues. Selenocysteine, the 21st amino acid incorporates into several antioxidant enzymes and therefore plays an important role in the protection of cells against oxidative stress. Se deficiency in humans can cause muscle weakness and inflammation, hypothyroidism, heart muscle dysfunction, weakness of the immune system, Keshan and Kashin-Beck diseases and others, whereas symptoms of Se toxicity include liver and kidney damage, necrosis of heart and liver, hair and nail loss. The selenium level in the European population is generally below the optimal, an Adequate Intake of 70 µg/day for adults and 85 µg/day for lactating women was determined by European Food Safety Authority (EFSA) in 2014 which can be provided by Se-rich/enriched foodstuff and food supplements (EFSA 2014).

There is a growing attention that not only the total intake of dietary Se is important to health, but the forms of the ingested Se can be also relevant due to the fact that different Se species can differ in bioavailability and can go together with beneficial or toxic health effects. The first step for making correct conclusions on health effects of different Se species is the adequate Se speciation in the food chain, especially in plants as being the main dietary sources of Se (Rayman *et al.* 2008).

Contrary to animals and humans, Se is not essential for higher plants but even toxic for most of them. A special group of plant species living on seleniferous soils evolved different metabolic pathways to cope with Se toxicity and adapted not only to tolerate but even to accumulate selenium in their tissues at high concentration level.

Selenium deficiency and toxicity are present side by side in China due to the high variances in soil Se content throughout the country. The controlled cultivation and

production of selenium enriched food on seleniferous areas can contribute to solve this health related issue of millions of people living in Se poor areas.

Cardamine violifolia, a selenium hyperaccumulator plant species originates from the naturally seleniferous region Yutangba, China and has been cultivated for phytoremediation purposes. The plant is also used for soil reclamation and food supplement production however the selenium species and metabolic pathways responsible for high Se content have not been elucidated yet. The work described here addressed the identification and quantification of selenium species and the investigation of Se related physiological properties of this selenium hyperaccumulator plant species.

2. OBJECTIVES

In my doctoral study I intended to investigate the selenium related characteristics of *Cardamine violifolia* selenium hyperaccumulator plant species. The experiments can be interpreted along two lanes.

For investigation of selenometabolites in *Cardamine violifolia* I intended:

- to purify the selenium containing fractions of selenium enriched *C. violifolia* plant extract with an ICP-MS assisted orthogonal chromatographic separation procedure;
- to detect selenium compounds by HPLC-ESI-QTOF-MS in the fractions;
- to putatively identify selenometabolites based on their accurate mass, chromatographic behaviour and MS/MS fragmentation pattern;
- to confirm the identification of the main selenocompound through synthesis;
- to quantify the main selenocompound without an authentic standard.

Comprehensive experiment was conducted to study the physiological effect of selenium on *Cardamine violifolia* with the comparison of the related non-accumulator *Cardamine pratensis* regarding:

- tolerance and accumulation of selenate;
- uptake capacity of different forms of selenium: selenate and selenite;
- interactions of selenate and sulphate, selenite and phosphate for selenium and sulphur uptake;
- effect of selenium treatment on chlorophyll fluorescence properties and antioxidant capacity;
- selenium localisation and speciation in intact plant tissues based on X-ray microprobe analysis.

3. REVIEW OF LITERATURE

3.1. SELENIUM IN PLANTS

3.1.1. Relation of selenium and plants

Selenium (Se) has not been shown essential for higher (vascular) plants in contrast to some microalgae, bacteria, animals and humans (Araie and Shiraiwa 2009, Guignardi and Schiavon 2017). Although not essential, Se can provide beneficial effects for plants (Pilon-Smits *et al.* 2009). Several studies have shown that proper levels of Se have a growth enhancing effect (Xue *et al.* 2001, Hartikainen 2005, Djanaguiraman *et al.* 2010) that can be associated with the enhanced accumulation of starch and sugar (Turakainen *et al.* 2004). Some plant species grown in Se-enriched media have shown increased tolerance against abiotic stresses like drought (Kuznetsov *et al.* 2003), cold stress (Chu *et al.* 2010), high temperature (Djanaguiraman *et al.* 2010), high ultraviolet-B radiation (Hartikainen and Xue 1999), salinity (Kong *et al.* 2005) and toxic metals (Fargasová *et al.* 2006). These physiological advantages may be related to the enhanced antioxidant capacity induced by Se against oxidative damage and lipid peroxidation (Xue *et al.* 2001, Hartikainen 2005); however, the exact molecular mechanisms that underlie these positive effects have not been elucidated yet (Feng *et al.* 2013).

Besides physiological advantages, even low Se levels (~10 µg Se g^{-1} dry weight (DW)) in tissues provide ecological advantage as well, such as protection against certain herbivores (Hanson *et al.* 2004). At higher tissue levels, Se protects not only against other herbivores but also some microbial pathogens. Also, Se provides allelopathic benefits as well because of the negative effects on Se sensitive plants (El Mehdawi and Pilon-Smits 2012).

All plants can take up and metabolise Se due to its chemical similarity to the essential macroelement sulphur (S) (Figure 1). On the other hand, there are huge differences in the degree to which different plant species can tolerate and accumulate Se.

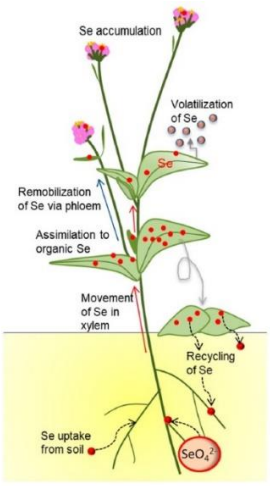

Figure 1. Accumulation and transformation of Se (red circles) in plants and the related effects on local Se cycling (Pilon-Smits 2019).

Based on the accumulated selenium level in plant tissues, three classes are most frequently distinguished in the literature. Species called Se hyperaccumulators can concentrate Se in the range of 1000-15000 µg Se g^{-1} DW. Non-accumulator species contain less than 100 µg Se g^{-1} DW. The third, distinct group of plants is named secondary accumulators (or simply accumulators) that accumulates Se in the range of 100-1000 µg Se g^{-1} DW while growing on seleniferous soils (Anderson 1993, Läuchli 1993). Additionally, several studies mention Se indicator plants that can colonise both non-seleniferous and seleniferous soils and can tolerate tissue Se concentration up to 1000 µg g^{-1} DW (White 2016). Different Se accumulation and tolerance capacity may be associated with the differences in Se metabolism and in tissue accumulation patterns (Pilon-Smits 2019). An overview about the biochemical and physiological characteristics used to differentiate these plant classes is given in Table 1. Secondary accumulator and non-accumulator plants take up Se and S proportionally to their abundance in the growth medium, which indicates that they are unable to distinguish these elements. Hyperaccumulator species appear to take up Se preferentially over S, which results in higher Se/S ratios in their tissues compared to growth media and surrounding vegetation (White *et al.* 2007, Harris *et al.* 2014). Mechanism of this qualitative difference is not known and there is a quantitative difference as well. Based on different studies it is assumed that the major genes involved in root sulphate/selenate uptake and assimilation are constitutively overexpressed in hyperaccumulators compared to non-hyperaccumulators (Pilon Smits 2017, Freeman *et al.* 2010, Schiavon *et al.* 2015, Cabannes *et al.* 2011).

Hyperaccumulators differ from other plants regarding the Se-S interactions as well. Sulphate uptake is more effectively inhibited by selenate while sulphate is less capable of inhibiting selenate uptake (Harris *et al.* 2014). Non-hyperaccumulator species tend to contain relatively more inorganic Se than hyperaccumulators do due to slower rate of selenate assimilation. *Brassica juncea* accumulator and *Arabidopsis thaliana* non-accumulator species were found to accumulate predominantly selenate while hyperaccumulator *Astragalus bisulcatus, Symphyotrichum ericoides, Stanleya pinnata* contain mostly organic Se species (Van Hoewyk *et al.* 2005, Freeman *et al.* 2006a, El Mehdawi *et al.* 2014). Hyperaccumulators show enhanced conversion of inorganic Se to organic Se and high activity to produce less toxic Se species from selenocysteine (SeCys) to avoid its non-specific incorporation into proteins. This explanation is often cited as "malformed protein theory", introduced in 1980 by Brown and Shrift. For example, methylation of SeCys to *Se*-(methyl)selenocysteine (MeSeCys) or producing volatile Se forms like dimethyldiselenide (DMDSe) offer ways for Se depletion (Pilon-Smits 2017).

Further differences have also been described in the translocation of Se between species. Hyperaccumulators translocate more Se in the xylem (from root to shoot), show higher phloem remobilisation (from leaves to reproductive organs) and often sequester Se in specialised tissues such as leaf hairs or epidermis (Pilon-Smits 2019, Quinn *et al.* 2011, Cappa *et al.* 2014).

Table 1. Classification of angiosperm species into ecological types according to their ability to accumulate Se in their tissues (White 2017, Moreno Rodriguez *et al.* 2005).

Classification	Leaf Se concentration (µg g^{-1} DW)	Soil ecology	Biochemical and physiological characteristics
non-accumulator ***e.g., Arabidopsis thaliana***	<10 - 100	non-seleniferous	Se uptake induced by S-starvation
			High S/Se selectivity for uptake
Se indicator ***e.g., Atriplex halimus***	<1000	seleniferous & non-seleniferous	Se transport to shoot induced by S-starvation
			Se volatilisation as dimethylselenide
			Sequestration highest in leaves
Se accumulator ***e.g., Brassica juncea***	>100	seleniferous	selenate as the main Se species (sometimes selenomethionine)
Se hyperaccumulator ***e.g., Stanleya pinnata***	>1000	seleniferous	Constitutive, S-independent Se uptake
			Low S/Se selectivity for uptake
			Constitutively large Se transport to shoot
			Constitutively large Se metabolic flux
			Large Se volatilisation as DMDSe
			Sequestration highest in reproductive organs
			MeSeCys is a common Se species

Selenium hyperaccumulation was discovered by Orville Beath and his coworkers in the 1930's (Rosenfeld and Beath 1964). Since then, hyperaccumulation has been reported in 45 taxa from 14 genera and from six eudicot orders: *Fabales*, *Brassicales*, *Caryophyllales*, *Gentianales*, *Lamiales* and *Asterales* (White 2016, Figure 2). It is assumed that Se hyperaccumulation has evolved independently in different clades possibly due to similar ecological and physiological circumstances (Pilon-Smits 2017).

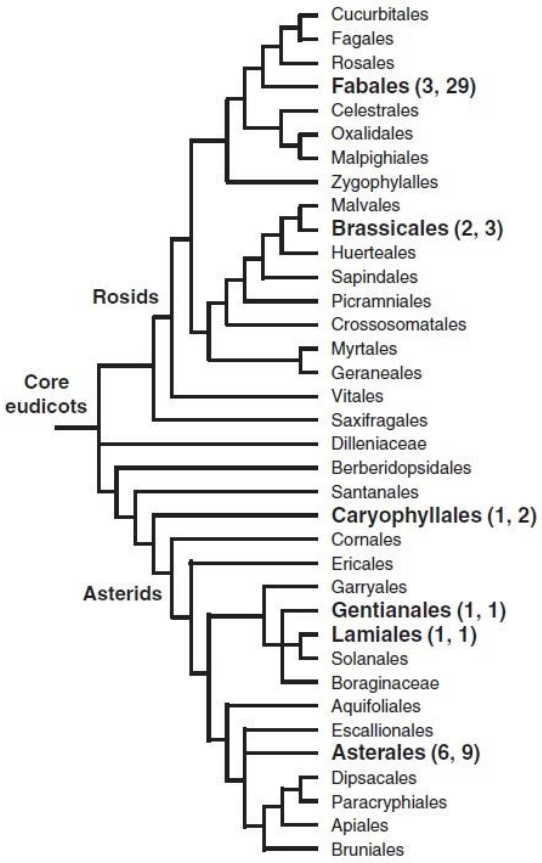

Figure 2. Distribution of proposed Se hyperaccumulating species among angiosperm orders. The number of Se hyperaccumulating genera and Se hyperaccumulating species in each order are given in parentheses, respectively (White 2016).

3.1.2. Seleniferous regions worldwide

Selenium is usually present in soils at trace level but high concentrations even above 1000 mg kg^{-1} have been reported for some regions (Fleming 1962, Zhu *et al.* 2008). There are several parts of the world where soils contain elevated levels of Se, which causes serious health problems due to Se accumulation in the food chain (Zhu *et al.* 2008). Soils with Se level > 0.1 mg kg^{-1} are considered seleniferous because

forages grown on such soils contain > 4 mg Se kg^{-1} – the maximum permissible level for animal consumption (Dhillon *et al.* 1992). Seleniferous regions are known in the United States, Ireland, Australia, Brazil, China, and India (Dhillon and Dhillon 2003). An overview of Se tolerant species collected in nature from these areas is presented in Table 2.

Similarly to normal soils, natural seleniferous soils have developed as a result of so-called active and passive factors of soil formation, and toxic Se levels are a direct consequence of geological processes. Toxic Se content of soils is determined by slight modifications in formations or rock outcrops, formations lying beneath the soil mantle, decomposition of parent rocks by wind and water and subsequent transport by ground or surface water, indicator plants (Dhillon and Dhillon 2003, Rosenfeld and Beath 1964). Besides natural processes industrial activities contribute to significant amounts of Se liberated to aquatic and terrestrial ecosystems, such as coal combustion, crude oil processing, metal refining, mining, and crop irrigation (Staicu *et al.* 2017a).

In Queensland (Australia) the high Se level of the soil is associated with limestone shale. Vegetation grown on these soils are known to cause selenosis in livestock. Selenium accumulator plants, *Morinda reticulata* and *Neptunia amplexicaulis* have been identified in Central Queensland (Knott and McCray 1959).

In Ireland the locations of toxic seleniferous soils are sporadic. Some of the highest soil Se concentration in the world are found in Limerick, Tipperary and Meath Counties. Level of total Se ranges between 3.2 – 132 mg kg^{-1} but can reach even 1200 mg Se kg^{-1} (Fleming and Walsh 1957, Fleming 1962, Rogers *et al.* 1990). Based on Fleming's descriptions (1962) these toxic soils have developed under highly humid conditions and air depression once occupied by old lakes.

Seleniferous soils are widespread in the Rocky Mountains and the Great Plains of Western United States of America (USA). Grazing on forages grown on these soils has been known since the 1930's to cause toxicity in livestock termed as blind staggers and alkali disease (Wilber 1980). The toxic soils are concentrated especially in the states of Wyoming, South Dakota, North Dakota, Montana, Nebraska, Kansas, Colorado, New Mexico, Utah, Arizona and the San Joaquin valley in California. Volcanic eruptions in Cretaceous age are thought to be the primary source of Se through deposition in Cretaceous seas that have flooded these areas in the USA. Toxic soils have developed from disintegrating these deposits (Dhillon and Dhillon 2003). Several Se hyperaccumulators have been reported occurring in these areas: 25 taxa within the genus *Astragalus* (Fabaceae), *Stanleya pinnata*, *Stanleya bipinnata*

(Brassicaceae) and genera from Asteraceae (*Oonopsis*, *Xylorhiza* and *Symphyotrichum*; Rosenfeld and Beath 1964, El Mehdawi *et al.* 2014).

Soils with toxic Se content in India are found in different states, the largest affected area (1000 ha) was located in Punjab (Dhillon and Dhillon 2003). Investigations of Dey *et al.* (1999) in northeast India found wild animal species suffering from Se toxicity with Se concentration exceeding toxic limits in their bones and hair. Soil and water Se concentration up to 17 µg g^{-1} and 1.4 µg g^{-1} were recorded, respectively, at certain living area of these animals.

Carbonaceous shale and carbonaceous chert strata are the major source of Se in Enshi, located in Hubei province, central China. Mining Se-rich rocks and weathering have caused Se release into the environment. In the 1960's high Se intake over short time caused Se poisoning in the local population (Zhu *et al.* 2004). Soils from this area were characterised with very high Se content in terms of total and water-soluble Se as well (up to 59 mg Se kg^{-1} soil and 2.4 mg Se kg^{-1} soil, respectively; Chang *et al.* 2019, Fordyce *et al.* 2000, Qin *et al.* 2012, Zhu *et al.* 2008, Zhu *et al.* 2004). Soil samples collected from croplands and discarded coal spoils were found to contain extremely high Se up to 2000 mg Se kg^{-1} soil (Zhu *et al.* 2008). Besides Enshi, selenium toxicity in human population has been recorded in Ziyang County, Shanxi Province as well (Fordyce et al. 2000).

Several studies reported high Se concentration in soil samples from the Amazon regions in Brazil up to 0.6 mg kg^{-1} and in Minas Gerais state even at 1.7 mg kg^{-1} (Shaltout *et al.* 2011, Silva Junior *et al.* 2017). Endemic Brazil nuts grown in Amazon regions are known for their high Se content. In some cases the consumption of one single piece of nuts would cover or even exceed the recommended dietary intake for an adult per day (Silva Junior *et al.* 2017, Lima *et al.* 2019).

In contrast to seleniferous areas there are several countries in the world where the soil is poor in Se therefore the Se content of foods and feeds is also extremely low, which causes Se deficiency in local population. One of the concerned countries is Finland where this issue was handled in a unique and efficient way: in 1984, the Ministry of Agriculture and Forestry started to regulate the supplementation of fertilisers with selenium in parallel with monitoring Se status through the whole food chain. Quantity of the allowed sodium selenite was 16 mg kg^{-1} in fertilisers for cereals and 6 mg kg^{-1} for grasses. This value has been continuously modified according to the actual monitoring results (Pirjo 2005). After 27 years, Se concentration of spring cereals has increased approximately 15-fold, while the mean increase in beef, pork and

milk was six-, two- and three-fold, respectively. Finally, the average dietary human intake has reached the actual recommendation (Alfthan *et al.* 2015).

Table 2. Plant species identified as Se (hyper)accumulators from natural environment (partly adopted from White, 2016).

Species	Location	Reference
Asteraceae		
Dieteria canescens	Midwest USA	Beath *et al.* (1939a)
Grindelia squarrosa	Lower Brule Reservation, SD, USA	Lakin and Byers (1941)
Gutierrezia microcephala	Thompson, UT, USA	Beath (1943)
Oonopsis foliosa	Lascar, CO, USA	Beath *et al.* (1939b)
Oonopsis wardii	Albany County, WY, USA	Byers (1935)
Symphyotrichum ascendens	Soda Springs, ID, USA	Pfister *et al.* (2013)
Symphyotrichum ericoides	Pine Ridge, Fort Collins, CO, USA	El Mehdawi *et al.* (2015)
Symphytrichum lateriflorum	SD, USA	Moxton *et al.* (1939)
Xylorhiza glabriuscula	Huerfano County, CO, USA	Byers *et al.* (1938)
Xylorhiza parryi	Albany County, WY, USA	Byers (1935)
Xylorhiza venusta	Midwest USA	Rosenfeld and Beath (1964)
Fabaceae		
Acacia cana	NW Queensland, Australia	McCray and Hurwood (1963)
Astragalus albulus	La Ventana, NM, USA	Beath *et al.* (1941)
Astragalus beathii	Cameron, AZ, USA	Beath et al (1940)
Astragalus beckwithii* var. *purpureus	Clark County, NE, USA	Lakin and Byers (1941)
Astragalus bisulcatus	Pine Ridge, Fort Collins, CO, USA	Sura-de Jong *et al.* (2015)
Astragalus canadensis	Las Vegas, NE, USA	Byers *et al.* (1938)
Astragalus crotalariae	Truckhaven, CA, USA	Beath *et al.* (1941)
Astragalus eastwoodiae	Utah, USA	Beath (1943)
Astragalus flavus	Aztec, NM, USA	Beath *et al.* (1941)
Astragalus flavus* var. *argillosus	Greenriver, UT, USA	Beath *et al.* (1941)
Astragalus flavus* var. *candicans	Thompson, UT, USA	Beath (1943)
Astragalus grayi	Carbon County, WY, USA	Byers (1935)
Astragalus osterhoutii	Kremmling, CO, USA	Beath *et al.* (1940)
Astragalus pattersonii	Thompson, UT, USA	Beath (1943)
Astragalus pectinatus	Teton County, MT, USA	Williams *et al.* (1940)
Astragalus praelongus	Leupp, AZ, USA	Beath *et al.* (1941)

Astragalus preussii	Thompson, UT, USA	Beath (1943)
Astragalus racemosus	WY, USA	Knight and Beath (1937)
Astragalus rafaelensis	Jensen, TX, USA	Beath *et al.* (1941)
Astragalus sabulosus	Thomspon, UT, USA	Beath *et al.* (1941)
Astragalus toanus	ID, USA	Lakin and Byers (1948)
Neptunia amplexicaulis	Richmond, Queensland, Australia	Knott and McCray (1959)
Brassicaceae		
Brassica juncea	Punjab, India	Eiche *et al.* (2015)
Cardamine hupingshanensis	Yutangba, Enshi, China	Yuan *et al.* (2013)
Stanleya bipinnata	Laramie, WY, USA	Beath *et al.* (1940)
Stanleya pinnata	Pine Ridge, Fort Collins, CO, USA	Galeas *et al.* (2007)
Amaranthaceae		
Artiplex confertifolia	Thompson, UT, USA	Beath (1943)
Artiplex nuttallii	WY, USA	Beath *et al.* (1937)
Rubiaceae		
Morinda reticulata	Cape York, Peninsula, Queensland, Australia	Knott and McCray (1959)
Orobanchaceae		
Castilleja angustifolia **var. *dubia***	Lysite, WY, USA	Beath *et al.* (1941)
Lecythidaceae		
Lecythis ollaria	San Juan de los Morros, Venezuela	Ferri *et al.* (2004)
Bertholletia excelsa	Amazon, Brazil	Silva Junior *et al.* (2017)
Lemnaceae		
Lemna minor	West Bengal, India	Singh *et al.* (2016)
Spirodela polyrhiza	West Bengal, India	Singh *et al.* (2016)

3.1.3. Biochemistry of selenium assimilation in plants

Plants take up Se from soil mainly in the form of selenate (SeO_4^{2-}) which is the prevalent bioavailable form in alkaline and well oxidised soils. The main bioavailable form of Se in anaerobic soils and wetlands is selenite (SeO_3^{2-}) that can be taken up by plants as well (Terry *et al.* 2000, Sors *et al.* 2005a). Plants are able to take up organic Se compounds but seem not to have the means to directly take up elemental Se or metal selenide compounds (White and Broadley 2009). Not only the concentration and chemical form (speciation) of Se available in the soil influence the rate and form of the Se uptake but rhizosphere conditions such as pH and the presence of sulphate and phosphate as well (Sors *et al.* 2005a). Due to its chemical similarity to sulphate, selenate is absorbed through sulphate transporters while selenite through phosphate transporters or anion channels (Shibagaki *et al.* 2002, Zhang *et al.* 2014). Sulphate transporters were characterised in *Arabidopsis thaliana* selenate resistant mutants (Shibagaki *et al.* 2002). Selenate enters the roots through the high affinity sulphate transporters SULTR1;1 and SULTR1;2 across the plasma membrane of root epidermal cells against their electrochemical gradients (Lass and Ullrich-Eberius 1984, Hawkesford et al. 1993). In *Stanleya pinnata* hyperaccumulator species selenate uptake and translocation rates were found to be constitutively elevated and not significantly inhibited by sulphate in contrast to *Stanleya elata* (non-accumulator) and *Brassica juncea* (secondary accumulator) species (El Mehdawi et al. 2018). Differences in the sulphate transporters were observed as well: the hyperaccumulator had an order of magnitude higher transcript levels of SULTR1;2 which may have enhanced Se:S specificity.

Selenite is taken up through a different pathway. Several studies showed reduced selenite uptake in the presence of higher phosphate concentration, *e.g.*, in perennial ryegrass (*Lolium perenne*) and strawberry clover (*Trifolium fragiferrum*) (Hopper and Parker 1999). These results indicate competition between these ions thus selenite uptake is assumed to be mediated by root phosphate transporters (Guignardi and Schiavon 2017). A silicon (Si) influx transporter (a nodulin 26-like intrinsic membrane protein subfamily of aquaporins) has been also shown to be permeable to selenite (Zhao et al. 2010).

Kikkert and Berkelaar (2013) investigated the uptake of organic Se compounds selenomethionine (SeMet), selenocystine ($SeCys_2$) in durum wheat (*Triticum turgidum*) and spring canola (*Brassica napus*). Their results showed higher rate in the

uptake of organic Se compound than of selenate or selenite. Organic Se compounds are assumed taken up via amino acid permeases (Guignardi and Schiavon 2017).

After uptake into the roots, selenate is converted into biologically active form for assimilation (Figure 3) through coupling to adenosine triphosphate (ATP) by the activity of ATP sulphurylase (ATPS, Enzyme Commission (EC) number 2.7.7.4), forming adenosine 5'-phosphoselenate (APSe). This reaction is thought to take place in the cytosol and plastids as well and was found to be rate liming in Se assimilation (Pilon-Smits and Le Duc 2009). Four isoforms of ATPS have been identified in *A. thaliana* (APS1-4). Overexpression of APS1 from *A. thaliana* in transgenic Indian mustard (*B. juncea*) resulted in enhanced Se assimilation, accumulation and tolerance (Pilon Smits *et al.* 1999). Jiang *et al.* (2018a) investigated the role of ATPS in hyperaccumulator *S. pinnata* compared to closely related non-accumulator *S. elata*. In roots of *S. pinnata* ATPS enzyme activity and ATPS2 transcript levels were found to be two- and six-fold higher, respectively. ATPS2 in *S. pinnata* showed purely cytosolic localisation while ATPS2 from *S. elata* was found to be localised in plastids and cytosol. Based on the activity studies the enzyme in *S. pinnata* likely acts on both selenate and sulphate as substrates too.

APSe is converted to selenite by the enzyme adenosine 5'phosphosulphate reductase (APR). This step is reported to be another rate limiting step in selenate assimilation and occurs exclusively in plastids (Sors *et al.* 2005a). Transgenic *A. thaliana* overexpressing APR showed significantly enhanced selenate reduction (Sors *et al.* 2005b) while the reduced activity in the loss-of-function allele of APR2 in *Arabidopsis* accessions led to decreased reduction of sulphate supporting the role of the enzyme in S and Se assimilation in plants (Chao *et al.* 2014). The next step is the reduction of selenite to selenide which may run either enzymatically or non-enzymatically. Sulphite reductase (SiR) is responsible for the conversion of sulphite to sulfide so it may catalyze the reduction of selenite as well while the non-enzymatic way is assumed to occur through an interaction between selenite and reduced glutathione (GSH) (Pilon-Smits 2012). Cysteine synthase enzyme complex (serine acetyltransferase (SAT) and *O*-acetylserine (thiol)-lyase (OAS-TL)) catalyses the formation of SeCys from *O*-acetylserine (OAS) and selenide (White 2016). *N.b.*, the official three letter amino acid code for selenocysteine is SeC; however, the abbreviation "SeCys" is also widely used in the literature. The reduction of selenite to selenide and SeCys formation are suggested to occur in the chloroplasts of cells, but

the latter step might take place in the cytosol and mitochondria as well (Ng and Anderson 1979).

SeCys can be incorporated non-specifically into proteins which then lose their function. Plants have evolved several ways to cope with Se-toxicity like producing non-protein building (*i.e.*, non-proteinaceous) Se species or volatile compounds. SeCys methyltransferase (SMT) enzyme localised in the chloroplasts is responsible for the methylation of SeCys to form MeSeCys which is a key mechanism to reduce the amount of SeCys (Guignardi and Schiavon 2017). Overexpression of SMT enzyme in *B. juncea* resulted in the increased accumulation of MeSeCys compared to the wild-type plant (LeDuc *et al.* 2006). In tobacco and tomato non-accumulator species the overexpression of the enzyme resulted in turning the plants into Se accumulators (Wiesner-Reinhold *et al.* 2017).

It is to highlight that only the Se hyperaccumulator species derived isoform of SMT enzyme from an *Astragalus ssp.* had the ability to produce MeSeCys in contrast with the isoform obtained from a non-accumulator species. Therefore, this enzyme is assumed to have an essential role in the toleration and accumulation of high levels of Se (Sors *et al.* 2009). MeSeCys is oxidised to methyl-selenocysteine-selenideoxide which can be further converted to methaneselenol *via* the action of the enzyme Cys sulfoxide lyase and volatilised in the form of DMDSe (Sors *et al.* 2005a). DMDSe production was detected in the Se hyperaccumulator *Astragalus racemosus* (Evans *et al.* 1968).

Condensation of SeCys and *O*-phosphohomoserine (OPH) results in selenocystathionine (SeCysta) by the activity of cystathionine-γ-synthase (CGS). Several hyperaccumulator species are known to contain Se in the form of SeCysta, *e.g.*, *S. pinnata* and *Astragalus praelongus* (Sors *et al.* 2005a). Overexpression of CGS from *A. thaliana* in *Brassica juncea* resulted two- to three-fold higher Se volatilisation rates compared to wild-type plants indicating that CGS is a rate-limiting enzyme for Se volatilisation (Van Huysen *et al.* 2003). Cysthathionine beta lyase calatalyses the reaction between SeCysta and water that ends up in selenohomocysteine (SeHCys) (Läuchli 1993). Conversion of SeHCys to SeMet may be catalyzed by the enzyme methionine synthase using methyl-tetrahydrofolate as a carbon donor (Cossins and Chen 1997). Methionine (Met) is synthesised in plants from *S*-methylmethionine and homocysteine *via* the activity of homocysteine *S*-methyltransferase (HMT) enzyme in the SMM cycle. In broccoli (*Brassica oleracea* var. *italica*) the gene BoSMT encodes an enzyme with high substrate specificity for the conversion of SeCys to MeSeCys

in vitro. The gene showed HMT activity as well and was upregulated in case of treating with selenate indicating remarkable role in selenium metabolism (Lyi *et al.* 2007).

In hyperaccumulators, SeMet is usually further metabolised to avoid its incorporation into proteins. SeMet can be methylated and converted to volatile dimethylselenide (DMSe). Tagmount and coworkers (2002) proved that the first step in the synthesis of DMSe is the methylation of SeMet which forms *Se*-methyl SeMet (SeMM). This process is catalyzed by the enzyme *S*-adenosyl-L-methionine: L-methionine *S*-methyltransferase (MMT). SeMM can be converted to DMSe by two pathways. It may first be converted into the intermediate molecule 3-dimethylselenonopropionate (DMSeP) or directly into DMSe *via* the enzyme methylmethionine hydrolase (Sors *et al.* 2005a). While DMDSe is primarly produced in hyperaccumulators, DMSe is the main volatile Se compound isolated from non-accumulator plants (Pilon Smits and Le Duc 2009).

A gene encoding C-methlytransferases involved in the biosynthesis of ubiquinone or coenzyme Q was isolated from broccoli (named BoCOQ5-2). Interestingly, its expression in bacteria and in *A. thaliana* resulted in increased Se volatilisation, which indicates that proteins outside of the Se metabolism pathway also have significant effects on Se volatilisation (Zhou *et al.* 2009).

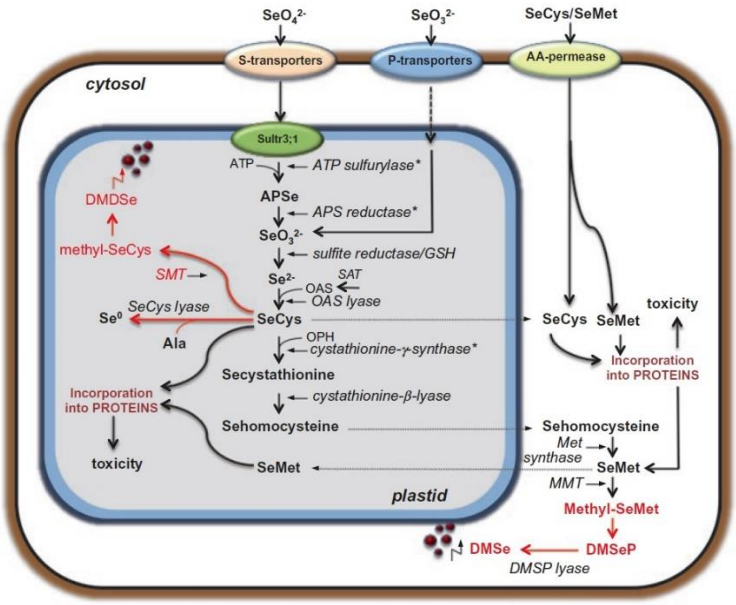

Figure 3. Schematic model of Se assimilation and metabolism in plant mesophyll cells. Red text and arrows indicate Se hyperaccumulator processes (Guignardi and Schiavon 2017).

Asterisks indicate enzymes overexpressed *via* genetic engineering. *Sultr* sulphate/selenite cotransporters, *APSe* adenosine phosphoselenate, *GSH* glutathione, *SAT* serine acetyltransferase, *OAS* *O*-acetylserine, *(Se)Cys* (seleno)cysteine, *OPH* *O*-phosphohomoserine, *(Se)Met* seleno(methionine), *MMT* methylmethionine methyltransferase, *DMSeP* dimethylselenoproprionate, *DM(D)Se* dimethyl-(di)selenide, *SMT* selenocysteine methyltranferase

Se can be incorporated into glucosinolates which conversion is suggested to proceed from SeMet as precursor. Selenoglucosinolates and their volatile hydrolysis products (methylselenoalkyl nitriles and isothiocyanates) were identified in *Brassica* species: broccoli, cauliflower, forage rape (Matich *et al.* 2012) and black mustard (Ouerdane *et al.* 2013).

Another mechanism in plants to avoid Se toxicity is the breakdown of SeCys into elemental Se and alanine by the enzyme selenocysteine lyase (EC 4.4.1.16), which is a way to reduce the amount of SeCys before its misincorporation into proteins (Van Hoewyk *et al.* 2005).

In the case when plant metabolism cannot detoxify excess Se, toxicity symptoms like chlorosis, withering, stunted shoot and root growth can be detected. Se toxicity induces damages in non-proteomic processes (*e.g.*, in lipid peroxidation and altered redox status) and in the proteome as well. Besides the malformed, selenium containing proteins, proteomic impairments include the protein damage associated with general abiotic stress (oxidised or nitrated proteins) as well (Kolbert *et al.* 2019).

Hypothesis of malformed selenoproteins asserts that Se toxicity occurs when a transfer ribonucleic acid^{cys} (tRNA) inadvertently binds to SeCys instead of Cys during translation, resulting in a Cys-to-SeCys substitution in a protein which might lose its specificity and activity. Several transgenic studies support the theory that diverting SeCys away from non-specific protein incorporation increases Se tolerance in plants (Van Hoewyk 2013). Indeed, Cys residues have critical roles in protein structure and function like catalysis, redox regulation, formation of disulfide bridges and metal binding sites. Despite the similarity in their structure, the physical and chemical differences between Cys and SeCys can be harmful in case of substitution in the protein (Van Hoewyk 2013). The different size of SeCys causes the alteration of the protein structure: a diselenide bond is 0.2Å longer than a disulfide bond. Moreover, SeCys possesses a lower redox potential, therefore its substitution can considerably alter enzyme kinetics: as cysteines are often found in the active site of enzymes, the higher reactivity of a SeCys residue dramatically influences all the enzymatic processes. In case of a protein residue that binds cofactors or ions, the related enzyme functions can be endangered due to the substitution. Additionally, Fe-Se clusters can also substitute for an Fe-S cluster in chloroplastic and mitochondrial proteins that participate in electron transport, which causes altered activity (Kolbert *et al.* 2019).

SeMet can also be accumulated non-specifically in selenium containing proteins (Eustice *et al.* 1981). However, it is not considered deleterious in plant proteins due to the lower reactivity of Met (Van Hoewyk 2013) and due to the quasi-specific accumulation of SeMet in Met-rich storage proteins (Németh and Dernovics 2015).

3.1.4. Selenium species identified in the Brassicaceae family

Se metabolism of Brassicaceae species has been in focus for a while due to their applicability for phytoremediation of seleniferous soils (White *et al.* 2007) and their evident presence in human diet. The actual known metabolic pathways of Se in *B. oleracea* based on the Kyoto Encyclopedia of Genes and Genomes (KEGG) database is shown in Figure 4. Green boxes refer to genes encoded in the organism genome: methyonil-tRNA synthetase (EC 6.1.1.10), homocysteine methyltransferase (MET), cystathionine β-lyase (CBL), cystathionine γ-synthase (CGS), methionine *S*-methyltransferase (EC 2.1.1.12), methionine γ-lyase (EC 4.4.1.11), thioredoxin reductase (EC 1.8.1.9), selenocysteine lyase (EC 4.4.1.16), and ATP sulphurylase (EC 2.7.7.4). Accordingly, the discovery of Se species that are either the substrate or the products of these enzymes has always been expected. The detection of SeMM, SeCysta, MeSeCys selenoxide, selenohomocystine, MeSeCys and SeMet with thin layer chromatography (TLC) in *B. oleraceae* was published by Hamilton (1975) however not all of these species have been confirmed since then with the spreading of more reliable analytical methods as detailed below. SeMet and MeSeCys were identified in different *Brassica* species, and the pathway of SeMet has been underlined by deoxyribonucleic acid (DNA) coded enzymes in contrast to MeSeCys.

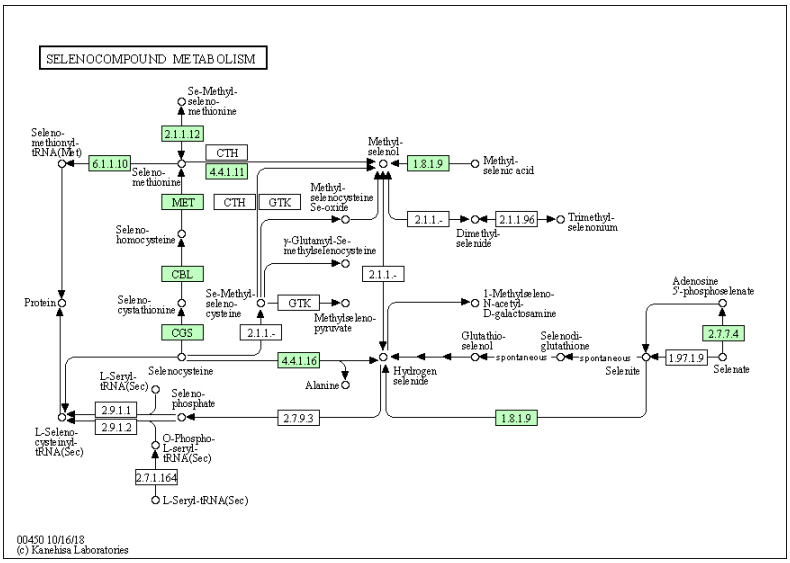

Figure 4. Metabolism of Se in *B. oleracea* (Kanehisa and Goto 2000).

Identification of Se species in plant tissues is an inevitable step on the way of exploring the pathways in Se metabolism. The most widespread analytical techniques for Se speciation are high performance liquid chromatography inductively coupled plasma mass spectrometry (HPLC-ICP-MS) which is complemented with electrospray ionisation mass spectrometry (ESI-MS) measurements and X-ray fluorescence (XRF) and X-ray absorption near-edge structure (XANES) spectroscopy. Latter technique provides information about the Se-related covalent bonds in the analysed compounds. Detailed applicability of the techniques is to be discussed in Chapter 3.2. In this actual chapter, an overview of Se speciation results in Brassicaceae species is presented that considers plants both from natural habitat and from artificial Se supplementation experiments as well. It is to underline that critical evaluation of the upcoming results, especially on the reliability of species identification, is also addressed later.

Protease and lipase digested enzymatic extracts of *A. thaliana* plant tissues were tested for Se speciation using strong anion exchange (SAX)-ICP-MS instrumentation. Identification of Se species was based on retention time matching with standards. When treated with selenate or selenite, the most abundant organic Se species was SeMet both in leaf and root samples. Inorganic selenate could be also identified and a small peak was supposed to be MeSeCys. Several peaks did not show any retention time matching with the available standards and remained unidentified, which called attention to the need for complementary – organic mass spectrometry derived – solutions (Wang 2010).

The main Se compound in the proteolytic extracts of *B. rapa* and *B. napus* seeds and meal was found to be SeMet after selenate or selenite treatment in the soil or with foliar spraying. SeMet accounted for 80% of the total Se while traces of inorganic selenate was detected as well (Seppänen *et al.* 2010). SAX chromatography was complemented with size exclusion chromatography (SEC), similarly to the experiment where the dynamics of organic Se species production in *B. napus* (Seppänen *et al.* 2010, Seppänen *et al.* 2018) was in focus. Results showed that 81% of the Se content in the leaves was in the form of selenate six hours after selenate application to the soil; this concentration decreased to 60% by 14 days. In the case of selenite treatment, the applied inorganic form was detected in the leaves even after 7 days and substantial after 14 days. SeMet was found to account for 15% of total Se after 6 hours, and this species increased to 33% after 14 days. After 6 hours, MeSeCys could be identified as well; however, it could not be detected after 14 days.

Broccoli (*B. oleracea* L. var. *Marathon*) accumulated mainly SeMet in the florets in an experiment where the plants were grown in soils that had been amended with ground shoots of the Se hyperaccumulator *S. pinnata*. Besides the main form SeMet (58% of total Se), $SeCys_2$ (15%), MeSeCys (7.4 %), selenate (6%) selenite (3.1%) were identified as well. These SAX-ICP-MS data of the protease enzymatic extracts were complemented with XANES measurements of finely ground broccoli florets, revealing the following composition: 55% of total Se was found in "C-Se-C" forms (that include both SeMet and MeSeCys), 23% as $SeCys_2$, 18% in oxidised SeMet and 4% as selenate (Banuelos *et al.* 2015). Indeed, several studies identified the main Se species in broccoli as MeSeCys: Cai *et al.* (1995) analysed broccoli samples with gas chromatography atomic emission spectroscopy (GC-AES), Sugihara *et al.* (2004) tested broccoli sprouts with reversed phase (RP)-ICP-MS, while Lyi *et al.* (2005) studied leaves and florets of broccoli with RP-fluorescence detection (FLD) setup. Extraction procedures in these experiments were carried out with different concentration of HCl (0.05 M-0.2 M) without any enzyme in contrast to the experiment of Banuelos *et al.* (2015). Actually, HCl is considered a good extraction solvent for free amino acids, as demonstrated by Cankur *et al.* (2006).

In another study where high Se environment was provided by sodium selenite, MeSeCys was found to be the main Se compound in several other vegetables sprouts belonging to Brassicaceae family, such as *B. campestris* (qing gin cai, Chinese cabbage, turnip, nozawana), *Lactuca sativa* (red-tip lettuce) and *Raphanus sativus* (daikon – Japanese radish, Kaiware daikon) (Sugihara *et al.* 2004). Pedrero *et al.* (2006) revealed differences in Se speciation regarding selenate and selenite treated radish (*R. sativus*), covering fresh and dried samples as well. Samples were extracted with a protease enzyme and analysed with SAX-ICP-MS. In plants grown in the selenite containing media, the main species was found to be MeSeCys, followed by SeMet and $SeCys_2$; selenate could be identified too. After drying at 50°C a clear decline in MeSeCys content was observed, together with the increase of selenate concentration and the appearance of an unknown compound. In the fresh samples of the selenate treated radish the main species was found to be selenate, while SeMet, $SeCys_2$ and MeSeCys were present to a lesser extent. After drying, the decrease of organic selenium compounds and the increase of inorganic selenate were detectable.

A pioneering and demanding study was published in 2007 by Ogra *et al.*: selenohomolanthionine (SeHLan) was identified in the water extract of a Se-enriched radish variant *(R. sativus* L. cv. 'Yukibijin'), accounting for ~5% of total Se. This was

the first time that a Se compound without any former assumption on a possible sulphur analogue was unambiguously identified in a Brassicaceae plant. Ten years later the same research group detected SeHLan in *Brassica juncea* with retention time matching of their in-house synthesised standard, but no traces of the compound could be detected in garlic (Ogra *et al.* 2017). Interestingly, the presence of SeHLan in garlic was reported by Ruszcynska *et al.* (2017) based on exact mass analysis. The MS/MS fragmentation pattern and spiking procedure could clarify the identity of the compound. The detection of SeHLan in several species indicates this compound is an important metabolite in selenium tolerance and depletion processes.

Se metabolism of nozawana (*B. rapa* var. *hakabura*) and komatsuna (*B. rapa* var. *peruviridis*), two popularly consumed leafy vegetables in Japan, were parallel analysed with the well-known Se accumulator *B. juncea* (Indian mustard). After selenate treatment, the main selenium form in the water extract of the four-week old plants was identified as selenate with SEC-ICP-MS. Traces of SeMet and MeSeCys could be detected as well (Yawata *et al.* 2010).

Several other studies focused on the Se speciation in the secondary accumulator *B. juncea*. Plants were grown under hydroponic conditions in the presence of sodium selenite. Proteolytic extraction resulted in a higher signal for SeMet in the RP chromatogram compared to the acidic extraction, but the main Se compounds remained unidentified (Montes-Bayón *et al.* 2002). Similarly, enzymatic extracts were analysed by Kahakachchi *et al.* (2004) with ion pairing reversed phase (IP-RP)-ICP-MS and GC-AED. In selenate treated *B. juncea* plants MeSeCys, SeMet and *S*-(methylseleno)cysteine were identified, while in case of selenite treatment SeMet and *S*-(methylseleno)cysteine were identified with both detection techniques. The Se-S amino acid *S*-(methylseleno)cysteine ($C_4O_2H_8NSeS$) was detected for the first time in plant shoots and roots. The main forms of Se in *B. juncea* plants were detected only with IP-RP-HPLC-ICP-MS: inorganic selenate and selenomethionine Se-oxide hydrate in case of selenate and selenite treatment, respectively.

Production of volatile Se compounds like DMSe and DMDSe was detected with GC-MS from *B. juncea* seedlings grown hydroponically in closed vials. Different enrichment forms (selenite, selenate, SeMet, selenocyanate) did not provide significant difference in terms of the species released by the plants (Meija *et al.* 2002). Overexpression of ATPS and SMT enzymes in *B. juncea* resulted shift in the volatilisation pathways towards the form of DMDSe compared to wild-type plants (Kubachka *et al.* 2007). The genetic modification allowed the identification of minor

volatile Se compounds: dimethyl selenosulfenate (CH_3-Se-S-CH_3), dimethyl triselenide (CH_3-Se-Se-Se-CH_3), dimethyl diselenyl sulfide (CH_3-Se-S-Se-CH_3), and ethyl methyl selenide (CH_3-Se-CH_2-CH_3).

The natural presence of selenoglucosinolates has been called into question due to their absence in *S. pinnata* grown at low or moderate Se concentration. Indeed, only high Se environment resulted in traces of detectable selenoglucosinolates (Bertelsen *et al.* 1988). Selenoglucosinolates were unambiguously identified first in *Brassica* species. Ethanolic extract of selenate treated forage rape (*B. napus*) and broccoli (*B. oleracea* L. var. *italica*) were analysed by RP-HPLC-MS. Glucoselenoiberverin and glucoselenoerucin were identified in both samples while forage rape contained glucoselenoberteroin as well (Matich *et al.* 2012). *R. sativus* was found to contain a different glucosinolate compound: 4-(methylseleno)-but-3-enyl glucosinolate (McKenzie *et al.* 2019).

Indeed, *S. pinnata* is one of the most studied Se hyperaccumulator plants. XANES spectra of *S. pinnata* leaves after selenate treatment revealed that the most prevalent form of Se is a "C-Se-C" type species. LC-MS measurements of extracts from the leaf edges and tips revealed that the main organic Se forms were MeSeCys (88%) and SeCysta (12%) (Freeman *et al.* 2006a). In comparison, the secondary accumulator *S. albescens* leaf spectra were different and showed the best fitting with a composition of 75% of "C-Se-C", 20% SeCys and 5% selenate. Only SeCysta could be detected as organic Se compound with LC-MS (Freeman *et al.* 2010). As supported by an upcoming study, several taxa in the *Stanleya* genus accumulate predominantly organic Se with the "C-Se-C" configuration (Cappa *et al.* 2015).

Cardamine hupingshanesis hyperaccumulator plants collected in a Se-mine drainage area in China were analysed with SAX-hydride generation atomic fluorescence spectrometry (HG-AFS) after Tris-HCl and enzymatic extractions. Authors denoted $SeCys_2$ as the main accumulated Se species in the plant (Yuan *et al.* 2013).

3.1.5. Selenium metabolism and the plant microbiome

Generally, Se uptake of plants depends on total Se concentration in soils, Se speciation, competing ions present in soils and soil physicochemical factors: $CaCO_3$, silt content, organic matter, clay content, pH, iron, exchangeable quantity, and redox potential among others (Zhao *et al.* 2005, Terry *et al.* 2000). On the other hand, several studies have recently investigated the effect of plant related soil microbiome on Se

metabolism, providing a novel approach in the interpretation of Se metabolism. Eventually, the interaction of microbes with definite selenium requirements with plants, the kingdom without direct selenium needs, must be ecologically active in sharing this microelement. Here, an overview of the results is presented with a main focus on rhizosphere.

Microbiomes include bacteria, archaea, fungi and some protists attending a particular environment. All tissues of a plant host a microbial community which often benefits its host *via* plant growth promoting properties, while the host offers protection and nutrients to the microbial symbiont. Plant microbiome can be divided into three parts: rhizosphere, endosphere and phyllosphere that all are unique and have intra- and intercommunity interactions (Figure 5). Phyllosphere consists of the group of microbes that occur on the surface of plant shoots and endophytes are microbes that live inside plant tissues. Rhizosphere is the underground area within 5 mm proximity of the roots and it possesses the highest abundance of microbes among the three spheres (Turner *et al.* 2013, Cochran 2017).

Rhizosphere microbiomes of Se hyperaccumulators were found to be significantly different from non-accumulators and to harbour a higher rhizobacterial species richness (Cochran *et al.* 2018).

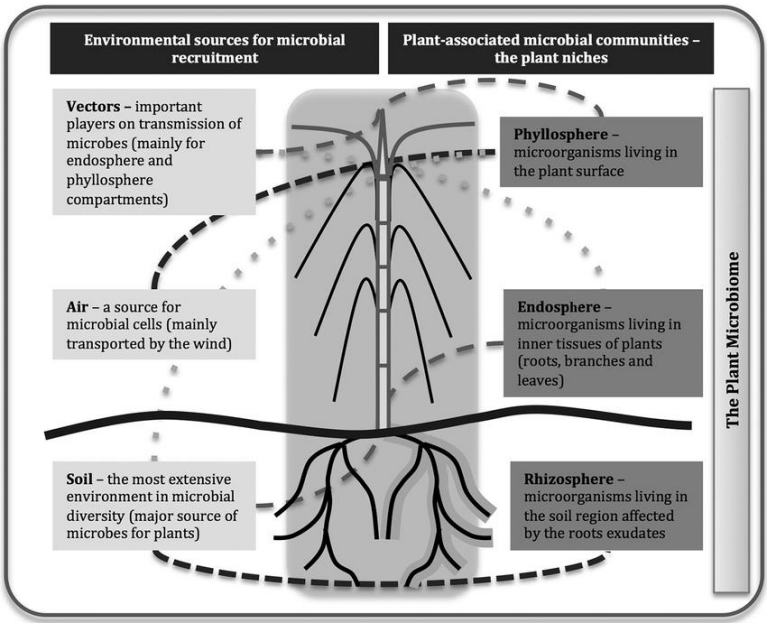

Figure 5. Schematic representation of the major sources of microbes that compose plant-associated communities (Andreote *et al.* 2014).

Bacteria in general seem to be tolerant to Se. Some bacteria are even selenium dependent, some synthesise selenoenzymes, or use selenium for respiration (Nancharaiah and Lens 2015). Most bacteria have capacity to assimilate inorganic Se

into organic forms and producing organic volatile forms similarly to plants' metabolism (Staicu *et al.* 2017b). Not all plant-associated microbes are resistant to Se; *e.g.*, fungi (for those selenium is *ab ovo* unessential) are much more sensitive than bacteria (Cochran 2017).

Contribution of soil microorganism to plant Se volatilisation was already studied decades ago. De-topped roots of broccoli were treated with antibiotics resulting in 95% inhibition of the Se volatilisation activity in case of selenate supplementation (Zayed and Terry 1994). Several studies showed that the presence of rhizosphere microbes can contribute to plant growth and enhanced Se accumulation. Experiments with ampicillin and selenate treatment showed that ampicillin inhibited Se volatilisation by about 35% of and tissue Se accumulation by about 70% of in *B. juncea*. Axenic plants inoculated with rhizosphere bacteria had 5-fold higher Se concentration in roots and 4-fold higher rates of Se volatilisation (de Souza *et al.* 1999). Inoculation with the rhizosphere extract of *S. ericoides* hyperaccumulator population from a seleniferous area stimulated growth and Se accumulation in the same species when it was grown upon surface-sterilised seed on autoclaved naturally seleniferous or non-seleniferous soils. The same inoculation enhanced shoot Se accumulation even in *S. ericoides* population originating from a non-seleniferous area grown on autoclaved seleniferous soil (El Mehdawi *et al.* 2015). Inoculation with a selenium tolerant environmental bacterium strain resulted in increased selenium uptake in wheat (Yasin *et al.* 2015).

Besides bacteria, rhizosphere fungi showed effects on plant Se accumulation as well. *Alternaria seleniiphila* and *Aspergillus leporis* from the rhizosphere of the hyperaccumulator *S. pinnata* were used to inoculate *S. pinnata* and the related non-hyperaccumulator *S. elata*. Reduced translocation of Se was detected in the hyperaccumulator species and increased root Se accumulation in the case of *A. seleniiphila – S. pinnata* and *A. leporis – S. elata* inoculation combinations; this observation indicated that the functional significance of fungal inoculation was host dependent. Similarly, in the case of comparing hyperaccumulator and non-accumulator *Astragalus* species, the hyperaccumulator plants showed decreased translocation of Se due to the inoculation with a *Fusarium* species previously isolated from the hyperaccumulator rhizosphere while the non-accumulator plant species was not influenced. Se speciation in roots was not affected by inoculation in these studies (Lindblom *et al.* 2013a, 2014). Only *Alternaria astragali* out of the four studied

rhizoplane fungi affected Se speciation in roots of *A. bisulcatus* and *S. pinnata* and gave rise to some elemental Se accumulation (Lindblom *et al.* 2013b).

Alford and coworkers (2014) investigated the nitrogen-Se relationship with the comparison of nodulated and non-nodulated *Astragalus* species. Enhanced nitrogen acquisition capacity associated with root nodulation was found to enhance Se accumulation in the form of selenoamino acids in hyperaccumulator *A. bisulcatus*. Microbial supply particularly seemed to provide glutamate for the formation of γ-glutamyl-(methyl)selenocysteine (γ -glu-MeSeCys).

Besides the rhizosphere microbiome, hyperaccumulator endophytes from *S. pinnata* and *A. bisulcatus* were also characterised with high Se resistance, high capacity to produce elemental Se and plant growth promoting properties (Sura-de Jong *et al.* 2015).

Besides plant-microbes, plant-plant interactions have been also in the focus of several studies. Soil collected nearby Se hyperaccumulators was found to be Se-enriched (and presumed to be) due to deposition of hyperaccumulator plant biomass (litter) and root exudation mainly in the form of organic Se compounds; this fact hypothesises an elemental allelopathic effect (El Mehdawi *et al.* 2011). The study of relative abundance of species occurring in seleniferous sites revealed that some species co-occurred either positively or negatively with hyperaccumulators compared to the overall vegetation. Neighbours of Se hyperaccumulators had higher tissue Se concentration compared to the cases the same species grew elsewhere in the area (Reynolds *et al.* 2020). The soil surrounding hyperaccumulators can easily become toxic to Se-sensitive species that leads to reduced germination and growth, while it can be beneficial for Se-tolerant species (Pilon-Smits 2019). It must be noted that the exact mechanisms of hyperaccumulators influencing their surrounding vegetation has not yet been fully elucidated.

3.1.6. Cultivation methods for selenium metabolism studies

Plant Se metabolism can be studied using different approaches in terms of the origin of analysed plant individuals. In case of field studies, plants are collected from their natural (usually seleniferous) habitat and soil samples are to be also analysed (Eiche *et al.* 2015). Even a particular individual can be analysed through several seasons, as global positioning system (GPS) coordinates can help to identify the exact location of individuals.

In contrast to field studies the cultivation of plants provides higher control over the growing environment. Glass- or greenhouses have usually transparent roof and/or walls that enable the light to enter during the day, which also contributes to upwarming. Greenhouses can be also equipped with several types of grow lights as sole light sources in growth chambers and growth rooms (Choi *et al.* 2015). Besides the intensity, the quality and the duration of light period, other factors can be monitored and/or controlled, such as temperature, irrigation, nutrient application and humidity.

Different media can be applied for plant cultivation (Figure 6). Plant seeds are often surface sterilised, *e.g.*, with ethanol, diluted bleach or $HgCl_2$ (Lindblom *et al.* 2013a, b, 2014, Cappa *et al.* 2015, Yasin *et al.* 2015). In most cases seeds are germinated and sometimes grown until sprout size on moisturised material like paper, cotton, rock wool, block wool, sheet of plywood or even coconut fiber before potting in the growing media or being analysed as sprouts (Montes-Bayón *et al.* 2002, Kahakachchi *et al.* 2004, Pedrero *et al.* 2006, Cappa *et al.* 2015, Sugihara *et al.* 2004, Finley *et al.* 2001, Yawata *et al.* 2010). In case of hydroponic set-ups, plants are grown until a certain size, evolving roots and shoots, then they are transplanted to float on a nutrient solution (Montes-Bayón *et al.* 2002, White *et al.* 2007). Main advantage of sand and gravel (Van Huysen *et al.* 2003, Freeman *et al.* 2010, Lindblom *et al.* 2013a, b, 2014, Harris *et al.* 2014, Schiavon *et al.* 2015) is their easier removal from the root in contrast to usual soil covering. The most widespread nutrient solution for watering and floating plants is Hoagland's solution that can be applied at different strength (Hoagland and Arnon 1950, de Souza *et al.* 1998, Kahakachchi *et al.* 2004, Lindblom *et al.* 2013a, b, 2014, Schiavon *et al.* 2015). Most commonly, plants can be cultivated under sterile conditions on agar media using Murashige-Skoog agar, which excludes any kind of microbial effects (Murashige and Skoog 1962, Freeman *et al.* 2006, Cappa *et al.* 2015, El Mehdawi *et al.* 2015).

For Se metabolism investigations Se is usually provided through the growing media, but surface foliar spraying was also addressed (Seppänen *et al.* 2010). Different forms of Se can be added: selenate, selenite, organic Se like SeMet, $SeCys_2$ (Montes-Bayón *et al.* 2002, Freeman *et al.* 2006, Kikkert and Berkelaar 2013, Cappa *et al.* 2015). Tolerance and accumulation experiments require Se supplementation at different concentrations (Harris *et al.* 2014, El Mehdawi *et al.* 2014, Jiang *et al.* 2018b). As indicated in Chapter 3.1.4, even grounded tissue of Se accumulating species can be used by mixing it with soil to provide available Se for plant uptake (Banuelos *et al.* 2015). Se metabolism should be studied in the known

(or hypothetical) accumulator species in comparison with a closely related non-accumulator species (if available).

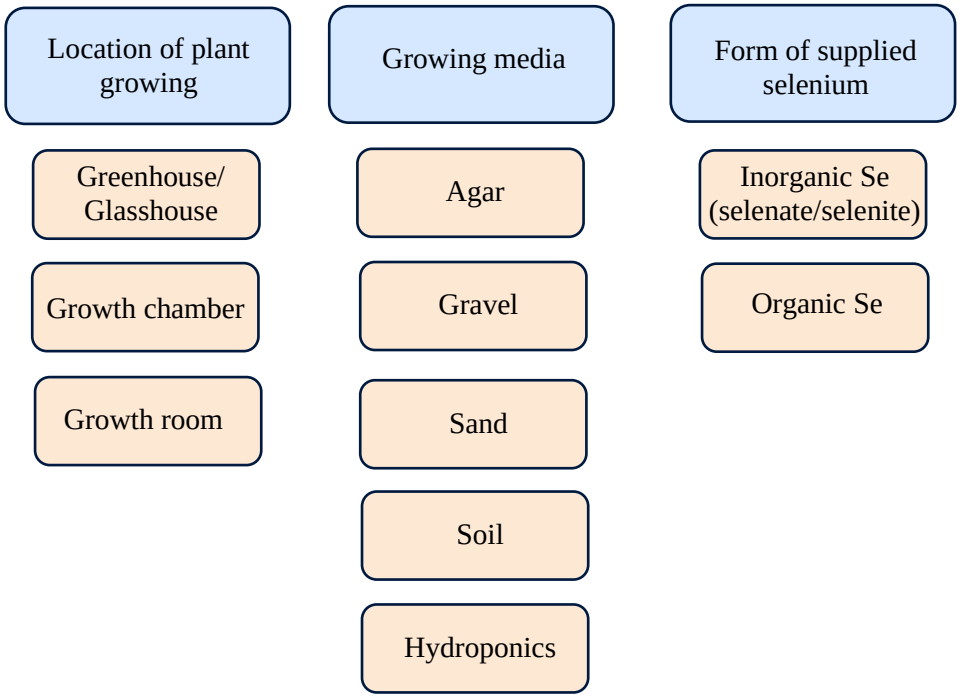

Figure 6. Overview of the most common cultivation set-ups used for Se metabolism studies.

3.2. ANALYTICAL APPROACHES IN SELENIUM SPECIATION

Recognition of the fact that effects of an element on living systems depends on its chemical form lead to increasing number of studies employing the term „speciation" in a number of different ways. The clarification of the terminology was found necessary by the International Union for Pure and Applied Chemistry (IUPAC). According to their recommendations (Templeton *et al.* 2000) speciation analysis is the analytical activity of identifying and/or measuring the quantities of one or more individual chemical species in a sample. Chemical species are specific forms of an element defined as to isotopic composition, electronic or oxidation state, and/or complex or molecular structure. The speciation of an element is the distribution of an element amongst defined chemical species in a system.

Similarly to some trace elements, different chemical forms of Se show different bioavailability, toxicity, and biochemical properties. Identification of Se species in plants is getting more attention as plants are the main Se source in human diet (Rayman *et al.* 2008). Analytical speciation contributes to the exploring of Se mobility and Se-specific metabolic pathways, and molecular and cell biological approaches are complementary needed to understand the whole process (Ogra and Anan 2009).

The two major challenges in elemental speciation in biological systems are the low concentration of trace elements and the complexity of the matrix (Szpunar *et al.* 2003). Several analytical methods have been used for speciation studies; the applied technique depends on among others the purpose of the study, the issue addressed by the researcher and the sample matrix.

3.2.1. Direct methods in selenium speciation

Analytical approaches for speciation studies can be direct methods where separation techniques are not required in the form of extraction or column separation (Kroukamp *et al.* 2016).

Synchotron based techniques are widespread in studying metal(loid)s in plants. The most common used approaches include X-ray fluorescence (XRF) and X-ray absorption spectroscopy (XAS). This latter technique makes possible to determine the chemical form of an element while XRF can be used for imaging its distribution in tissues and cells and also for its quantification (Sarret *et al.* 2013).

During XRF the energy of the X-ray excites core electrons in the elements, creating a photoelectron and a core hole. The hole is filled by dipole-allowed decay of higher

bound electrons with concomitant emission of an X-ray fluorescence photon or with the emission of an Auger electron (Pushie *et al.* 2014). In case of Se, K-edge absorption corresponds to the excitation of the most tightly bound 1s electrons, and occurs at energies close to 12 658 eV (Dolgova *et al.* 2018). Schematic diagram of the underlying physics and the fluorescence emission spectra of a selenium-containing sample exposed to X-rays above and below the Se K-absorption edge are shown in Figure 7. The spectrum with the incident X-ray energy below the Se K-edge shows only scattered X-rays, whereas peaks due to the Se K_α and Se K_β X-ray fluorescence are clearly detected when the incident X-ray energy is above the Se K-edge (Pushie *et al.* 2014).

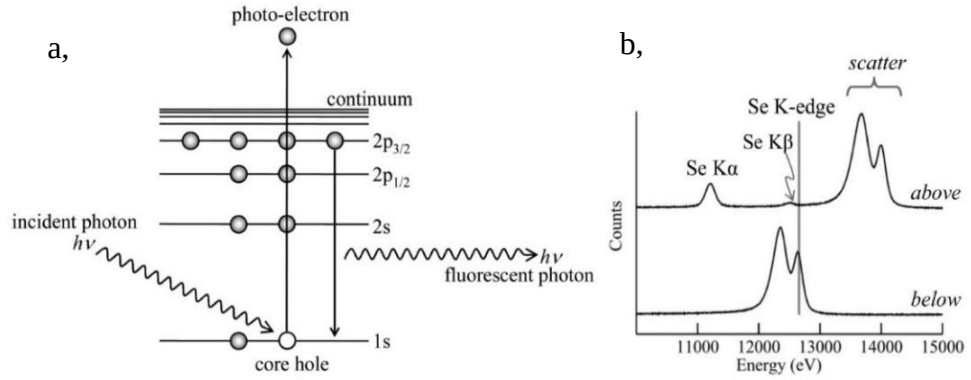

Figure 7. Physics of X-ray absorption and X-ray fluorescence. (a) Schematic diagram of the physics. (b) Experimental X-ray emission spectra collected with incident X-ray energy above and below the selenium K-absorption edge of a biological sample (Pushie *et al.* 2014).

A basic XRF experimental apparatus consists of a magnet source, a crystal monochromator, slits and focusing optics, a beam intensity monitor, a motorised sample stage and a fluorescence detector (Sarret *et al.* 2013). A schematic figure of a set-up is shown in Figure 8.

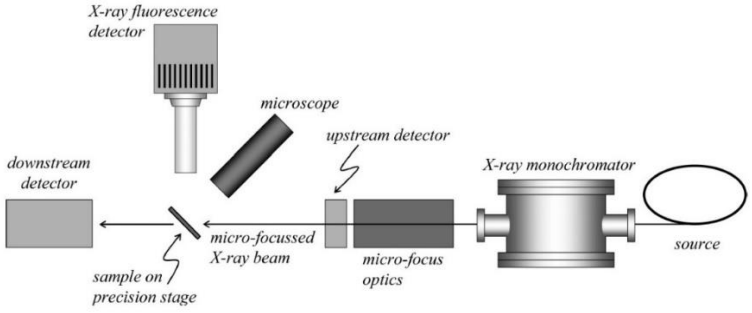

Figure 8. Schematic plan view of basic X-ray fluorescence microprobe (Pushie *et al.* 2014).

Due to the minimal required pretreatment, wide spectra of biological samples can be analysed *in situ*, including purified biomolecules, cell cultures, tissues, intact small organs or organisms, soil, sediment, dust or water (Dolgova *et al.* 2018). Synchrotron radiation microprobe can reach the spatial resolution of 0.1 – 1 µm (Lobinski *et al.* 2006a). To avoid the alteration of elemental distributions and chemical speciation in the sample careful fixation protocol is preferred. In case of some sample types chemical fixation of tissues can cause inaccuracies in the studied parameters. For hydrated tissue analysis, thin tissues can be cryo-preserved with immersion in liquid nitrogen, while in case of thick tissues high-pressure freezing provides homogeneous vitrification to yield the closest results to the *in vivo* state. Thin sections can be also prepared from frozen hydrated samples using a cryomicrotome. The samples must be kept in frozen state until analysis which is also carried out on a cryostage. Air-dried and dehydrated samples can be analysed at room temperature. In case of experiments carried out *in vivo*, radiation damage should be monitored carefully and exposure time should be reduced as much as possible (Sarret *et al.* 2013, Pushie *et al.* 2014).

Emission of characteristic X-rays from sample spots is recorded for µXRF imaging. High resolution optics focus X-rays into a small spot and the sample is scanned through the focal spot. Different visualisation approaches can be applied like plotting a gray-scale image for elements separately, scatterplotting, or making a red-green-blue (RGB) image where the RGB values of each pixel are proportional to the amounts of the elements they represent. µXRF images can be evaluated for quantification as well using standards for each element of interest or an internal standard element if the bulk composition, sample density and thickness are estimated reasonably (Sarret *et al.* 2013).

During XAS experiment the absorption of a monochromatic beam of X-rays is monitored as a function of the incident energy. Fingerprint information can be found in the X-ray absorption near edge structure (XANES) region of the XAS spectrum. This energy region lasts from 50 eV below the element absorption edge to 200 eV above it. The spectra depend on the electronic structure, thus they provide information about valence state and local structure. This means that XANES based speciation determines the chemical form of Se in the biological sample rather than the individual Se-containing molecules. Evaluation is done by least-squares fitting (LSF) of the linear combinations of spectra of known Se standards (Sarret *et al.* 2013, Dolgova *et al.* 2018).

In Se research the most common application of X-ray based methods is the investigation of the spatial distribution and chemical speciation in plant tissues. In some studies ecological partners of plants have been analysed as well. Se can be present in the oxidation states of +6, +4, 0, -2 and bound to different neighboring atoms, mostly to C, S, O, Se and H. Different selenocompounds show different XANES spectra, however the organic forms with ”C-Se-C” bonds are indistinguishable and their speciation requires complementation with further methods.

XANES analysis of leaf and root tissues of non-accumulator *A. thaliana* species showed that Se was accumulated primarily in the form of inorganic selenate while hyperaccumulator *A. bisulcatus* and *S. pinnata* tissues contained predominantly organic selenocompounds with “C-Se-C” configuration. Further LC-MS analysis identified the compounds responsible for “C-Se-C” signal as MeSeCys and γ-glu-MeSeCys in *A. bisulcatus* and MeSeCys and SeCysta in *S. pinnata*. Differences in the localisation of Se in leaves of hyperaccumulator and non-accumulator species were also revealed. Hyperaccumulator *A. bisulcatus* accumulated Se mainly in the leaf hairs, *S. pinnata* did so in its epidermis (particularly along the leaf edge), while non-hyperaccumulator *B. juncea* and *A. thaliana* showed higher Se concentration in the vasculature (Freeman *et al.* 2006a, Van Hoewyk *et al.* 2005). Differences in moth populations originating from seleniferous and non-seleniferous areas were revealed with μXANES and LC-MS. The Se-tolerant moth accumulated MeSeCys similarly to its parasitic wasp while the Se-sensitive moth population accumulated SeCys that is toxic due to its non-specific incorporation into proteins (Freeman *et al.* 2006b).

Laser ablation inductively coupled plasma mass spectrometry (LA-ICP-MS) has been also employed to map the distribution of Se in biological tissues as a direct method, *e.g.*, in thin sections of Se-treated slugs and sunflower leaves (Becker *et al.* 2007, da Silva and Arruda 2013, Cruz *et al.* 2018). The method could be indirectly used to detect selenium-containing proteins after extraction and gel electrophoresis. Selenoproteins in wheat were analysed after two dimensional poliacrylamide gel electrophoresis (2D-PAGE) using one dimensional isoelectric focusing electrophoresis (1D - IEF) and 1D sodium dodecyl sulphate PAGE (SDS PAGE) to shorten the time required to locate the position of proteins (Bianga *et al.* 2013). LA-ICP-MS technique allows for isotope specific analyses and ensures lower detection limit (down to 0.01 μg Se g^{-1}) compared to μXRF (0.1-1 μg g^{-1}) however its resolution is generally insufficient to map sub-cellular distribution (Lobinski *et al.* 2006a).

3.2.2. Orthogonal LC-MS techniques

Indirect methods require the separation of species prior to analysis, which can be carried out in the form of sequential extractions and/or column separation (Kroukamp *et al.* 2016). Speciation studies require the combination of separation techniques with element-specific detectors and often a molecule-specific detector as well. The set-up is expressed with the term "hyphenated" and the choice among the several possibilities available depends primarily on the objective of the research (Szpunar and Lobinski 2003). Schematic overview about hyphenated techniques for general bio-inorganic speciation analysis is shown in Figure 9. However, ICP-MS cannot be used for some elements (*e.g.*, F), its role is unquestionable for quantification and species localisation purposes.

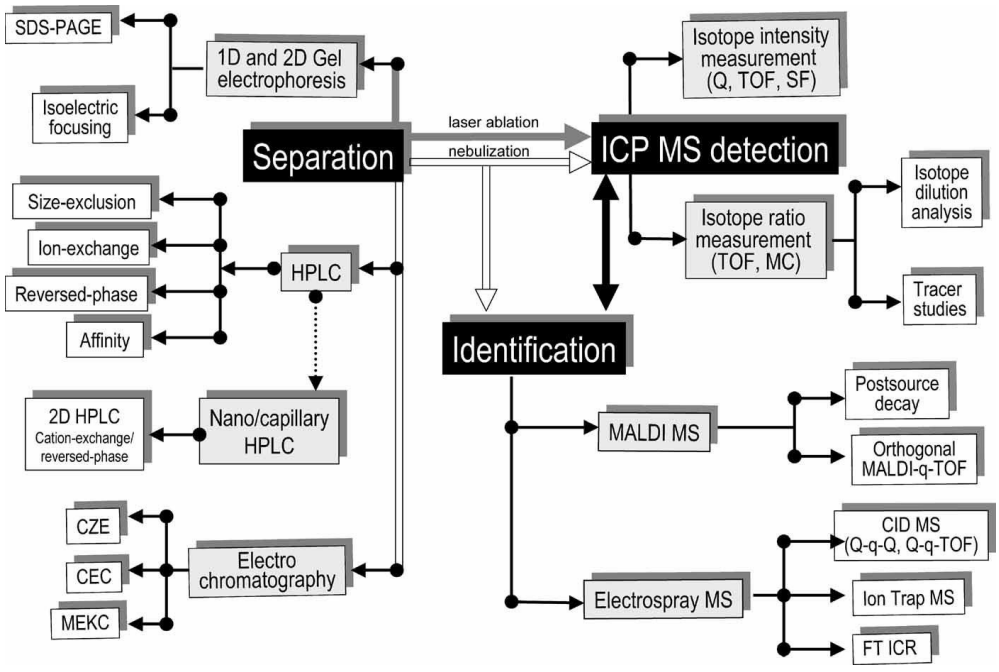

Figure 9. Hyphenated techniques for the speciation analysis of non-volatile species (Lobinski *et al.* 2006b).

1D one dimensional, *2D* two dimensional, *HPLC* high performance liquid chromatography, *CZE* capillary zone electrophoresis, *CEC* capillary electrochromatography, *MEKC* micellar electrokinetic chromatography, *Q* quadrupole, *TOF* time of flight, *SF* sector field, *MC* multicollector, *ICP MS* inductively coupled plasma mass spectrometry, *MALDI MS* matrix assisted laser desorption ionisation mass spectrometry, *FT ICR* Fourier-transform ion cyclotron resonance

Volatile Se species and some selenoamino acids after derivatisation can be analysed with gas chromatography, but the most widespread approach in plant Se speciation is HPLC separation of plant extracts and monitoring Se with an element specific detector (mostly ICP-MS).

Steps of sample pretreatment/preparation can influence the accuracy and quality of the final result, therefore the chosen extraction methods should fit for the purpose depending on the matrix, the expected chemical form of selenium and the selected instrumentation. One should also keep in mind the quantitative extraction of selenium species and avoiding their interconversion/decomposition (Pedrero and Madrid 2009, Dernovics *et al.* 2006). Besides choosing a given extraction method, sequential extraction procedures can also be applied as developed for the characterisation of different classes of selenium species in garlic including water extraction, enzymatic cell wall lysis, proteolysis, and extractions with HCl, sulphite and CS_2 (Monicou *et al.* 2009). Recently, nanomaterial based extraction and preconcentration techniques have also been investigated for Se speciation studies (Clough *et al.* 2017).

One of the challenges in Se speciation is that most biological samples contain Se at low concentration levels and it is distributed among a wide variety of Se species (Pedrero and Madrid 2009). Due to the very low detection limit achievable, ICP-MS is the most frequently used detection method, however structural information of the compounds cannot be directly gained. During the so-called hard ionisation the covalent and non-covalent bonds are completely broken in molecules and monoatomic positive ions are guided to the mass analyser. Molecular (structural) identification is mostly based on retention time matching if standards are available (Lobinski *et al.* 2006b). As the majority of species have not been purified/synthesised yet for bioinorganic trace element speciation analysis, the parallel application of molecule specific detectors (ESI-MS, MALDI-MS) became inevitable for the standardless identification in Se speciation studies (Szpunar and Lobinski 2003).

Different types of liquid chromatography have been used for Se speciation analysis such as size exclusion, reversed phase, strong anion/cation exchange (SAX/SCX) or hydrophilic interaction (HILIC). Among these, SAX is applied in a considerable part of speciation studies because several important species (*e.g.*, inorganic Se oxyanions) can be targeted. However, some species are hardly retained in SAX and co-elute close to the chromatographic void volume, *e.g.*, $SeCys_2$, SeHLan and selenomethionine-selenoxide (SeMetO). Interestingly, this aspect is not always taken into account and the presence of $SeCys_2$ has been continuously published without any further confirmation by other separation or structural assignment techniques (Clough *et al.* 2019). Indeed, SAX usually enables the identification of SeMet, selenite, selenate, γ-glu-MeSeCys and MeSeCys on the basis of retention time matching in vegetable samples (Michalska-Kacmyrov *et al.* 2014, Ruszcynska *et al.* 2017).

RP chromatography is also used for the analysis of Se species, although selenoamino acids are too hydrophilic to be retained on typical non-polar stationary phases (C_8 or C_{18}). Their retention can be increased by using ion pairing reagents (for example, perfluorocarboxylic acids, alkyl sulfonic salts or tetraalkylammonium salts) in the mobile phase (Pryzynska *et al.* 2019).

Hydrophilic interaction chromatography is an alternative to RP separations of highly polar selenocompounds. In comparison with RP, HILIC mode showed higher and better separated signals, particularly for inorganic forms of Se and a shorter run when analysing onion extracts (Sentkowska and Pyrzynska 2018). The main advantage of HILIC in contrast to ion exchange separations is that the used mobile phases are compatible with the electrospray ion source therefore direct hyphenation can be carried out. This approach was first applied for yeast and yeast based food supplements analysis in the field of Se speciation (Dernovics and Lobinski 2008a, 2009).

SEC enables the separation of the compounds according to their hydrodynamic volume that is more or less proportional to their molecular mass and it can be tuned for the separation of low molecular mass Se species when low ionic strength SEC is addressed (Szpunar and Lobinski 2002, Encinar *et al.* 2003a). SEC usually is followed by a different separation, preferably orthogonally: even three-dimensional chromatography purifications have been used by the sequential application of SEC, anion and cation exchange separations for selenocompounds (McSheehy *et al.* 2002, Dernovics *et al.* 2007). Multidimensional HPLC separations are necessary not only because of the high number of selenocompounds present at low concentration in the samples but also to decrease matrix complexity (Szpunar and Lobinski 2002).

Molecular mass spectrometry based methods apply soft ionisation. In electrospray ion sources covalent and non-covalent bonds are usually preserved while during matrix-assisted laser desorption ionisation (MALDI) the covalent bonds are preserved and non-covalent bonds are often destroyed. Structural analysis and standardless identification of low molecular mass Se compounds is enabled by ESI (up to ~1000 Da) (Lobinski *et al.* 2006b). Casiot and coworkers (1999) were the first to successfully apply a generic approach where the purification of selenocompounds was monitored with ICP-MS prior to ESI-MS(/MS) identification.

The parallel coupling of ICP-MS and ESI-MS to chromatographic separation requires careful harmonisation, especially in terms of the solvent eluting into ion sources (Szpunar and Lobinski 2003). The purification and concentration of the fraction of a selenocompound detected by the ICP-MS may be necessary before ESI-

MS analysis, because of its high exposure to signal suppression events (McSheehy *et al.* 2002). The application of orthogonal separations and detections is mostly related to selenised yeast Se speciation in the literature (Lobinski *et al.* 2006a), but some examples for the application related to plants can also be found (Table 3).

Table 3. Application of orthogonal separation for Se speciation in plants.

Sample	Instrumentation	Identified compound(s)	Reference
Brassica juncea roots	IP-RP-HPLC-ICP-MS, SCX-HPLC-ICP-MS, ESI-QTOF-MS	*Se*-methyl selenomethionine	Grant *et al.* 2004
Allium fistulosum (green onion)	SEC-ICP-MS, IP-RP-HPLC-ICP-MS, ESI-Iontrap-MS	γ -glu-*Se*-(methylseleno)cysteine	Shah *et al.* 2004
Allium sativum (garlic)	SEC-ICP-MS, RP-HPLC-ICP-MS, ESI-QQQ-MS	γ -glu-*Se*-(methylseleno)cysteine	McSheehy *et al.* 2000
Phaseolus vulgaris vulgaris (green bean)	SAX-HPLC-ICP-MS, RP-HPLC-ICP-MS, RP-HPLC-ESI-TOF-MS, RP-HPLC-ESI-Orbitrap-MS	*Se*-(methyl)selenocysteine, γ -glu-*Se*-(methyl)selenocysteine	Shao *et al.* 2014
Lecythis minor (monkeypot nut) *Betholletia excelsa* (Brazil nut)	SEC-ICP-MS, SCX-HPLC-ICP-MS, IP-RP-HPLC-ICP-MS, RP-HPLC-ESI-QTOF-MS	Derivatives of SeMet, SeCys and selenohomocysteine, polyselenides	Németh *et al.* 2013
Allium sativum (garlic) *Helianthus annuus* sprouts (sunflower) *Raphanus sativus* sprouts (radish)	SAX-HPLC-ICP-MS, RP-HPLC-Orbitrap-MS	SeHLan, *Se*-(methylseleno)cysteine, SeMet, SeMetO, deaminohydroxy-SeHLan, *N*-acetylCys-SeMet, γ-glu-*Se*-(methylseleno)cysteine, methyl-seleno-*Se*-pentose-hexose, *Se*-methyl-selenoglutathione, 2,3-dihydroxy-propionyl-SeCys-Cys, methyltio-selenoglutathione and 2,3-dihydroxypropionyl-SeLan, 2,3-dihydroxypropionyl-SeCys-Cys-alanine	Ruszcynska *et al.* 2017
Lecythis minor (monkeypot nut)	SEC-ICP-MS, SCX-HPLC-ICP-MS, IP-RP-HPLC-ICP-MS, nanoRP-HPLC-ESI-QTOF-MS	SeCysta, γ -glu-SeCysta	Dernovics *et al.* 2007

3.2.3. Detection and basics of structural identification of selenocompounds by LC-ESI-MS and MS/MS

Apart from the evident option to search for previously reported selenium species with the help of a custom database, the detection of Se containing molecules in full scan ESI-MS spectra was first carried out by manual pattern exploration. Basically, the unique isotope distribution pattern of Se makes the detection of Se containing molecule possible (Figure 10).

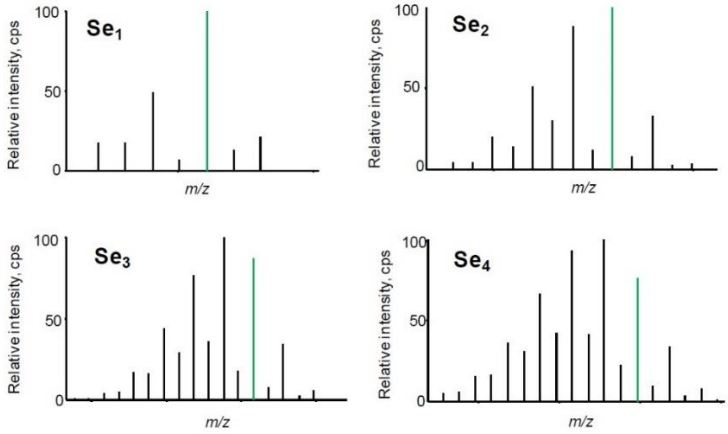

Figure 10. The characteristic isotopic distribution of Se containing compounds. The green isotopologues correspond to the monoisotopic mass (Németh 2015).

Successful visual seeking not only requires sufficient signal-to-noise (S/N) ratio (Dernovics *et al.* 2007) but adequate resolution to be able to unambiguously recognise the isotopic pattern of Se. In the case of low resolution (single or triple quadrupole) instruments the spotting of Se pattern was a difficult task, especially when real world samples were faced, as evidenced by a series of studies by McSheehy *et al.* (2000, 2001, 2002). Indeed, usually the characteristic ^{78}Se – ^{80}Se isotope ratio could only be spotted and a subsequent MS/MS step was required to prove the presence of a formerly reported selenium specific fragment, *e.g.*, selenohomocysteine. With the introduction of high resolution (HR) MS instruments, the possibility to look for the specific mass defect of selenium (for ^{80}Se: 79.9165 – 80 = -0.0835 amu) was an evident tool to detect Se containing molecules (García-Reyes *et al.* 2007). The mass defect feature, together with the specific isotopologue pattern, unambiguously pinpoints selenium carrying molecules – however, manual screening ("walking the chromatogram") is extremely time consuming and must be assisted with some kind of pre-filtering. However, when no software assistance is provided, such an approach is a must and calls for a personal experience to spot the mass defect carrying molecules in each full scan spectrum.

Software based pre-filtering can be based on the extraction of "diagnostic" (characteristic) Se-containing in-source fragments. These fragments are highly stable, carry an evident mass defect and their structure is known, which also determines their position in the final molecule. The most important in-source (or, as sometimes referred, ion-source) fragments on ^{80}Se are the two different SeHCys residue derived forms ($C_4H_8NO_2Se^+$ at *m/z* 181.97148 and $C_4H_{10}NO_2Se^+$ at *m/z* 183.98713), their derivatives after formic acid loss (especially from the first form, $C_3H_6NSe^+$ at *m/z* 135.96600), the selenocysteine derived fragment ($C_3H_6NO_2Se^+$ at *m/z* 167.95583), the NH_3-loss derived structure of *Se*-(methyl)selenocysteine ($C_4H_7O_2Se^+$ at *m/z* 166.96058) and the methyl-seleno group (CH_3Se^+ at *m/z* 94.93945) (Németh *et al.* 2013; Dernovics and Lobinski 2008b). Among these, the $C_4H_{10}NO_2Se^+$ fragment is highly specific to selenohomolanthionine, *Se*-(methyl)selenocysteine and their derivatives (Ogra *et al.* 2007, Dernovics *et al.* 2009), $C_3H_6NO_2Se^+$ to selenocysteine and its derivatives (McSheehy *et al.* 2000, 2002), while $C_4H_8NO_2Se^+$ is the least specific and therefore the most useful stable fragment to locate any compound that is derived from the highly central selenocysteine – selenomethionine pathway in selenium metabolism. Once a peak is obtained in the EIC of an in-source fragment, the full scan spectrum at the apex should be opened, the in-source fragment must be checked (whether it has been a false positive hit or not), and the parent molecule(s) should be looked for. If no hypothetic parent is found, the relevant ion source voltage setting (*e.g.*, "declustering potential", "cone voltage", "fragmentor voltage", etc.) should be decreased to give a rise to the potentially completely fragmented parent ion. Unfortunately, no useful selenised in-source fragment ions can be provided for negative ion mode measurements, which considerably hampers species spotting in the case of plant samples (Németh *et al.* 2013).

A semi-automated approach to detect selenium containing molecules, actually peptides, was published by McSheehy *et al.* (2005), taking advantage of automated peptide listing options of proteomic softwares. In case there is no ICP-MS assisted purification and enrichment of selenium containing peptides from the tryptic digest (*cf.* Encinar *et al.* 2003b), the sulphur and selenium analogues of the same peptides are present in the same sample to analyse with the RP-LC-ESI-MS proteomic setup. The search and fragmentation at + 48 amu masses related to automatically detected Met-containing peptides (regarding the + 48 amu as a variable /non-fixed/ modification of Met to arrive at SeMet) promote the detection and identification of peptides where SeMet was non-specifically built into the place of Met.

An attempt to automated screening for Se species was first developed by coupling an on-line 2D chromatographic system with parallel diode array UV, ICP-MS and linear trap-Orbitrap (ESI-MS^n) detection. The Metworks and Mass Frontier software (Thermo Fisher Scientific) enabled automatic isotopic pattern recognition in a full MS scan mode and structural identification based on the isotopic ratio, intra-isotope mass defect and the addition of a parent ion in the MS^3 target list (Preud'homme *et al.* 2012). Indeed, as no vendor independent (freeware) tools are available at the moment, analysts should explore the instrument derived software options whether they can be tuned to help to filter selenium containing species, *e.g.*, by modifying the widespread tool intended for detecting chlorine containing molecules. In such cases, the intra-isotope mass defect based ($^{37}Cl - {}^{35}Cl$ = 1.9970 amu) accurate mass filtering might be changed for $^{80}Se - {}^{78}Se$ (= 1.9992 amu), which can provide a considerable decrease in hits if applied with highly stable accurate mass measurements, even without taking into account isotopologue ratios.

Before the spread of LC-ESI-MS techniques the structural characterisation of selenocompounds was only possible with time and reagent consuming procedures. For example, the isolation and identification of two isomers of γ-glu-SeCysta from seeds of *Astragalus pectinatus* required long and solvent consuming extraction from more than 200 g sample, followed by resin chromatography, acid hydrolysis, amino acid analysis, derivatisation, paper electrophoresis, ninhidrin reaction, starch-iodide reaction, and Raney-Ni hydrogenolysis (Nigam and McConnell 1976). The application of LC-MS enables faster identification, however it must be noted that in modern organic chemistry, nuclear magnetic resonance (NMR) spectroscopy is the designated method for the definitive identification of compounds. The amount of the pure compound (~ 1-1.5 mg) required for NMR spectroscopy cannot often be extracted and purified from biological samples, therefore ESI-MS and ESI-MS/MS based identification might be adequate in selenium speciation in most cases.

Casiot *et al.* (1999) published the first ESI-MS based standardless identification of Se-metabolites in a yeast sample. The principle of the sulphur-selenium analogy could be followed as Se can incorporate into compounds instead of S resulting a +48 amu difference in the molecular mass. The compound at *m/z* 433 showing the characteristic Se isotope pattern was fragmented, resulting in two Se-containing fragments with masses of *m/z* 182 and 298 and in Se-free fragments of *m/z* 250 and 136. The hypothetic identity (*Se*-adenosyl-selenohomocysteine, AdoSeHCys) was confirmed through the fragmentation of its sulphur analogue standard (*S*-adenosyl-

homocysteine). Wrobel *et al.* (2002) assumed the S-Se analogy throughout the overall sulphur metabolic pathway and looked for selenoadenosylmethionine (AdoSeMet) as this compound should be the preceding compound leading to the synthesis of AdoSeHCys. Similarly, the identification was confirmed through the fragmentation of the sulphur analogue and also by a custom synthesised standard. Well, following the S metabolic pathway in the exploration of Se compounds can be successful mainly in case of stable compounds that are present at considerable concentration in the sample. For instance, cystathionine is another key compound in S metabolism and it is ubiquitous in all living organisms, however, its concentration is highly organism-dependent. The Se analogue SeCysta and its γ-glutamyl derivatives have been found in monkeypot nut following the S-Se analogy method (Dernovics *et al.* 2007).

The Met metabolism pathway towards *S*-methyl-5'-thioadenosine in the general Met salvage process has been also found to function in Se metabolism, as proven by the identification *Se*-methyl-5-selenoadenosine in *Hericium erinaceus* (lion's mane mushroom; Egressy-Molnár *et al.* 2016). Species of Allium family are known to possess remarkable S metabolism; Se-rich garlic was found to contain mainly γ-glu-MeSeCys which has been graded as one of the main compound for Se deposition in Se accumulator plants (Larsen *et al.* 2006).

Active metabolites with disulfide bonds naturally play roles in the metabolism of cells in the glutathionine cycle. However, the *ex vivo* formation of compounds with Se-S bond has also been associated with oxidation processes due to, *e.g.*, long storage (Uden *et al.* 2004). The presence of glutathionine S-conjugates with selenocompounds in yeast was reported first time by McSheehy *et al.* (2001). After the reduction of the detected selenocompounds glutathione and selenium-containing moieties could be partly identified with low mass resolution MS. HR MS data and MS/MS fragmentation allowed for the ultimate identification of conjugates of glutathionine with Se-glutathionine and glutathione with a methylseleno group through Se-S bridges (Infante *et al.* 2006). Similarly, the search for free thiol and selenol containing building block moieties (including glutamyl/seleno/cysteine or /seleno/cysteinylglycine among others) offers an effective tool in the exploration of Se-S(e) conjugates: the application of this strategy, together with the assignment of the *m/z* 167.96 in-source fragment referring to SeCys allowed for the identification of a series of conjugated (seleno)glutathione and 2,3-dihydroxy-propionyl-L-(seleno)cysteine derivatives (Dernovics and Lobinski 2008b). This latter, previously unreported moiety was confirmed by chemical synthesis as well (Egressy-Molnár *et al.* 2014). The same

"building block" identification methodology allowed for the detection of 19 Se-S(e) bond containing compounds in yeast samples by Gil Casal *et al.* (2010). Theoretical and experimental masses, isotopic patterns, empiric formulas and proposed structures of two newly detected selenocompounds are shown in Figure 11 as examples.

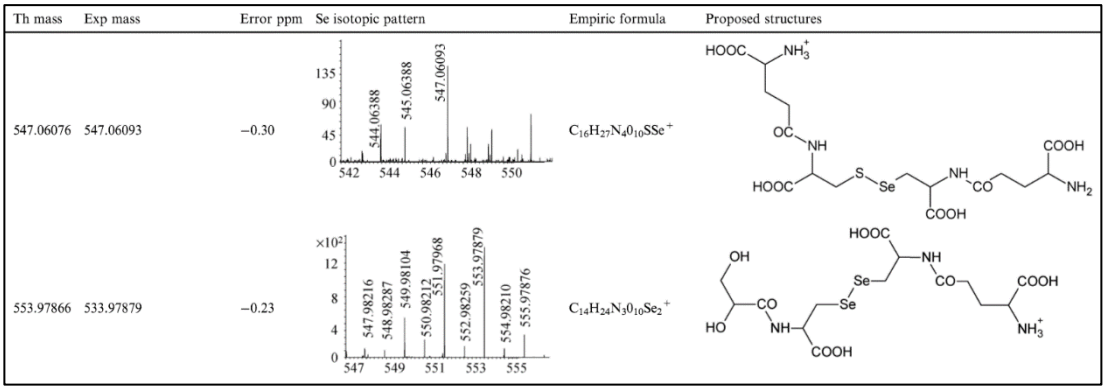

Figure 11. Two new selenocompounds detected by Gil Casal *et al.* (2010).

Taking into account the chromatographic behaviour of unknown selenium species might contribute to successful structural elucidation. MS/MS fragmentation of a Se compound detected at *m/z* 360.057 in *H. erinaceus* indicated the losses of adenosyl, adenine and ribose groups which fragments could relate to two possible structures: *Se*-ethyl-5-selenoadenosine and *Se*-dimethyl-5-selenonium-adenosine. Taking into account that the retention of the compound was close to the void on an RP column, an ethyl group containing compound should have eluted later, so this structure was excluded and the compound was assigned as *Se*-dimethyl-5-selenonium-adenosine (Egressy-Molnár *et al.* 2016). Similarly, the addition of a functional group to a detected compound appears not only in the *m/z* value but can considerably change the hydrophobicity of the compound as well. The addition of a hydroxyl group to geranyl-SeHCys contributed to a less hydrophobic character and therefore showed shorter retention time on an RP column while in the case of an additional carboxyl group the retention showed higher hydrophobicity compared to the hydroxyl group possessing compound (Németh *et al.* 2013).

Finally, when neither preconception nor additional information (*e.g.*, glutathione related structure) is available on an unknown selenium species, the following general steps might be taken to arrive at a possible structure on the basis of LC-HR-MS/(MS) data:

a) elemental composition should be determined for the parent and for the at least medium intensity fragments as well, taking into account the number of participating selenium atoms (dedicated from the isotopologue pattern);
b) in-source and MS/MS fragments should be matched to decide whether co-eluting selenium species are present;
c) fragments arriving from co-fragmented isotopologues of the parent ion (*e.g.*, from ^{78}Se or ^{82}Se) should be clearly assigned;
d) characteristic (diagnostic) fragments should be searched for, especially selenium containing ones, in the low abundance section of the MS/MS spectra;
e) characteristic losses (*e.g.*, hexose /-162.05 Da/, formic acid /-46.00 Da/, water /-18.01 Da/, ammonia /-17.03 Da/, ^{80}Se /-79.92 Da/) should be checked;
f) fragments completing each other to the parent mass should be looked for;
g) structure elucidation might be started at the characteristic selenium fragments with the following notes: (i) fragmentation often occurs at both sides of selenoethers that might stabilise either as $R\text{-}Se^+$ or $R\text{-}SeH_2^+$; (ii) free selenols (-R-SeH) should not be accounted for neither in MS, nor under MS/MS conditions; (iii) Se-S(e) bridges hardly dissociate in positive ion mode fragmentation;
h) in case of low abundance, looking for and fragmenting a surrogating higher intense sulphur analogue might provide additional information.

3.3. QUANTIFICATION WITHOUT AUTHENTIC STANDARDS

3.3.1. Background

LC based quantification procedures usually require authentic standards that can be applied with different calibration protocols: external-, matrix matched calibration or standard addition. Unfortunately, lots of compounds are not commercially available in the form of standards due to their instability, low consumer demand, low natural concentration or when the extraction/purification from natural sources or the synthesis is expensive. Besides purchasing costs, there are several further problematic issues regarding the handling of standards: limited shelf life, cost of storage (*e.g.*, -80 °C), administrative costs, introduction of standard deviation and biases during the

preparation of calibration solutions (*e.g.*, components missing from a multi-component calibration), *etc*. Also, the separate handling of standards might be also required when they are incompatible (*e.g.*, selenate oxidises selenite). Definitely, there are numerous cases in (bio)analytical studies when quantification must be carried out with a limited number of standards. In such situations, several analytical approaches might be addressed.

3.3.2. Making uniform analytes: general aspects

Adequate solution may be provided by the reduction of the number of target compounds. It is possible that the required information can be gained by summing the target compounds when their individual concentration is not important. For example, this is the case for vitamin C and dehydroascorbic acid (DHAA): they both have the same vitamin effect. A former (out-of-date) European Standard specifying a method for the determination of vitamin C in foodstuffs (EN 14130:2003) prescribed the reduction of DHAA, thus making a uniform analyte (vitamin C) from the two compounds. However, such protocol cannot be followed if the goal is the monitoring of degradation of vitamin C, *e.g.*, in foodstuffs during heat treatments (Xanthakis *et al.* 2018). Anyhow, making uniform analytes is an established approach and it is presented with examples as follows.

3.3.2.1. Making uniform analytes for LC-ultraviolet and fluorescence detections through sample preparation and/or methodology

If a compound can exist both in reduced and oxidised forms, making one uniform analyte (one state) facilitates the quantification. In case of coenzyme Q10 (CoQ10) the application of an oxidizing agent drives the equilibrium to the fully oxidised state and total CoQ10 can be determined with LC-ultraviolet (UV) spectroscopy at 275 nm (Orozco *et al.* 2007).

Another situation is where the analytes differ in a functional group or in a moiety from each other. Steviol glycosides are often determined with UV absorbance with external calibration; however, there can be dozens of glycosides present in a sweetener mixture that are not available in the form of standards. This approach doesn’t take into account that principally non-UV chromophore aglycon side chains also influence the spectra besides the common aglycone moiety (JECFA 2010). Therefore, uniform

analytes can be prepared through the hydrolysis of the glycosyl chains, resulting in the common aglycone molecule, steviol (Bartholomees *et al.* 2016).

Quantification of vitamin B_9 content in foods also requires uniform analytes due to the presence of several vitamers. Enzymatic hydrolysis is applied for the conversion of folates and polyglutamate folates into monoglutamates, while 10-formyl-tetrahydrofolate (THF) is converted to 5-formyl-THF with a heat treatment to efficiently reduce the number of structures for analysis (Quinlivan *et al.* 2006). Similarly, acidic hydrolysis breaks the glycoside bonds in flavonoid glycosides which allows for their quantification in vegetables and fruits through their aglycones (Wach *et al.* 2007).

3.3.2.2. Making uniform analytes through LC-ESI-QQQ methodology

As indicated above, the quantification of flavonoids is a challenging task: with thousands of glycosylated flavonoids, there have not been and never will be standards for most compounds, which makes the identification very difficult as well. Although, the hyphenation of LC with a diode-array detector (DAD) and mass spectrometry (MS) also can provide a solution (Harnly *et al.* 2007). Retention time, wavelengths of maximal UV/VIS absorbance, molecular mass and fragmentation pattern allow for the structural characterisation of flavonoid compounds whereas the quantification is based on the UV signal from the structurally closest matching available standard (Lin *et al.* 2007). An elegant example of this comprehensive approach was published by Abrankó *et al.* (2015): the authors could quantify a novel, tentatively identified genisteine-hexoside in cherry samples with the calibration equation of genistin using the UV signal at 260 nm. To achieve this, the novel compound had to be proven a part of the genistein-derived flavonoids, which was made by in-source fragmentation and high resolution (TOF) mass spectrometric data as well.

3.3.3. Solutions with LC-ICP-MS; Part 1

While signal intensity is considered to be independent from the matrix in UV measurements, the analyte signal in MS is influenced by several factors, *e.g.*, the eluent and the coeluting matrix components. When there is no authentic standard available, these effects should be considerably reduced or making compromises is needed.

In metallomics studies where some standards are available, unknowns might be quantified by using the closest eluting standard: Sloth *et al.* (2004) assumed that the

LC-ICP-MS setup would show similar matrix effects for the arsenic species eluting close to each other in a short retention time window (*i.e.*, with similar HPLC eluent composition), therefore the instrumental sensitivity for these arsenicals should be quite similar. However sample derived matrix effects cannot be evidently monitored/ruled out (especially when non-UV chromophore compounds are eluting, *e.g.*, sugars), but the monoisotopic feature of arsenic considerably decreases the number of quantification possibilities. Another possibility is the application of low flow rates on microbore (capillary, nano) columns together with isocratic separation: this combination increases the stability of the ICP-MS plasma in time, removes eluent-derived changes in sensitivity, and this way, calibration can be carried out with only one authentic standard (Far *et al.* 2010).

In case isocratic separation is not an option, and gradient separation is a must, different methods should be addressed. Indeed, constant elemental response can be a requirement for the absolute quantification with LC-ICP-MS but the increasing ratio of organic solvents in RP gradient separations influences the ionisation efficiency of certain elements in ICP either in negative (signal suppression) or in positive (carbon charge effect) manner. In the study of Pröfrock and Prange (2009), counter-current compensation was applied: the gradient separation was carried out on the analytical column, while a second matched reversed gradient was post-column mixed before entering the pooled flow into the ICP-MS. Another approach was published by Moller *et al.* (2005): the modification of the LC eluent prior to the ICP plasma was made by the use of a membrane desolvation system to remove a considerable part of the organic solvent from the eluent. However the desolvator system had to be individually optimised for each analysed element and the species independent sensitivity was lost for selenium compounds, the method was successfully validated for platinum compounds.

The most recent approach to achieve constant signal response factors has been published by Spanish scientists. Calderon-Celis *et al.* (2018, 2019) developed and optimised a method for six elements (S, P, As, Se, Br, I) with the help of CH_4 or CO_2 addition to the plasma following capillary LC (that is, low flow rate, < 5 µL min^{-1}) based separation. The so-called carbon saturation technique adds an adequately high amount of carbon in the plasma to reach special ICP conditions where neither the LC eluents, nor the matrix constituents, nor species dependent ionisation efficiency can significantly change elemental response factors. This approach also has the advantage that no additional instrumentation is needed.

3.3.4. Possibilities in LC-ICP-MS Part 2: isotope dilution

Isotope dilution analysis (IDA) has been widely used for quantification purposes both with standalone ICP-MS and together with LC hyphenation. The technique is based on the measurement of isotope ratios in samples where the isotopic composition has been altered by the addition of a known amount of an isotopically enriched standard. The method has excellent precision and accuracy because signal influencing factors equally affect isotope signals, therefore their ratios remain unchanged. Only a few disadvantages can be listed about this technique: it can be used only for stable multi-isotopic elements, additional equipment and software tools are required (however, none of them calls for extraordinary investments), and the isotopically enriched standards might not be easily available commercially (Fassett and Paulsen 1989).

When it comes to LC-IDA-ICP-MS, basically two approaches have been used. Species-specific IDA requires the isotopically labelled (molecular) entity of the compound to be analysed in the form of standards, which have far lower commercial availability than the related standards with normal isotope distribution. However this method can offer highly accurate and unbiased quantification due to the compensation of extraction efficiency losses, analyte decomposition and on-column analyte loss, only a few compounds can be purchased directly (that is, methyl-$^{198/199/201}$Hg, mono/di/tributyl-^{119}Sn and ^{76}Se-selenomethionine), which acts as a real bottleneck in the application of this approach. On the other hand, the so-called species-unspecific spiking mode enables the quantification of structurally unknown compounds or when standard is not commercially available. The addition of the isotope spike is carried out after the separation in the form of post-column spiking and the spike with a known isotopic distribution exists in a chemical form that is different from that of the species. If the standard is in solution form, the isotope distribution is given on the certificate, while if the standard is solid the exact isotope distribution must be determined through isotope dilution, which is called reverse isotope dilution and it involves a standard with natural isotopic composition. This type of spiking mode does not correct for any error occurring during sample preparation or separation and corrects only for errors derived from instrumental instabilities and matrix effects (Rodríguez-González *et al.* 2005).

The first species-unspecific isotope dilution analysis was carried out in 1994 by Rottmann and Heumann; the schematic overview of their instrumental set-up is shown in Figure 12.

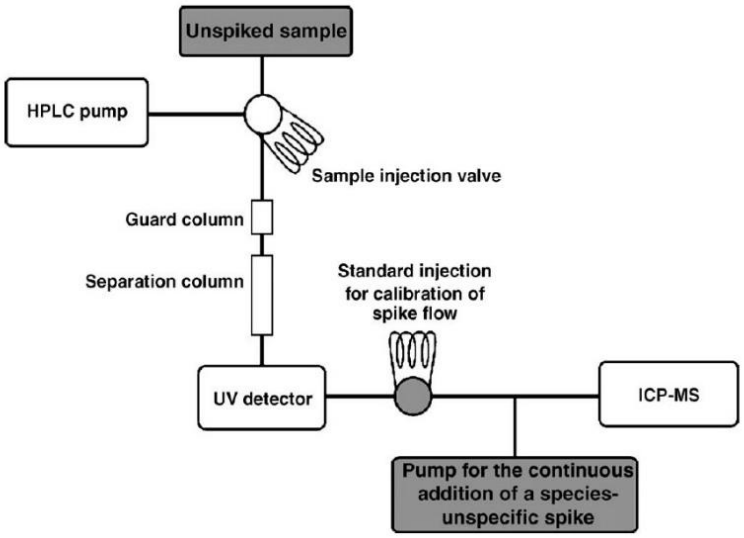

Figure 12. Schematic diagram of a species-unspecific isotope dilution analysis set-up by HPLC-ICP-MS
(Rottmann and Heumann 1994, Rodríguez-González *et al.* 2005).

This on-line isotope dilution technique relies on the plotting of the mass flow *vs.* retention time. The mass flow is calculated by measuring the corresponding isotope ratio throughout the whole chromatographic run, then the peaks detected have to be integrated and normalised to the injection volume to obtain final concentration data.

Elemental isotope dilution analysis can be performed only if at least two isotopes can be measured free of spectral interferences. There are several ways to eliminate spectral interferences, like the use of double focusing HR-ICP-MS or addressing quadrupole analysers combined with collision and dynamic reaction cells (Reyes *et al.* 2003a). Isobaric interferences and polyatomic interferences from the sample matrix can be eliminated during the chromatographic separation or mathematical corrections can be applied. Moreover, the signal intensities must be corrected with the dead time of the detector, which is usually done automatically by the instrument, and the mass bias which is caused by the phenomenon that heavier isotopes are transmitted more efficiently than lighter isotopes into the MS part from the ICP (Rodríguez-González *et al.* 2005).

The application of IDA in Se studies is a powerful tool for quantification as the number of commercially available standard is especially limited. The most abundant Se isotopes are affected by the presence of Ar dimer ions in ICP-MS, which can be eliminated by the introduction of He, H_2, O_2, NH_3 or CH_4 in collision/reaction cells. In the case of H_2, the SeH^+ and BrH^+ formation requires mathematically correction as

well (Huerta *et al.* 2003). Examples about the application of IDA in Se studies are shown in Table 4.

Isotope pattern deconvolution (IPD) is a more recent method of calculation and it is based on the determination of the molar fractions for each pure isotope pattern (natural abundance or labeled) contributing to the isotope pattern observed in the mixture of natural (native) and labeled analytes (added) by multiple linear regression. This approach has been applied also for Se studies (Rodríguez-Castrillón *et al.* 2008, Castillo *et al.* 2013).

Table 4. IDA applications for quantifications in Se studies.

Type of spiking	Instrumentation	Sample(s)	Quantified compounds	Enriched isotope in spike	Isotope ratio used for calculation	Reference
species-specific	RP-HPLC-ICP-MS	human serum	SeMet, $SeCys_2$*	^{77}SeMet	77/80	Encinar *et al.* 2004
species-unspecific	Affinity HPLC-ICP-MS	human serum	selenoprotein P, albumin, glutathione peroxidase	^{77}Se	78/77 80/77	Reyes *et al.* 2003b
species-unspecific	IP-RP-HPLC-ICP-MS	wheat, triticale, flour, wheat biscuits	SeMet, SeMetO	^{76}Se	76/78	Kirby *et al.* 2008
species-unspecifc	SAX-HPLC-ICP-MS	yeast, wheat flour	yeast: SeMet, Se(IV) wheat flour: SeMet	^{77}Se	78/77	Huerta *et al.* 2003
species-specific species-unspecific	SAX-HPLC-ICP-MS	certified reference materials, skimmed powdered milk, wheat flour, enriched yeast	SeMet	^{76}SeMet ^{77}Se	77/76 78/76 78/77	Krata *et al.* 2008
species specific double IDA	RP-HPLC-ICP-MS	garlic	γ -glu-MeSeCys	^{77}γ -glu-MeSeCys	78/77 82/77	Infante *et al.* 2008
species-unspecific	2D SEC-AF-HPLC-ICP-MS	mouse plasma	selenoprotein P, extracellular glutathione peroxidase, selenoalbumin, seleno-metabolites	^{74}Se	78/74	García-Sevillano *et al.* 2014

* The accurately determined SeMet was used as an internal standard for $SeCys_2$ quantification

4. EXPERIMENTAL

4.1. INVESTIGATION OF SELENOMETABOLITES IN *CARDAMINE VIOLIFOLIA*

4.1.1. Reagents and samples

Heptafluorobutyric acid (HFBA; ≥99%), sodium borohydride (≥98%), *Se*-(methyl)selenocysteine hydrochloride (≥95%), D,L-lanthionine (≥98%), L-selenocystine (95%) and formic acid (~98% for MS) were supplied by the Merck-Sigma group (Schnelldorf, Germany). Deionised water (18.2MΩ cm) was obtained from a Millipore purification system (Merck-Millipore; Darmstadt, Germany). Acetonitrile (Super Gradient Grade, UPLC-MS grade), and sodium sulphite (98%) and formic acid (~98%) were supplied by VWR (Radnor, Pennsylvania, USA), while carbon disulphide (extra pure), hydrochloric acid (37%), sodium selenite pentahydrate (≥99%), ammonia solution (25%), Pronase E (4,000,000 PU g^{-1}), hydrogen peroxide (a.r. 30 m/m%), the 1.000 g/l standards of S, Se and Rh were obtained from Merck. Nitric acid (a.r., 65≥m/m%), formic acid (98–100%, used for liquid chromatographic purposes) and acetic acid (100%) were purchased from Scharlau (Barcelona, Spain). Ethanol (96%), Tris(hydroxymethyl)aminomethane (a.r.) and ammonium acetate (> 99%) were supplied by Reanal (Budapest, Hungary). Methanol (HPLC Gradient Grade), pyridine (99.5%) and D,L-dithiothreitol (≥98%) were obtained from Fisher Scientific (Loughborough, UK). β-Chloro-L-alanine (98%) was purchased from Santa Cruz Biotechnology (Dallas, USA), L-selenomethionine (99+%) was obtained from Acros Organics (Geel, Belgium). Certified ^{82}Se isotopic abundance solution (10 µg mL^{-1} ^{82}Se in 5% nitric acid) was bought from Inorganic Ventures (Christiansburg, VA, USA).

Cardamine violifolia was identified and registered by the Wuhan Botanical Garden (Chinese Academy of Sciences; Wuhan, China). Pooled sample of stems and leaves was harvested in the springtime of 2016 in the natural seleniferous region Yutangba, Enshi (Hubei Province, China). Leaves and root samples of *C. violifolia* were collected separately in the springtime of 2017. Plant biomass was cleaned with deionised water, lyophilised and milled.

4.1.2. Selenium distribution in *C. violifolia*

4.1.2.1. Total selenium and sulphur determination

Total selenium and sulphur concentrations were determined after acidic digestion. Microwave digestion of the samples, the extraction residues and aliquots of extraction solutions was carried out in a CEM Mars-5 digestion system (CEM; Matthews, NC, USA). Samples (50 mg *C. violifolia*; entire extraction residues; 1.0–2.0 mL aliquots) were mixed with 5.0 mL HNO_3 in polytetrafluorethylene (PTFE) digestion tubes and after 24 h 3.0 mL H_2O_2 was added prior to the microwave digestion process. The pressure was raised to 250 psi over 20 min and held for 15 min.

Total Se concentration was determined with an Agilent 7500ce ICP-MS (Agilent Technologies, Santa Clara, CA, USA) on the ^{77}Se and ^{82}Se isotopes by the method of standard addition using rhodium (^{103}Rh) as an internal standard.

Total S concentration was determined with a Perkin Elmer Optima 8000 ICP-OES instrument (Waltham, MA, USA) with external calibration at the wavelengths of 180.669, 181.975, 182.037 and 182.563 nm.

4.1.2.2. Sequential extraction procedure

Sequential extraction protocol was adapted from Mounicou *et al.* (2009):

1. Water extraction: 200 mg of the *C. violifolia* sample was extracted with an ultrasonic probe (UP100H, Hielscher Ultrasound Technology, Teltow, Germany) at ambient temperature. Extraction was carried out with sonication in two steps: first in 6.0 mL deionised water for 2×1 min then with 3.0 mL deionised water for 2×1 min. Supernatants were recovered by centrifugation (30 min at 4000*g*), then they were pooled and filled up to 10.0 mL. This procedure was carried out in six replicates.

2. Extraction with sulphite: 5.0 mL of 1.0 M Na_2SO_3 was added to the water insoluble residue; the sample was vortexed and shaken in an orbital shaker at 180 1 min^{-1} for 24 h at 37 °C. Supernatants and residues were separated by centrifugation (30 min at 4000*g*). The residues were washed with 4.0 mL deionised water and the relevant supernatants (Na_2SO_3 and water) were pooled and made up to 10.0 mL with deionised water. This procedure was carried out in three replicates.

3. CS_2 extraction: this procedure was carried out with the three residues obtained after the sulphite extraction. First, 2.0 mL deionised water was added to the residues that were afterwards vortexed, then 4.0 mL CS_2 was added, followed again by vortexing and incubating for 4 h. The mixture was hand-shaken regularly in 20-min

intervals. Afterwards the samples were centrifuged (10 min at 4000*g*) and three phases were separated: the upper water phase, the plant tissue debris and the CS_2-containing layer. These three phases were treated separately: the CS_2 phase was evaporated at room temperature and the dried-in residue was digested, while the plant debris and the water phase were digested as they were, without evaporation. The selenium content of the extracts and phases was determined by ICP-MS following the HNO_3-H_2O_2 digestion procedure.

4.1.3. Identification of selenocompounds in *C. violifolia*

4.1.3.1. Extractions

Selenium speciation experiments were carried out from the water extract and from the enzymatic extract of the sample:

- 250 mg of lyophilised and pooled plant material (stems + leaves) was enzymatically digested according to the method described by Shao *et al.* (2014) with Pronase E in two subsequent steps in Tris-buffered medium. Supernatant arising from the treatments was decanted and made up to 10.0 mL with deionised water in a volumetric flask and filtered through 0.45 μm PTFE disposable syringe filters. The entire sample preparation was executed in three replicates.
- 250 mg of lyophilised and pooled plant material (stems + leaves) was extracted with an ultrasonic probe (UP100H) with 10.0 mL deionised water for 2x1min. Supernatant was recovered by centrifugation (10 min 4000*g*) and 5 mL was lyophilised, dissolved, filtered through a 0.45 μm cellulose acetate syringe filter and diluted with eluent buffer applied in the corresponding chromatography.
- 50 mg of the *C. violifolia* leaf sample was extracted with an ultrasonic probe (UP100H) at ambient temperature with 10.0 mL deionised water for 1 min. Supernatant was recovered by centrifugation (10 min at 4000*g*, filtered (0.45 μm, cellulose acetate syringe filter) and lyophilised in 2.225 mL aliquots.

4.1.3.2. LC-ICP-MS set-ups (SAX, SCX and IP-RP)

All strong anion exchange, strong cation exchange and ion-pairing reversed phase chromatography set-ups were achieved with an Agilent 1200 HPLC system connected to an Agilent 7500cs ICP-MS for element-specific detection of ^{77}Se, ^{82}Se and ^{88}Sr. In the case of IP-RP hyphenation, oxygen (40 mL min^{-1}) was used as optional gas. The applied columns and chromatographic conditions are presented in Table 5.

Selenite was quantified with SAX, while *Se*-(methyl)selenocysteine was quantified with IP-RP, both through the method of three-point standard addition.

Table 5. Chromatographic conditions for LC-ICP-MS set-ups.

Column	Flow rate	Eluent A	Eluent B	Gradient program	Injection volume
SAX: PRP-X100 (250mm×4.1mm× 10 μm; Hamilton, Reno, NV, USA)	1.5 mL min^{-1}	10 mM ammonium acetate buffer pH=6	250 mM ammonium acetate buffer pH=6	0-5 min 100%A 5-20 min up to 40% B 20-22min up to 100% B 22-25 min 100 % B 25-26 min down to 0%B 26-31 min 0% B	100 μL
SCX: Zorbax 300 (150mm×4.6mm× 5 μm, Agilent)	1.2 mL min^{-1}	1 mM pyridine formate buffer pH=2.2	40 mM pyridine formate buffer pH=2.2	0-2 min 100% A 2-15 min up to 30% B 15-16 min up to 100% B 16-20 min 100% B 20-21 min 100% A	5/10 μL
IP-RP: XTerra MS-C_{18} (250mm×4.6mm× 5 μm; Waters, Milford, MA, USA)	0.6 mL min^{-1}	deionised water with 0.05 v/v% HFBA	methanol with 0.05 v/v% HFBA	0-2 min 5% B 2-10 min up to 65% B 10-15 min 65% B 15-16 min down to 5% B 16-22 min 5 % B	25 μL

4.1.3.3. LC-ESI-QTOF-MS set-up

For the HPLC-ESI-MS experiments, a 6530 Accurate Mass ESI-QTOF-MS system (Agilent) equipped with an Agilent 6220 derived dual ion spray source was applied. Chromatographic elution was provided by an Agilent 1200 HPLC system using a Zorbax XDB C_{18} RP HPLC column (50 mm × 2.1 mm × 3.5 μm; Agilent). Isocratic elution with deionised water containing 5 v/v% acetonitrile and 0.1 v/v% formic acid was carried out at the flow rate of 0.35 mL min^{-1}. ESI ion source was used in positive ionisation mode. The default fragmentor voltage was 170 V in MS and 145 V in MS/MS experiments. Other related instrumental parameters are shown in the appendix (Table A1).

4.1.3.4. LC-Unispray-QTOF-MS set-up

A Vion ion mobility QTOF-MS (Waters) equipped with a UniSpray (Waters) ion spray source was applied coupled to an Acquity UPLC I-Class system (Waters) using a BEH-C_{18} RP UPLC column (100 mm × 2.1 mm × 1.7 µm; Waters). Deionised water with 0.1 v/v% formic acid (A) and acetonitrile with 0.1 v/v% formic acid (B) were used as mobile phase at the flow rate of 0.4 mL min^{-1}. The column was kept at 25 °C. Gradient elution program was applied as follows: 0-1 min 10% B, 1-4 min up to 80% B, 4-4.5 min 80% B, 4.5-5 min down to 10% B, 5-7 min 10% B. UniSpray ion source was used both in positive and negative ionisation modes either in MS^E or MS^E → MSMS functions. Related instrumental parameters are described in the appendix (Table A2). Data evaluation was carried out with the help of the Unifi software (version 1.9.4; Waters).

Mass defect based Se species filtering was carried out in the frame of an iterative approach. Default settings (mass padding: 15 Da; defect padding: 40 mDa; isotope defect: ^{80}Se-^{78}Se; minimal compound response: 2000 counts) were tested whether they allowed for the detection of known Se species (selenolanthionine and selenocystathionine among others) that had been detected in the fractions by database derived searching. Afterwards, the list of Se species was step-by-step completed with newly detected species resulting from the in-source selenohomocysteine fragment search (*m/z* 135.9660 /$C_3H_6NSe^+$/ and 181.9715 /$C_4H_8O_2NSe^+$/) and from the manual Se isotopologue pattern searching processes; with these, the mass padding and defect padding settings were recursively tuned to include the newly introduced species in the result list. After each tuning step, the updated mass defect based Se species filtering was run on the LC-QTOF-MS data to look for still undiscovered selenium species that met the actual search settings. All positive hits were manually checked and individually validated to remove false positives.

4.1.4. Synthesis of selenolanthionine

4.1.4.1. Chemical synthesis

The chemical synthesis of selenolanthionine was based on a modified procedure originally described by Block *et al.* (2001). 200 mg L-selenocystine was suspended in 5 mL ethanol under argon atmosphere and 100 mg solid $NaBH_4$ was added. The solution was refluxed for 20 min then an additional volume of ethanol (5 mL) was added and the solution was refluxed for further 20 min. 150 mg β-chloro-L-alanine was added to the still yellowish solution that was refluxed for 10 min and cooled to room temperature. The resulting suspension was filtered, the solid residue was dried and dissolved in 0.1 M HCl solution.

4.1.4.2. Chromatographic purification – analytical scale

Prior to SCX-ICP-MS analysis and purification the synthesised mixture was dissolved to a concentration 12.5 mg mL^{-1} in MQ water with 10% HCOOH and 500-fold diluted with pyridine formate (1 mM, buffer A for SCX), filtered through a 0.45 μm cellulose acetate filter and injected onto the SCX-ICP-MS chromatographic set-up. The same chromatographic conditions were used as described in Table 5. The amount of residual L-selenocystine was quantified using the method of three-point standard addition to estimate the yield of selenolanthionine synthesis. The peak corresponding to selenolanthionine was fractionated (50×), pooled and lyophilised.

4.1.4.3. Chromatographic purification – semi-preparative scale

Preparative chromatographic purification was needed to yield higher amount of pure selenolanthionine for recording XANES spectra. Synthesised mixture was dissolved in 0.1 M HCl to the concentration of 10 mg mL^{-1}. A Luna strong cation exchange column (250 mm × 10 mm × 10 μm; Phenomenex, Torrance, CA, USA) was used with gradient elution using pyridine formate eluent (pH 3.55; buffer A: 1 mM; buffer B: 40 mM). The optimised program was as follows: 0–15 min from 0% up to 30% B (2.5 mL min^{-1}), 15.1–16 min up to 100% B (2.5 mL min^{-1}), 16.1–17 min 100% B (3.0 mL min^{-1}), 17.1–17.5 min down to 0% B (3.0 mL min^{-1}), 17.6–25.9 min 0% B (3.0 mL min^{-1}), 25.9–26 min 0% B (2.5 mL min^{-1}). Injection volume was 10 μL. The peak corresponding to selenolanthionine was collected from 20 subsequent runs, pooled and lyophilised.

4.1.5. Quantification procedures

4.1.5.1. Quantification of selenolanthionine standard

In order to determine the approximate concentration of the synthesised selenolanthionine, an isocratic SCX method was applied with a three-point standard addition of *Se*-(methyl)selenocysteine as the closest eluting Se species, according to a method introduced by Sloth *et al.* (2004) for arsenic speciation. The chromatographic system was identical as described above for the SCX-ICP-MS analyses; the eluent was 1 mM pyridine formate (pH 2.2; 0–5 min).

4.1.5.2. Quantification of lanthionine and selenolanthionine with LC-ESI-QQQ-MS

A QTRAP3200 triple quadrupole-linear ion trap mass spectrometer (Applied Biosystems/Sciex; Foster City, CA, USA) was applied in MRM (multiple reaction monitoring) mode. The instrument was coupled to an Agilent 1100 series HPLC set-up using a Luna HILIC 200 Å (150 mm × 4.6 mm × 5 μm; Phenomenex) HPLC column. For the gradient elution method, the mobile phase consisted of 98:1:1 v/v% deionised water/formic acid/acetonitrile (eluent A) and 98:1:1 v/v% acetonitrile/formic acid/deionised water (eluent B). The flow rate was 0.8 mL min^{-1} and the gradient elution was performed as follows: 0–1 min 10% A, 1–10 min linear gradient up to 90% A, 10–11 min 90% A, 11–12 min linear gradient down to 10% A, 12–20 min 10% A. The injection volume was 5 μL and the column was kept at 25 °C.

The instrument was optimised in positive MRM mode for lanthionine (Lan) and selenolanthionine by introducing a 2 mg mL^{-1} stock solution of each compound containing acetonitrile/water/formic acid (60:39:1; v/v%) with the help of a syringe pump at the flow rate of 10 μL min^{-1}. Lanthionine was monitored with the precursor ion set at *m/z* 209, while the transitions were set for 209/74, 209/120, and 209/146, with the quantifier product ion at *m/z* 120. The precursor ion for selenolanthionine was set to *m/z* 257 for the transitions at 257/168, 257/140, and 257/74, showing the most intensive (quantifier) product ion at *m/z* 168. The optimal parameters and other related instrumental data are described in the appendix (Table A3).

4.1.5.3. Quantification of selenolanthionine with isotope dilution analysis (IDA)

HPLC-ICP-MS set up was achieved by using an Agilent 1200 HPLC system connected to an Agilent 7500cs ICP-MS for the element-specific detection of ^{76}Se,

^{77}Se, ^{78}Se, ^{79}Br, ^{80}Se, ^{81}Br, ^{82}Se and ^{83}Kr. H_2 was used as collision/reaction gas in the flow rate of 2.5 mL min^{-1} and oxygen (40 mL min^{-1}) as optional gas.

XTerra MS-C_{18} (250 mm × 4.6 mm × 5 µm; Waters) column was used. The mobile phase consisted of deionised water (eluent A) and methanol (eluent B) both containing 0.1 v/v% HFBA. The flow rate was 0.6 mL min^{-1} and the gradient elution program was: 0–2 min, 5% B; 2–10 min, up to 65% B; 10–15 min, 65% B; 15–16 min, down to 5% B; 16–19 min 5% B. Injection volume was 40 µL.

The outlet of the RP column was connected through a T-piece where the ^{82}Se standard solution was continuously added in the concentration of 20 ng g^{-1} in 0.1% nitric acid with a flow rate of 0.1 mL min^{-1} with the help of a peristaltic pump. Mass bias was determined with the repeated injections of 20 µL of *Se*-(methyl)selenocysteine standard solution (0.5 mg L^{-1} as Se) and correction was carried out using the exponential approach (Reyes *et al.* 2003, Rodriguez-González *et al.* 2005). Dead time correction was automatically carried out by the instrument.

Second aliquot of the lyophilised water extract of *C. violifolia* leaf sample was dissolved in 2 mL deionised water, diluted 15x with deionised water containing 0.1 v/v% HFBA. Sample injection volume was 40 µL. IDA calculations were based on the equations published by Koellensperger *et al.* 2003:

$$M_x(t) = M_y(t) \times \frac{R_y - R_b\,(t)}{R_b\,(t) - R_x} \times \frac{h_{iy}}{h_{ix}} - M_y(t) \times \frac{R_y - R_{bblank}\,(t)}{R_{bblank}\,(t) - R_x} \times \frac{h_{iy}}{h_{ix}}$$

where:

M_x: mass flow of the analyte (ng min^{-1});

M_y: mass flow of the spike (ng min^{-1});

R_y: corresponding isotope ratio in the isotopically enriched spike standard solution (certificate);

R_x: corresponding natural isotope ratio;

R_b: measured isotope ratio of the sample blended with spike (corrected for dead time and mass bias);

R_{bblank}: measured isotope ratio of the blank blended with spike (corrected for dead time and mass bias);

h_{iy}: isotopic abundance of the reference isotope in the spike;

h_{ix}: isotopic abundance of the reference isotope in the sample.

4.2. COMPARISON OF SELENIUM METABOLISM IN *C. VIOLIFOLIA* AND *C. PRATENSIS*

4.2.1. Reagents and biological materials

Murashige and Skoog agar (MS agar) medium, ethanol, sucrose (≥99%), sodium selenate (≥95%), L-selenocystine (95%), sodium selenite (≥98%), trolox (97%), Folin & Ciocalteu's phenol reagent and salts used for nutrient solution: ammonium nitrate, calcium nitrate tetrahydrate, ethylenediaminetetraacetic acid ferric sodium salt, potassium nitrate, potassium hydroxide, magnesium sulphate heptahydrate, potassium phosphate monobasic, magnesium chloride hexahydrate, boric acid, manganese (II) sulphate monohydrate, zinc sulphate heptahydrate, copper (II) sulphate pentahydrate, molybdenum (VI) oxide were obtained from the Merck-Sigma group. Phytoagar was purchased from Research Products International (Mt. Prospect, IL, USA). Pyridine (a.r.) was obtained from Carlo Erba (Peypin, France), while formic acid (98–100%, used for liquid chromatographic purposes) was purchased from Scharlau. Standards for ICP-OES calibration were obtained from Elemental Scientific (Omaha, NE, USA).

Cardamine violifolia leaves and roots were collected in the springtime of 2017 in the natural seleniferous region Yutangba, Enshi (Hubei Province, China). Seeds were collected in the Yutangba region and were provided by the Academy of Agricultural Sciences of Enshi Tujia and Miao Autonomous Prefecture (Wuhan, China). *Cardamine pratensis* (cuckooflower) seeds were purchased from Seedaholic (Cloghbrack, Clonbur, Ireland).

4.2.2. Cultivation of plants

Different types of cultivation were applied to study several Se-related features of the two *Cardamine* species, which are summerised in Table 6. For cultivation on sterile half-strength MS agar medium (Murashige and Skoog 1962) the seeds were surface-sterilised by rinsing consecutively with 70% ethanol (1 min), sterilised distilled water (10 min), 10% household bleach (10 min) and finally five times (10 min each) with sterilised distilled water. The agar was sterilised by heating to 120 °C for 20 min and cooled to 55 °C before supplementation with Se and pouring in Petri dishes. For the study of root length, germinated seeds were carefully placed on the solidified medium along a line approximately 2 cm from one of the edges, with 1 cm distance (10 seeds per plate). Petri dishes were sealed with a double layer of parafilm and placed vertically in an incubator, with the seeds forming a horizontal line along the top rim of the Petri dishes. After 26 days, photos were taken and root lengths were determined using Image

J2 software (Rueden *et al.* 2017). Plants were then harvested, rinsed in distilled water, separated into shoots and roots and dried at 50 °C for 48 h. Dry weight data of shoots were determined (roots were too small to be weighed accurately), and the shoots from the different selenate treatments were used for elemental analysis as described below.

In case of the round Petri dishes using 25 μM selenate in the agar media, the plates were incubated horizontally and the seeds distributed across the entire surface.

In case of cultivation in gravels the strength of the Hoagland's nutrient solution (Hoagland and Arnon 1950) was gradually increased. In order to investigate the uptake capacity of different forms of Se (selenate, selenite) and the interactions of sulphate and phosphate, five different treatments were applied (see Table 6). After the 10-day long treatments, chlorophyll (Chl) fluorescence measurements were carried out. Plants were then harvested, rinsed, shoots and roots were separated and dried (50 °C for 48 h) for elemental analysis as described below. For LC-ICP-MS analysis the leaves and stems of cultivated *C. pratensis* were rinsed, lyophilised and milled.

Table 6. Cultivations of *Cardamine* species.

Plant species	Seed treatment	Germination	Growth media	Circumstances	Dish/pot	Treatment	Measurements
C. violifolia *C. pratensis*	Surface sterilisation Cold treatment in distilled water: 2 days at 4 °C	On wet filter paper	½ strength MS agar: 2.22 g L^{-1} MS basalt salt mixture 10 g L^{-1} sucrose 8 g L^{-1} Phytoagar pH 5.6-5.8 (set with KOH)	Growth cabinet 23 °C 16 h: 8 h (light:dark photoperiod)	square petri dishes (12 × 12 cm)	Na_2SeO_4: 0, 50, 100, 200, 400 μM	Root length Dry weight of shoots Elemental analysis
					round petri dishes (d=25 cm)	Na_2SeO_4: 25 μM	X-ray analysis Total phenolic content Antioxidant capacity
C. violifolia *C. pratensis*	Cold treatment in distilled water: 2 days at 4 °C	In the growth media – water treatment	Turface® growth medium (pH 5.5) (PROFILE Products LLC; Buffalo Grove, IL, USA)	Growth room 23 °C 10 h: 14 h (light:dark photoperiod)	10 × 10 cm pots	After germination: 7 days: 1/8th Hoagland's 7 days: 1/4th Hoagland's 10 days: A: control: 1/4th Hoagland's B: 1/4th Hoagland's + 20 μM Na_2SeO_4 C: 1/4th Hoagland's + 20 μM Na_2SeO_4 and 5 mM $MgSO_4$ D: 1/4th Hoagland's + 20 μM Na_2SeO_3 E: 1/4th Hoagland's + 20 μM Na_2SeO_3 and 2.4 mM KH_2PO_4	Chlorophyll fluorescence Elemental analysis X-ray analysis
C. pratensis	Cold treatment in distilled water: 2 days at 4 °C	In sterilised garden soil – water treatment	Vermex vermiculite (Soprema; Strasbourg, France)	Growth room 21 °C 16 h: 8 h (light:dark photoperiod)	20 × 10 cm pots	After germination: 3 days: 1/16th Hoagland's 7 days: 1/8th Hoagland's 4 days: 1/4th Hoagland's 9 days: 1/4th Hoagland's + 20 μM Na_2SeO_4 and $MgSO_4$ changed for $MgCl_2$	LC-ICP-MS

4.2.3. Elemental analysis

Se and S concentrations of the cultivated plants were determined with inductively coupled plasma optical emission spectrometry (ICP-OES) as described by Fassel (1978) using a Perkin Elmer Optima 7000 DV ICP-OES, at 196.026 nm (Se) and 181.975 nm (S), respectively after nitric acid digestion. The nitric acid digestion was carried out in glass tubes with heating for 2 h at 60°C and for 6 h at 125 °C. The limits of quantification for Se and S were ~1 mg kg^{-1} and ~0.2 mg kg^{-1} DW in plant samples, respectively.

Total Se content of *C. pratensis* grown for LC-ICP-MS analysis was determined with the method described in Chapter 4.1.2.1.

4.2.4. Selenium distribution and speciation analysis using X-ray microprobe analysis

X-ray microprobe analyses were performed at beamline 10.3.2 (X-Ray Fluorescence Microprobe) of the Advanced Light Source (ALS), at Lawrence Berkeley National Lab (Berkeley, CA, USA) using a Peltier cooling stage (-25 °C). Entire *C. violifolia* and *C. pratensis* seedlings grown on agar media containing 25 μM selenate were collected at harvest, rinsed, flash-frozen in liquid nitrogen and stored at -80 °C. Furthermore, young leaves from the plants grown on Turface® media (selenate and selenite treatment /treatment 'B' and 'D', respectively see Table 6/) were collected at harvest, flash-frozen and stored at -80 °C. Samples were shipped on dry ice for microprobe analyses. Selenium, calcium (Ca) and potassium (K) distribution were mapped using micro-focused X-ray fluorescence (μXRF), and Se speciation was investigated using X-ray absorption near-edge structure (μXANES) spectroscopy, essentially as described by Jiang *et al.* (2018b). XANES spectra of selenolanthionine standard was recorded from frozen droplet on the Peltier cooling stage (-25 °C). The μXRF maps were recorded at 13 keV incident energy, using 20 mm × 20 mm pixel size, a beam spot size of 7 mm × 7 mm, using 50 ms dwell time. Maps were deadtime-corrected and decontaminated. Selenium K-edge μXANES (in the range 12500–13070 eV) was used to analyse Se speciation on different spots, close to areas showing high Se concentration in the μXRF maps. Spectra were energy calibrated using a red amorphous Se standard, with the main peak set at 12660 eV.

Least-square linear combination fitting of the μXANES data was performed in the range of 12630–12850 eV using a library of 52 standard selenocompounds and procedures described by Fakra *et al.* (2018). All data were recorded in fluorescence mode using a seven-element Ge solid state detector (Canberra, ON, Canada) and processed using custom LabVIEW programs (National Instruments, Austin, TX, USA) available at the beamline.

4.2.5. Physiological parameters: chlorophyll fluorescence, antioxidant capacity analysis and total phenolic content

Chl fluorescence measurements were carried out on the leaves of plants cultivated on Turface® media before harvest, using a MultispeQ 2.0 instrument (Photosynq LLC, East Lansing, MI, USA) using the company's recommended protocol.

Seedlings of *C. violifolia* and *C. pratensis* grown on agar media containing 25 μM selenate or without selenate were harvested and flash frozen. Samples were lyophilised, powdered and weighed. The freeze-dried material was extracted with 80% acetone at a ratio of 25 μL mg^{-1} tissue while rotated in the dark at 4 °C for 30 min. Supernatant was collected, diluted with additional acetone at 1:10 or 1:20 depending on the sample, and stored on ice until used. For the antioxidant capacity assay, the absorbancies of the diluted supernatants were recorded at λ = 734 nm with a UV–Vis spectrophotometer (PowerWaveXS2; BioTek Instruments, Winooski, VT) using the method of Miller and Rice-Evans (1996). Trolox (a water-soluble analogue of vitamin E) was used as standard for this assay, and results were expressed as micromoles of trolox-equivalent antioxidant capacity (TEAC) per gram dry weight (μmole TE g^{-1} DW). Diluted supernatant collected from extraction described above was used for total phenolics. Folin & Ciocalteu's reagent was used as described by Singleton and Rossi (1965). All samples for this assay were recorded at λ = 765 nm using gallic acid as a standard with results expressed as milligrams of gallic acid equivalent (GAE) per gram of dry weight (mg GAE g^{-1} DW).

4.2.6. Strong cation exchange (SCX) – ICP MS analysis

0.5 g of *C. violifolia* leaf and root from China were extracted with 10.0 mL deionised water using an ultrasonic probe (UP100H) at ambient temperature. Supernatants were recovered by centrifugation (10 min at 4000*g*) and filtered through 0.45 μm cellulose acetate filters. 2.225 mL of the leaf extract and 3.0 mL of the root

extract were lyophilised and redissolved in 2.0 mL deionised water. 0.1 mL sample was diluted with 1.4 mL eluent buffer and 20 µL was injected onto the column. In case of spiking, the samples were spiked to 200 ng mL^{-1} $SeCys_2$ concentration (calculated as Se). Same HPLC-ICP-MS set up was used as described in Chapter 4.1.3.2.

0.3 g of lyophilised *C. pratensis* biomass was extracted with 10.0 mL deionised water using a vortex shaking device for 5 min. The supernatant was recovered by centrifugation (10 min at 9000*g*), filtered through 0.45 µm PTFE filters and 20 µL was injected onto the column without any dilution. In case of spiking, the samples were spiked to 500 ng mL^{-1} $SeCys_2$ (calculated as Se). The chromatographic set-up consisted of a Thermo Spectra System P4000 HPLC pump (Thermo Fisher Scientific) connected to the Thermo Scientific X-Series II ICP-MS for element specific detection of ^{78}Se and ^{80}Se, using 7% H_2-93% He as collision gas, introduced at 6.0 mL min^{-1}. A Luna SCX column (250 mm × 4.6 mm × 10 µm; Phenomenex) was used in gradient elution mode with pyridine formate (pH 3.0; buffer A: 1 mM; buffer B: 40 mM). The program was as follows: 0–1 min 0% B (1.7 mL min^{-1}), 1–15 min from 0% up to 30% B (1.7 mL min^{-1}), 15–16 min up to 100% B (1.9 mL min^{-1}), 16–21 min 100% B (1.9 mL min^{-1}), 21–21.5 min down to 0% B (1.7 mL min^{-1}), 21.5–26 min 0% B (1.7 mL min^{-1}).

4.2.7. Statistical analysis

Statistical analysis was performed with the IBM SPSS v.20 software (Armonk, NY, USA). Two-way ANOVA model was applied to compare the means of the measured parameters with the factors “species” and “treatment”. The normality of residuals and the homogeneity of variances were checked. In case of non-normality, data transformation was carried out. Tukey-Kramer’s (Tukey 1977) or Games-Howell’s post-hoc test (Games and Howell 1976) was used, depending on the fulfilment of homogeneity of variances assumption. Student’s t-test or Welch’s t-test was applied to compare two means, depending on the fulfilment of homogeneity of variances assumption (Jaccard *et al.* 1984).

5. RESULTS AND DISCUSSION

5.1. SELENIUM METABOLITES IN *CARDAMINE VIOLIFOLIA*

5.1.1. Total selenium, sulphur contents and selenium distribution

Total Se concentration of the pooled stem and leaves *C. violifolia* sample harvested in the natural seleniferous region in China was found to be 3.7 ± 0.2 g Se kg^{-1} DW. This result places the plant among the hyperaccumulator species in agreement with other reports (Yuan *et al.* 2013, Cui *et al.* 2018). The sulphur concentration (15.2 g S kg^{-1} DW) falls in the range of sulphur accumulation of other Se (hyper)accumulator Brassicaceae species, *e.g.*, *Stanleya pinnata* var. *pinnata* (14.0-19.3 g S kg^{-1} DW, Cappa *et al.* 2014), *Sinapsis alba*, *Brassica arvense*, *B. oleracea* and *B. juncea* (12.9-21.8 g S kg^{-1} DW, White *et al.* 2007). The ratio of Se:S (1:10 molar ratio) is unusually high among the known Brassicaceae species; however, Se and S concentration data of the growing media is required to be taken into account when evaluating the Se enrichment factor. Figure 13 shows the distribution of selenium among different fractions. Water extract contained 60 ± 1.5 % of the total Se while the sum of Se in Na_2SO_3 extract (assigned as elemental selenium) and CS_2 extract (assigned as selenides) accounted for ~ 18% of the Se originally present in the sample. Different observations are found in the literature discussing the extraction efficiency and selectivity of Na_2SO_3 and CS_2 solvents in case of elemental selenium and selenides (Aborode *et al.* 2015, Chen *et al.* 2006, Gao *et al.* 2000, Velinsky and Cutter 1990). Considerable elemental selenium content is usually a feature of secondary and non-accumulator plants such as garlic (Mounicou *et al.* 2009) and Black-eyed Susan (Aborode *et al.* 2015), however some *Astragalu*s and *Stanleya* hyperaccumulator species have been also shown to contain up to 35 % of total Se in this form (Lindblom *et al.* 2013b). Although in this latter case, the high elemental Se fraction was found in the roots and was attributed to the microbial activity of endophytic bacteria or fungi.

The overall Se recovery was 88%. The missing amount from the mass balance can be attributed to the physical loss observed during the laborious collection of the CS_2 phase and therefore might be assigned as insoluble Se after the triple stage extraction process.

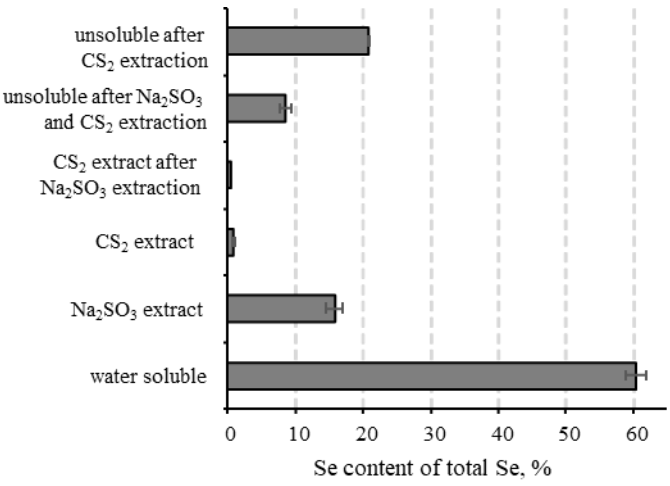

Figure 13. Distribution of Se in *C. violifolia* sample on the basis of the sequential extraction procedure. Error bars indicate ±1 standard deviation.

5.1.2. Chromatographic characterisations

High water-soluble Se content and considerable elemental Se concentration could indicate the accumulation of inorganic (anionic) Se species, selenate and selenite therefore strong anion exchange chromatography (SAX) was chosen for further characterisation. The aqueous extract of *C. violifolia* contained only a negligible amount of selenite (48 μg g^{-1} as Se) that accounts for only 1.3% of total Se (Figure 14).

The SAX-ICP-MS chromatogram also indicates that most of the soluble Se compounds are either neutral or cationic at the pH of the separation (pH 6.0) and elute in the void volume.

Ion-pairing RP chromatography has also been chosen for characterisation as it is a well established method for the efficient separation of selenoamino acids and their derivatives arising from proteolytic extracts (Kotrebai *et al.* 2000). Figure 14 shows the elution of the proteolytic extract with the indication of the elution time of *Se*-(methyl)selenocysteine (MeSeCys) and selenomethionine (SeMet). SeMet was detected in traces, the amount of MeSeCys was quantified accounting for ~ 0.4% of total Se (13 μg g^{-1} as Se). The two most abundant peaks could not be identified with any of the available standards with retention time matching; however, their retention at the acidic pH of the elution (pH < 3) with the actual anionic ion pairing agent (HFBA) provided useful information.

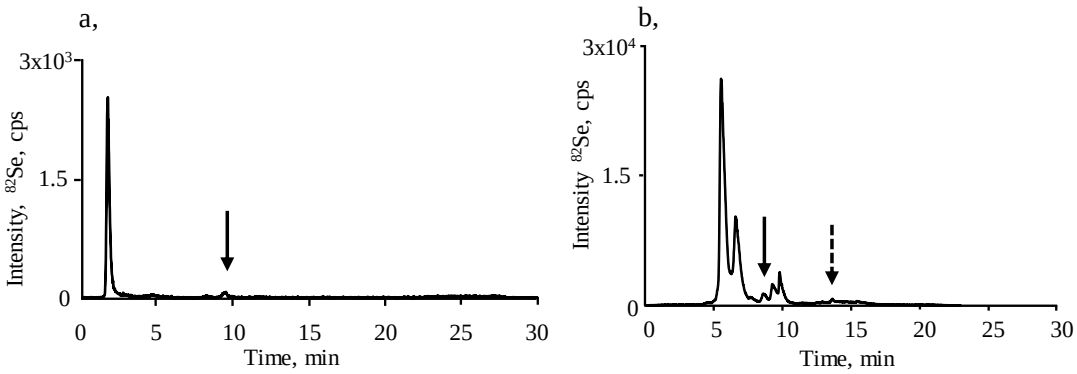

Figure 14. (a) Strong anion exchange (SAX)-ICP-MS chromatogram of the *C. violifolia* water extract. The arrow indicates the retention time of selenite. (b) Ion-pairing reversed phase (IP-RP)-ICP-MS chromatogram of the *C. violifolia* enzymatic extract. The solid arrow indicates the retention time of *Se*-(methyl)selenocysteine, while the dashed arrow points at that of selenomethionine.

Water extract of the sample was analysed with strong cation-exchange (SCX) chromatography (Figure 15) showing one dominant peak at the retention time of 3.7 min and several minor peaks. Repeated fraction collection was carried out for the major one to obtain the compound in adequately pure form for ESI-MS based identifications. The collected and pooled fractions of the peak were re-analysed with IP-RP chromatography. The IP-RP chromatogram of the major peak indicated that the fraction of the major compound consists of mostly one Se compound however it was re-fractionated with IP-RP as well to eliminate further matrix compounds for ESI-MS analysis.

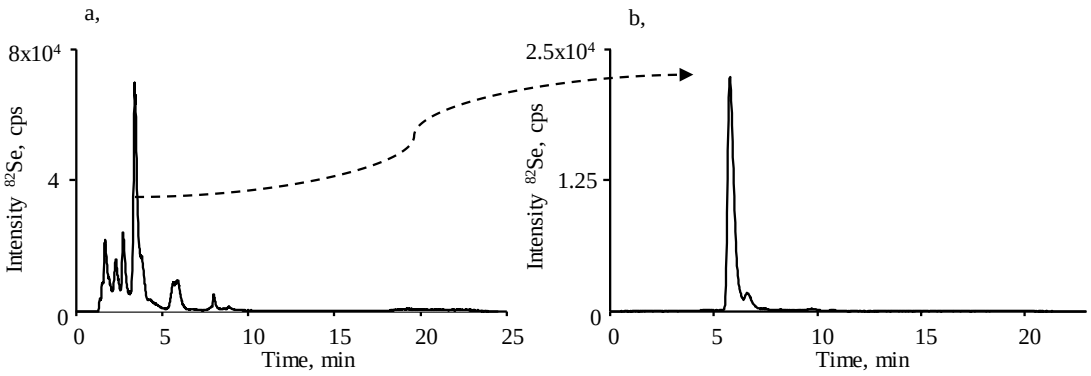

Figure 15. (a) Strong cation exchange (SCX)-ICP-MS chromatogram of the *C. violifolia* water extract. The dashed line indicates the major fraction. (b) Ion-pairing reversed phase (IP-RP)-ICP-MS chromatogram of the major fraction collected from the SCX chromatographic set-up.

5.1.3. Identification of the major selenocompound by HPLC-ESI-QTOF-MS and -MS/MS

The orthogonal sample clean-up procedure ensured the elimination of matrix interferences and the pre-concentration of the analytes required for the ESI-QTOF-MS analysis. The fraction of the major peak collected by IP-RP-HPLC was introduced into the ESI-QTOF-MS instrument by the means of an RP-HPLC system which provided an additional separation to achieve better S/N ratios. Selenium-containing molecules were searched by visual seeking for the characteristic selenium isotopic pattern. Two components with the mass to charge ratios (*m/z*) 257.0032 and 167.9555 were found in the full scan spectrum showing the one Se atom containing isotopic pattern (Figure 16). The assumption that the ion at *m/z* 167.9555 is the in-source fragment of the compound with *m/z* 257.0032 was confirmed by matching their extracted ion chromatograms (EIC), as showed in Figure 16b and by decreasing the fragmentor potential of the ion source from 170 V to 150 V, which practically eliminated the in-source fragment.

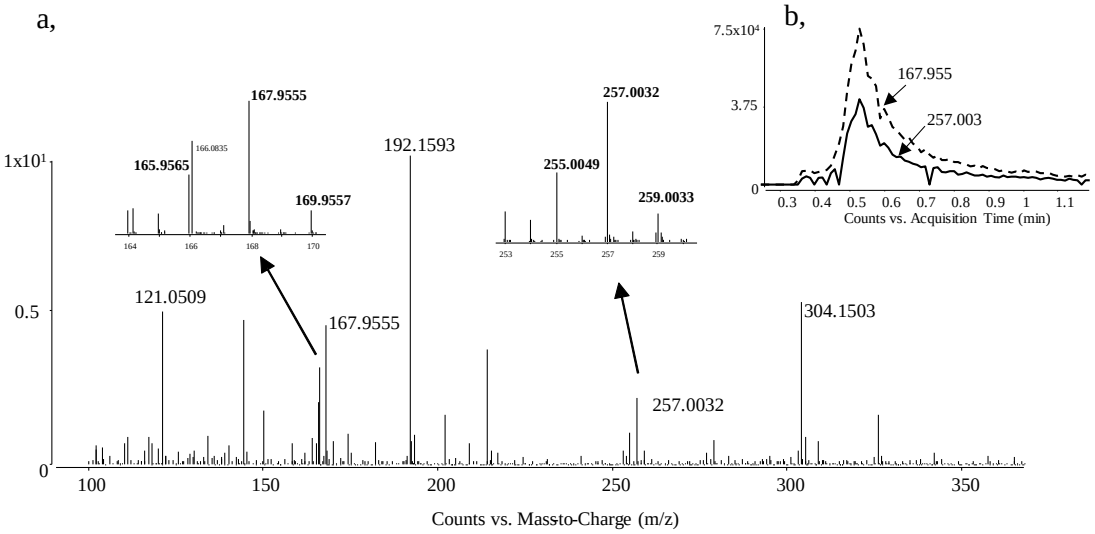

Figure 16. (a) HPLC-ESI-QTOF-MS full scan spectrum recorded at 0.502 min of the most abundant selenium containing fraction of *C. violifolia*. The spectrum presents the isotopologue patterns of selenolanthionine and its in-source fragment in the insets. Masses highlighted in bold refer to the ^{78}Se, ^{80}Se and ^{82}Se isotopologues. The mass with *m/z* 166.0835 arrives from an interference on the ^{78}Se isotopologue of the in-source fragment. (b) Extracted ion chromatograms (EICs) of the ions *m/z* 257.003 (solid line) and *m/z* 167.955 (dashed line).

Accurate mass measurement offers the opportunity to calculate the elemental composition of the molecule. The calculating tool setting is shown in appendix (Table A4). Only one possible composition was found within 5 ppm: $C_6H_{13}N_2O_4Se^+$;

theoretical *m/z* 257.0035, Δ=−1.16 ppm. This composition and the note from Block *et al.* (2001) about the most significant fragment detected at *m/z* 168 indicated this molecule is selenolanthionine (SeLan). For further confirmation of the compound identity, MS/MS experiment was carried out on the ^{80}Se and ^{77}Se isotope containing isotopologues (Figure 17, Table 7).

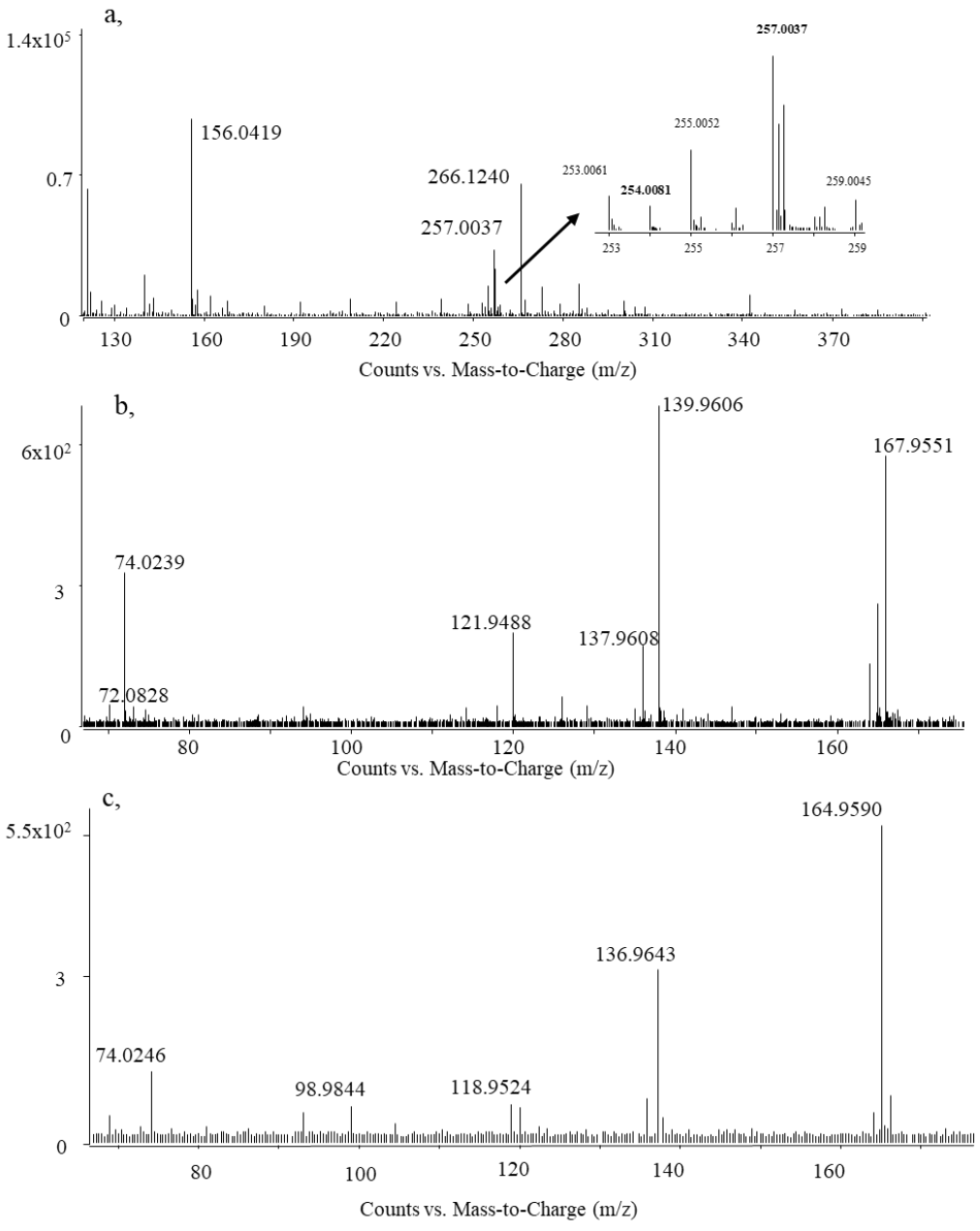

Figure 17. (a) HPLC-ESI-QTOF-MS full scan spectrum of selenolanthionine prior to MS/MS analysis. The inset shows the isotopologue pattern, together with the fragmented ions highlighted in bold. (b) HPLC-ESI-QTOF-MS/MS collision induced dissociation (CID) spectrum of selenolanthionine fragmented on the ^{80}Se isotopologue and (c) on the ^{77}Se isotopologue.

Table 7. MS/MS fragmentation data of selenolanthionine purified from *C. violifolia* water extract.

Composition	Theoretical mass, *m/z*	Experimental mass, *m/z*	Δ, ppm
$C_6H_{13}N_2O_4(^{80}Se)^+$	257.0035	257.0037	0.78
$C_6H_{13}N_2O_4(^{77}Se)^+$	254.0068	254.0081	5.12
$C_3H_6NO_2(^{80}Se)^+$	167.9558	167.9551	-4.17
$C_3H_6NO_2(^{77}Se)^+$	164.9592	164.9590	-1.21
$C_2H_6NO(^{80}Se)^+$	139.9609	139.9606	-2.14
$C_2H_6NO(^{77}Se)^+$	136.9642	136.9643	0.73
$C_2H_4NO_2^+$	74.0236	74.0239	4.05
$C_2H_4NO_2^+$	74.0236	74.0246	13.5

The possible structure of the fragments together with selenolanthionine structure is shown in Figure 18. The structures presented here are meant to present the origin of the fragments in the molecule, and they are not intended to show the actually formed fragment structure. Up to now only one record on SeLan has been published: Kotrebai *et al.* (2000) assigned this species in selenised yeast based on retention time matching in an HPLC-ICP-MS chromatogram on a shoulder of an eluting selenium containing peak (Figure 19).

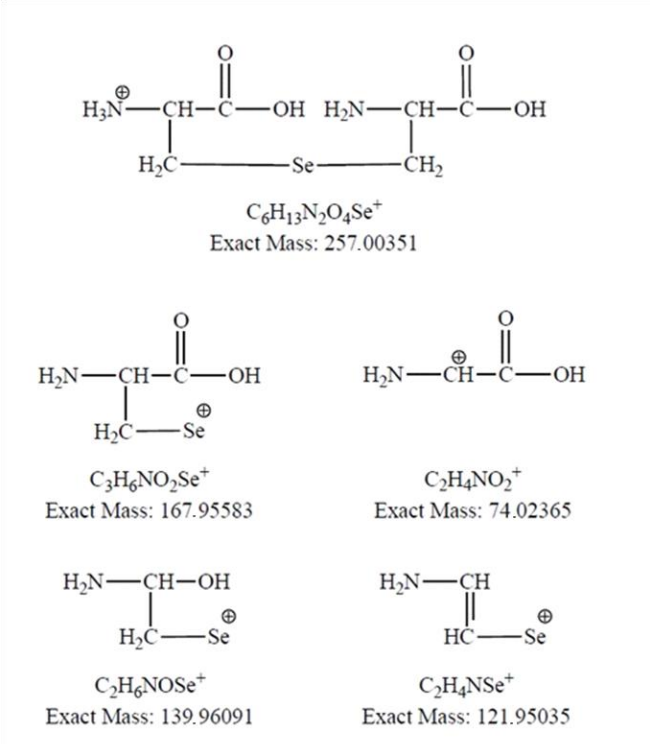

Figure 18. Structure of selenolanthionine and the possible fragments with their accurate masses.

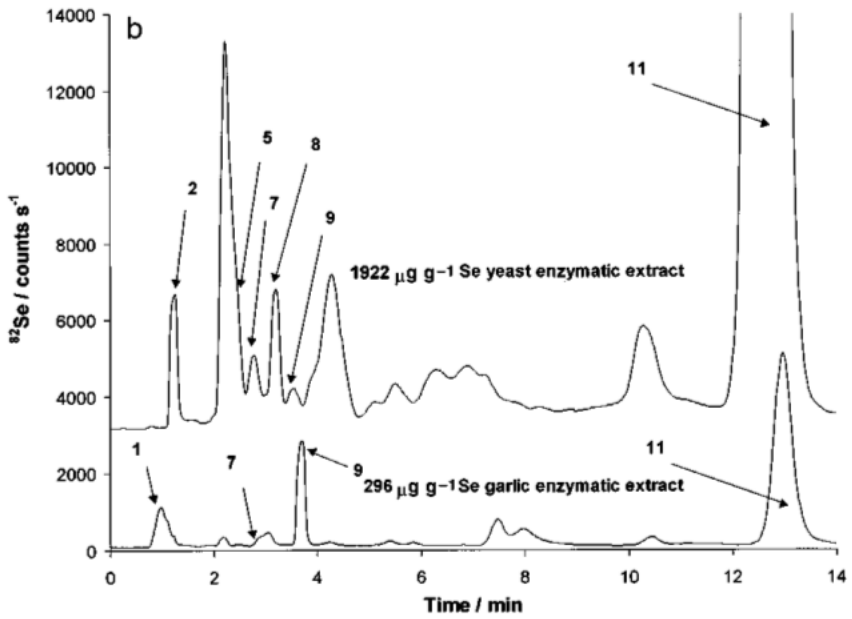

Figure 19. Selenolanthionine identification in selenised yeast (denoted with number "5") based on retention time matching by Kotrebai *et al.* (2000).

Even though all the isotopic pattern, accurate mass data, fragmentation pattern and cationic chromatographic behaviour (Sykora 1984) confirmed the identity of this compound, it was found necessary to confirm the identification by the chemical synthesis of selenolanthionine as well especially in the light of the fact that only the derivatives of SeLan have been found so far in Se-containing plant (Aureli *et al.* 2012) and yeast (Far *et al.* 2010) samples.

5.1.4. Analytical and semi-preparative chromatographic purification of synthesised selenolanthionine

As the synthesis described by Block *et al.* (2001) could not be completely reproduced, the synthesised material was analysed by SCX-ICP-MS. Several selenium species could be found in the synthesised mixture (Figure 20). The highest peak eluting at 5.3 min was identified as residual selenocystine ($SeCys_2$) based on retention time matching. Its concentration indicated that about 70% of $SeCys_2$ did not react, which resulted in a yield of ≤30% for the SeLan synthesis. Repeated fraction collection was carried out for the compound eluting at 4.3 min that was supposed to be SeLan.

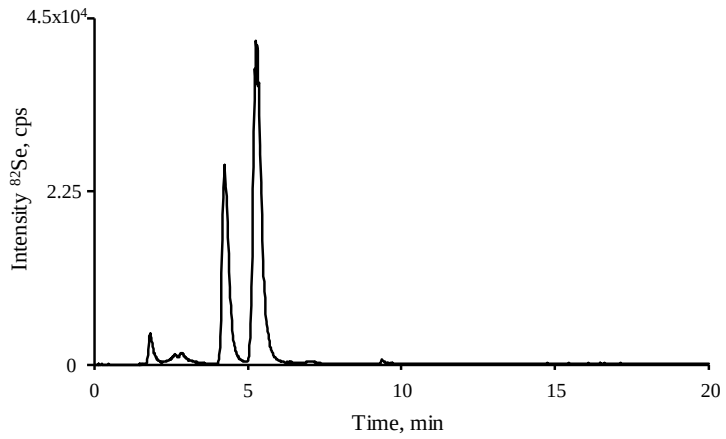

Figure 20. SCX – ICP-MS chromatogram of the synthesised selenolanthionine standard. The peak eluting at 5.3 min refers to residual selenocystine, while selenolanthionine eluted at 4.3 min.

Collected fractions were lyophilised for preconcentration and dissolved in 1.0 mL. Its concentration was estimated with an isocratic SCX method that ended up in a concentration of ~ 15.5 μg Se mL^{-1}.

Semi-preparative purification was needed to yield higher amount of pure SeLan standard for recording its XANES spectra (Chapter 5.2.3). The separation of SeLan and $SeCys_2$ required optimisation process as the method adaptation from Zorbax SCX (Agilent) analytical column did not provide adequate separation on the semi-preparative Luna SCX (Phenomenex) column (Figure 21a). Chromatographic parameters of the optimisation process are described in Table 8. However their experimental pKa values were unknown, SeLan (eluting before $SeCys_2$) seemed to be a stronger acid and the appropriate pH could be set up only through the approach called "trial and error". The applied pH was increased stepwise (pH 2.15, 2.55, 3.05, 3.55) applying the chromatographic method #1 (Table 8); finally, pH 3.55 provided an acceptable separation of the two compounds (Figure 21).

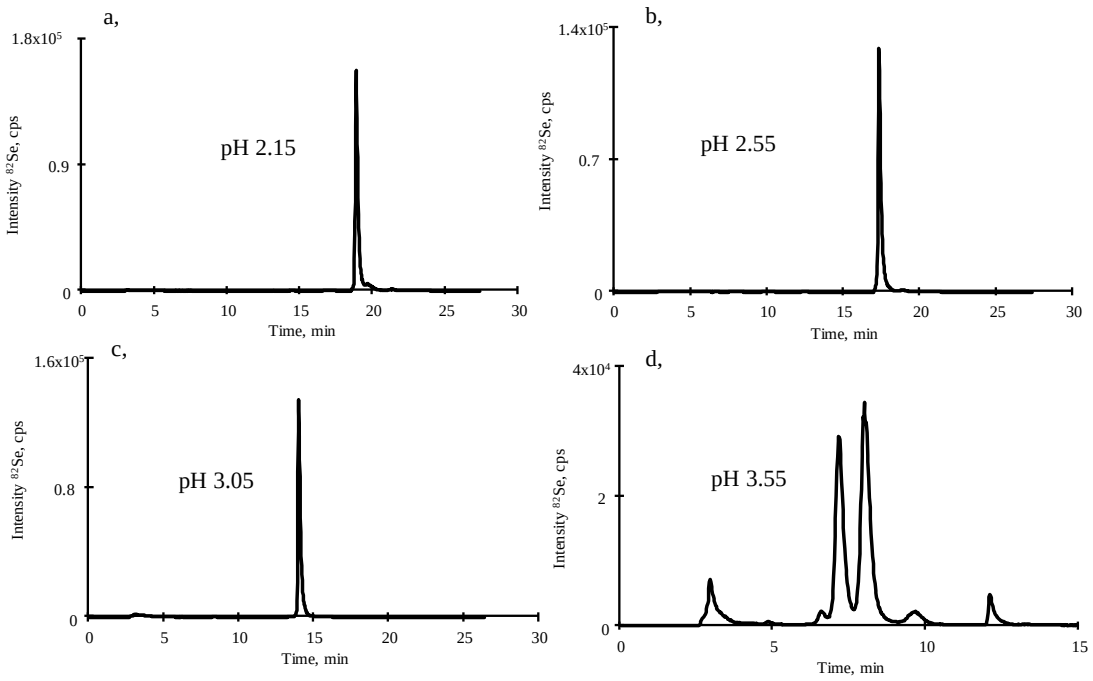

Figure 21. Semi-preparative strong cation exchange chromatograms of the synthesised SeLan mixture at four different pH settings: (a) pH 2.15 (b) pH 2.55 (c) pH 3.05 (d) pH 3.55.

Isocratic approach could also be applied instead of a gradient separation but this case the two compounds partly overlapped, even after a careful optimisation of the isocratic method #2 (Table 8, Figure 22).

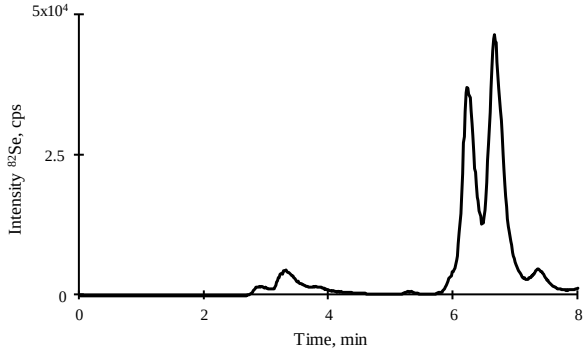

Figure 22. Separation of the synthesised SeLan mixture on the semi-preparative strong cation exchange column with isocratic method at pH=3.55.

The resolution and the retention factor (k') of the compounds could be improved by cooling the column from 23 °C to 20 °C, flattening the gradient slope and decreasing the flow rate from 3.0 mL min^{-1} to 2.5 mL min^{-1}, as presented in method #3 (Table 8, Figure 23). The k' of SeLan was increased from 1.77 to 2.28, and the k' of $SeCys_2$ reached 2.8 after the former 2.1 value. However adequate resolution (~ 1) was finally achieved, fraction collection was set to stop earlier to exclude the traces of

$SeCys_2$ and the purity was checked after lyophilisation. Injection volume of the synthesised mixture was 5 µL (dissolved at concentration 10 mg mL^{-1}) for optimisation and 10 µL for fraction collection; the injection of 25 µL resulted in saturated and tailing peaks.

The collected and pooled fraction was dissolved in 100 µL distilled water after the lyophilisation, its concentration was estimated with isocratic SCX method that indicated the concentration of ~ 120 µg Se mL^{-1}; this concentration was found high enough for recording the XANES spectra.

Table 8. Chromatographic parameters for the separation of selenolanthionine and selenocystine on a semi-preparative strong cation exchange column.

Method	Eluents	Column temperature	Flow rate	Gradient
#1	A: 1 mM pyridine formate pH: 2.15; 2.55; 3.05; 3.55 B: 40 mM pyridine formate pH: 2.15; 2.55; 3.05; 3.55	23 °C	3 mL min^{-1}	0-2 min 0% B 2-20 min up to 100% B 20-21 min 100% B 21-21.5 min down to 0% B 21.5-30 min 0% B
#2	A: 1 mM pyridine formate pH 3.55 B: 40 mM pyridine formate pH 3.55	23 °C	3 mL min^{-1}	0-15 min 10% B 15-15.5 min up to 100% B 15.5.-17 min 100% B 17-17.5 min down to 10% B 17.5-26 min 10% B
#3	A: 1 mM pyridine formate pH: 3.55 B: 40 mM pyridine formate pH: 3.55	20 °C	2.5 mL min^{-1} (during gradient) 3 mL min^{-1}	0-15 min up to 30% B (2.5 mL min^{-1}) 15-15.1 min 30% B 15.1-16 min up to 100% B 16-17 min 100% B 17-17.5 min down to 0% B 17.5-25.9 min 0% B 25.9-26 min 0% B

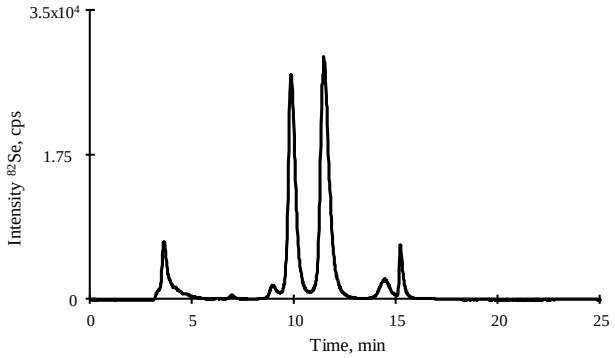

Figure 23. Separation of the synthesised mixture on the semi-preparative strong cation exchange column with optimised parameters.

5.1.5. Confirmation of selenolanthionine by chemical synthesis

The compound collected from analytical cation-exchange fraction collection (eluting at 4.3 min) was used for spiking the water extract of the *C. violifolia* sample. Exact retention time matching with the peak of the previously identified SeLan was detected with SCX-ICP-MS (Figure 24).

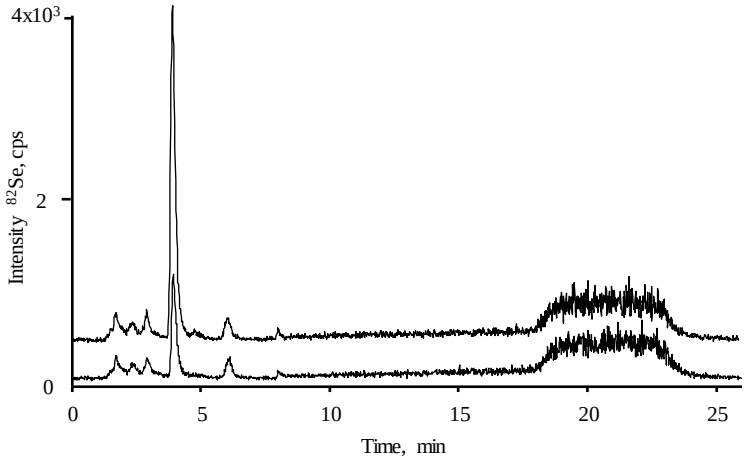

Figure 24. SCX – ICP-MS chromatograms of the *C. violifolia* water extract (lower chromatogram) and that of the water extract spiked with the synthesised selenolanthionine standard (upper chromatogram).

The synthesised compound and the spiked *C. violifolia* extract were analysed by RP-LC-ESI-QTOF-MS in MS and MS/MS experiments. Figure 25a shows the full-scan spectra where the *m/z* 257.0038 and *m/z* 167.9557 ions were both found with the characteristic Se isotopic pattern and also the MS/MS fragments showed matching with those detected in *C. violifolia* extract (Figure 25b).

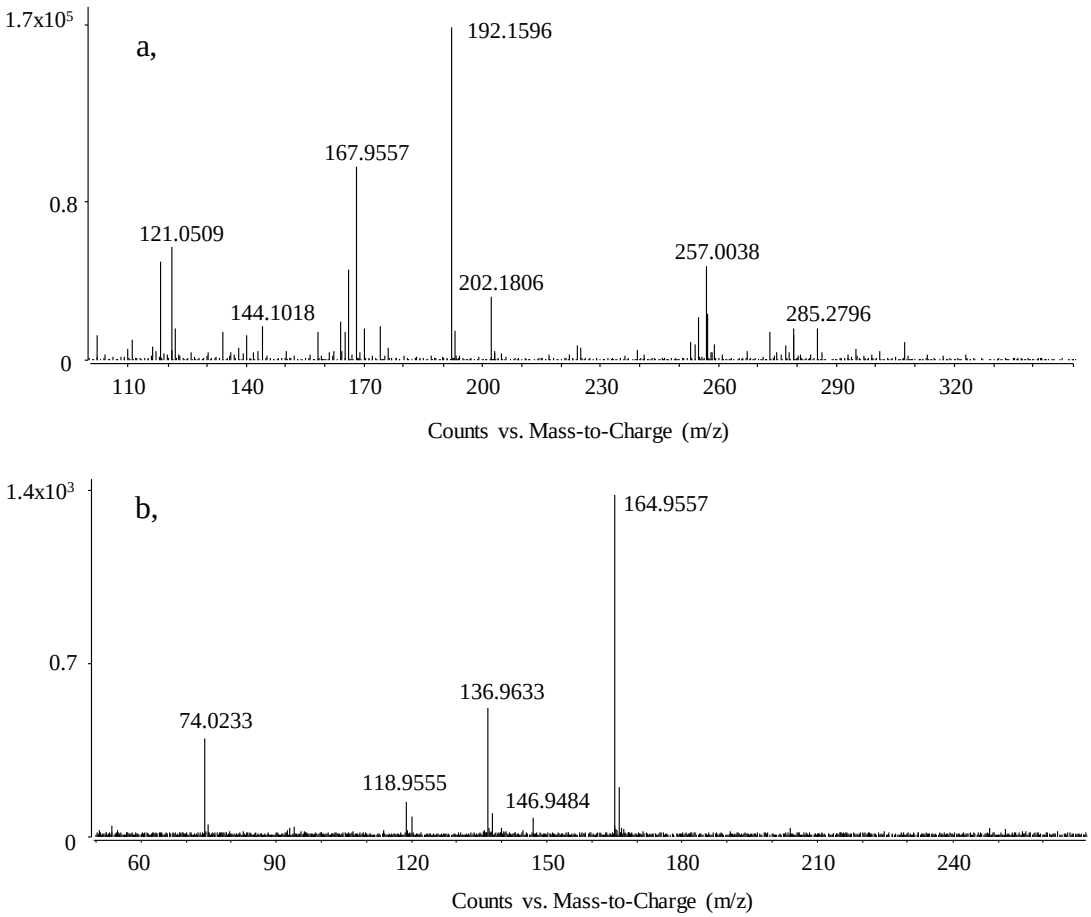

Figure 25. (a) HPLC-ESI-QTOF-MS full scan spectrum of the synthesised selenolanthionine prior to MS/MS analysis. (b) HPLC-ESI-QTOF-MS/MS collision induced dissociation (CID) spectrum of the synthesised selenolanthionine fragmented on the ^{77}Se isotopologue.

The extracted ion chromatograms of SeLan and its in-source fragment showed matching in the spiked extract of *C. violifolia* which corresponds to another, orthogonal verification to the previous SCX chromatography (Figure 26).

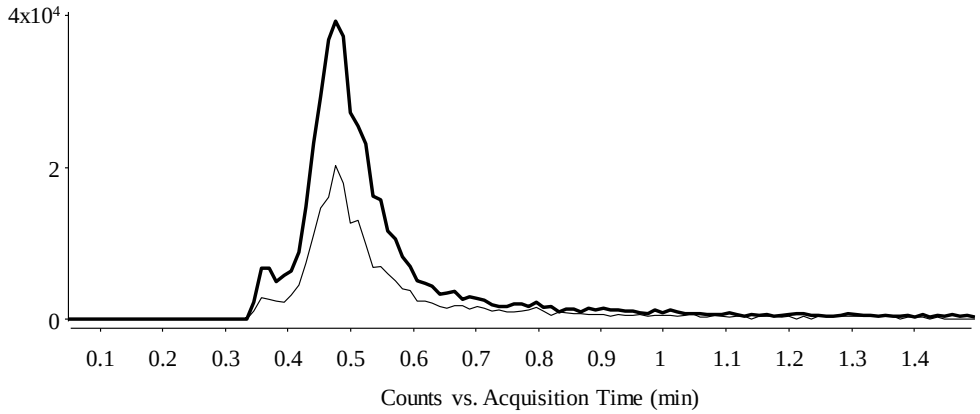

Figure 26. EICs of the ions *m/z* 257.003 (lower line) and *m/z* 167.955 (upper line) from the *C. violifolia* water extract spiked with the synthesised selenolanthionine standard.

It must be mentioned that seemingly contradictory speciation results have been reported for this plant under an alternative name *C. hupinshanesis*: selenocystine was identified as the main Se compound (Yuan *et al.* 2013). Indeed, this report was based on only one separation approach (SAX, pH=6.0) that cannot evidently separate $SeCys_2$ from SeLan.

5.1.6. Identification of minor selenocompounds in *C. violifolia*

5.1.6.1. Chromatographic characterisation

Water extract of *C. violifolia* leaf sample (261 mg total Se kg^{-1} DW) was analysed by SCX-ICP-MS chromatography (Figure 27). The most intense selenolanthionine peak (eluting at 3.04 min) is surrounded by several less intense peaks, which were fraction collected for further analysis (indicated with Fr1 to Fr4). Figure 27b shows the respective and overlaid IP-RP-ICP-MS chromatograms of the fractions. Despite that the peaks could be slightly separated on SCX, three fractions (Fr1, 2 and 3) could not be clearly differentiated by IP-RP and eluted between 4.8-6.6 min; no adequate (baseline) separation could be achieved for the first three fraction eluting close to the void volume ($k<2$). Fr 4 was the only one fraction that showed an adequately retained and distinct peak at 6.9 min with no considerable overlapping. Each fraction consisted of several peaks indicating that numerous selenium species should be expected in the ESI-MS acquisitions. Fraction collection was carried out for each fraction that were afterwards concentrated by lyophilisation and subjected to LC-Unispray-QTOF-MS. No selenium species could be detected after the two dimensional (SCX+IP-RP) purification, which might be explained by unstable retention time parameters on IP-RP that hampered reproducible fraction collection. Therefore, the SCX-ICP-MS derived fractions were addressed for LC-Unispray-QTOF-MS analysis.

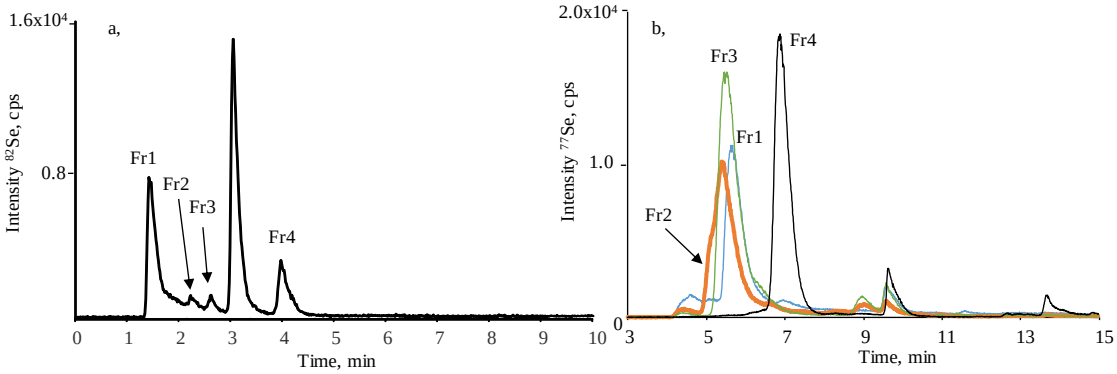

Figure 27. (a) Strong cation exchange (SCX) – ICP-MS chromatogram of water soluble extract of *C. violifolia*, recorded on the ^{82}Se isotope. Fractions labelled #1 - #4 were collected for further characterisation on LC-Unispray-QTOFMS. (b) Ion-pairing reversed phase (IP-RP) – ICP-MS chromatograms of the fractions #1 - #4 collected from SCX – ICP-MS, recorded on the ^{77}Se isotope.

5.1.6.2. Screening for selenium species in the LC-Unispray-QTOF-MS acquisitions

Intra-isotope mass defect based extraction, manual pattern exploration, extracting diagnostic ion source fragments and database dependent search allowed the detection of numerous selenium compound in the four fractions, which are listed in Table 9. As the first three fractions were co-eluting during fraction collection, and selenium species were often found in more than one fraction, they are positioned into the fraction where they showed the highest abundance. The most contributing technique to discover the given species is indicated, however most of them could be localised by more than one search method. Manual pattern exploration was crucial for discovering the higher (*m/z* > 370) molecular mass species. Full scan spectra under *m/z* 300 are of relatively high density ("crowded"), the most visible mass spectral features of selenium containing molecules (*i.e.*, characteristic /7-12 isotopologue wide/ base, unique isotope ratio of ^{80}Se and ^{78}Se, high /0.1-0.2 amu/ absolute mass defect compared to neighbouring ions) are difficult to explore. In contrast to the SeHCys in-source fragment, extracting the diagnostic ion source fragment at *m/z* 183.9871 ($C_4H_{10}O_2NSe^+$) did not reveal any hit, which indicates no derivatives of SeHLan were present in the fractions at high concentration. The selenocysteinyl moiety ($C_3H_6O_2NSe^+$, *m/z* 167.9558) could only be found in MS/MS spectra, possibly due to the fact that in-source and MS^E fragmentation usually run at lower fragmentation voltage compared to MS/MS analysis.

Table 9. Summary of selenium species detected in the water soluble selenometabolome of *C. violifolia*. 'n.p.' denotes to 'not provided'; 'n.a.' denotes to 'not available'. MS/MS quality scaling indicates high signal-to-noise ratio with good quality MS/MS spectrum obtained ('+++'), moderate signal-to-noise ratio with moderate quality MS/MS spectrum ('++') and low signal-to-noise ratio with missing or low quality MS/MS spectrum ('+').

Experimental *m/z*	Elemental composition, $[M+H]^+$	Theoretical *m/z*	Difference ppm	Retention time, min	Detected in fraction				Isomers detected	Detected also in negative ion mode	Contains one or two (deoxy)hexose moiety(ies)	Detected first on the basis of				SeHCys derivative	Characteristic non-SeHCys fragment on ^{80}Se	Characteristic non-Se fragment	MS/MS quality	Reference
					#1	#2	#3	#4				manual screening	mass defect	database search	SeHCys in-source fragments					
197.00725	$C_6H_{13}O_2Se^+$	197.00753	-1.42	2.13			x						x			-	94.94, 108.95	-	+++	
241.99302	$C_6H_{12}NO_2Se^+$	241.99261	1.69	0.74			x								x	x	108.95	-	++	
241.99296	$C_6H_{12}NO_2Se^+$	241.99261	1.45	1.48	x							x				-	108.95, 138.98, 152.94, 195.98	130.05	+	
254.02883	$C_8H_{16}NO_2Se^+$	254.02899	-0.63	0.93, 1.04				x	x						x	x	106.94, 134.97	-	++	
268.04482	$C_9H_{18}NO_2Se^+$	268.04464	0.67	1.36			x						x			-	133.00	86.06	++	
270.02341	$C_8H_{16}NO_3Se^+$	270.02391	-1.85	0.73			x					x				n.a.	-	-	+	
271.02005	$C_7H_{15}N_2O_2Se^+$	271.01916	3.28	0.60				x						x		x	-	109.08	++	Virupaksha and Shrift (1963)
282.06027	$C_{10}H_{20}NO_2Se^+$	282.06029	-0.07	2.34				x							x	x	163.00	81.07	+++	
284.03997	$C_9H_{18}NO_3Se^+$	284.03956	1.44	0.66, 0.79				x	x						x	x	-	85.06, 102.06, 124.04	+++	
285.05998	$C_{10}H_{21}O_4Se^+$	285.05996	0.07	1.63, 1.69		x			x				x			-	132.96, 134.97, 168.98	85.06	++	
301.09063	$C_{11}H_{25}O_4Se^+$	301.09126	-2.09	2.95, 3.09		x			x			x				n.a.	n.a.	n.a.	+	
312.03454	$C_{10}H_{18}NO_3Se^+$	312.03447	0.22	1.17, 1.36				x	x						x	x	146.97, 164.98, 192.98	102.10	++	
313.02949	$C_9H_{17}N_2O_3Se^+$	313.02972	-0.73	0.76				x						x		x	-	108.05, 154.09	++	
364.95162	$C_8H_{17}N_2O_4Se_2^+$	364.95133	0.79	0.70				x						x		x	-	-	+	Hamilton (1975)
377.07037	$C_{12}H_{25}O_6Se^+$	377.07092	-1.46	1.76, 2.09, 2.34	x				x		x	x				-	215.02	85.06, 103.07	++	
391.08672	$C_{13}H_{27}O_6Se^+$	391.08657	0.38	2.33, 2.42	x				x		x	x				-	229.03	85.03, 99.08	++	
405.06603	$C_{13}H_{25}O_7Se^+$	405.06583	0.49	0.60		x					x	x				-	243.01	97,03, 145.05	++	
407.04499	$C_{12}H_{23}O_{10}Se^+$	407.04510	-0.27	1.04	x					x	x			x		-	244.99	89.02	+++	Aureli *et al.* (2012)
416.08051	$C_{14}H_{28}NO_6Se^+$	416.08182	-3.15	0.85		x						x				x	134.97, 168.98, 193.97, 326.02	114.05	+	
419.05681	$C_{12}H_{23}N_2O_8Se^+$	419.05633	1.15	0.59		x				x	x	x				-	167.95, 257.00, 401.04	96.05, 104.11, 196.06, 214.07, 232.08, 258.11	+++	
434.09228	$C_{14}H_{28}NO_8Se^+$	434.09238	-0.23	0.76		x						x				-	134.97, 168.98, 293.98, 312.00, 416.08	130.05	+	
435.04004	$C_{13}H_{23}O_{11}Se^+$	435.04001	0.07	2.01	x						x	x				-	244.99	108.05	+	
444.86739	$C_8H_{17}N_2O_4Se_3^+$	444.86785	-1.03	1.03				x						x		x	244.86, 347.84	80.05	+	Németh *et al.* (2013)
446.09233	$C_{15}H_{28}NO_8Se^+$	446.09238	-0.11	0.65, 0.72			x		x						x	x	193.97, 326.02	114.05, 152.06, 172.06, 218.06	++	
447.11604	n.p.	n.p.	n.p.	1.50, 1.54	x				x			x				n.a.	n.a.	n.a.	+	
448.10670	n.p.	n.p.	n.p.	0.76, 1.32	x				x			x				x	326.02	-	+	
460.10880	n.p.	n.p.	n.p.	0.84, 0.90	x				x			x				x	326.02	99.08	+	
463.02100	n.p.	n.p.	n.p.	0.60			x				x	x				-	196.91, 211.92, 300.97, 304.02	160.03	++	
482.99120	n.p.	n.p.	n.p.	1.02	x							x				n.a.	n.a.	n.a.	+	
489.05794	n.p.	n.p.	n.p.	0.72				x				x				x	-	76.02, 116.01, 162.02, 179.05, 233.06, 308.09	+	
523.12784	$C_{16}H_{35}O_{12}Se^+$	523.12883	-1.89	2.08, 2.18	x				x		x	x				-	215.02, 377.07	-	+	
537.14451	$C_{17}H_{37}O_{12}Se^+$	537.14448	0.06	2.33, 2.39		x			x		x	x				-	229.03, 391.08	99.08	+	
552.06109	n.p.	n.p.	n.p.	1.02	x							x				-	284.97	153.06, 177.05	+	
581.10958	$C_{18}H_{33}N_2O_{14}Se^+$	581.10915	0.74	0.60		x				x	x	x				-	167.95, 257.00, 296.00, 314.01, 332.03, 401.04, 545.08	110.06, 166.05, 170.08, 214.07, 232.08	+++	
614.14680	n.p.	n.p.	n.p.	0.77	x						x	x				-	434.08, 596.14	116.04, 235.11	++	

Optimisation of the intra-isotope mass defect filter settings was carried out with using all the 35 compounds detected. A compromise must be set as an increase in the mass padding or in the defect padding parameters increase the lists of both the true and false positive hits. After setting 200 Da for mass padding and 80 mDa for defect padding, the total number of compounds assigned for pattern validation as potentially Se carrying molecules ranged between 206-457, accounting for 4.5-6.3 % of the total number of detected compounds (Table A5). These data seem to cover too many false positive hits, however the practical implementation is reasonable. The outcome of some hundreds of compounds can be easily shortlisted on the basis of absolute mass defect and isotopologue redundancy. Finally, these settings allowed to recover 16 Se species out of the 35 involved in the optimisation process at signal intensity of 2000 counts (Table A6 and A7). Another benefit of this searching method is that several detected species eluted further from the void volume, where the generally hydrophilic Se species are less evidently occurring (*e.g.*, *m/z* 197 and *m/z* 282).

Six accurate mass values matched with previously detected species but only four species could be marked as known in Table 9: selenocystathionine at *m/z* 271.02005 (Figure A2), selenohomocystine at *m/z* 364.95162 (Figure A3), a selenosugar at *m/z* 407.04499 (Figure A4) and *Se*-selenohomocysteinyl-diseleno-homocysteine at *m/z* 444.86739 (Figure A5). In two cases, at *m/z* 254.02899 and *m/z* 313.02972, the MS/MS fragments did not matched of the formerly reported species (that is, *N*-acetyl-*Se*-methylselenomethionine (Németh *et al.* 2013) and γ-glu-*Se*-(methyl)selenocysteine (McSheehy *et al.* 2000) or *N*-acetyl-selenocystathionine (Dernovics *et al.* 2009), respectively). This calls the attention to the fact that accurate mass data is necessary but not sufficient for the identification of Se species.

As an example, the MS and MS/MS spectra of one detected species is presented in the appendix (Figure A6).

5.1.6.3. Structural elucidation of novel selenocompounds: *N*-glycosylated selenolanthionines

The characteristic loss of hexoses (162.05 Da) could be detected during MS/MS fragmentation of eleven species; three of them could be detected in negative ion mode as well ($[M-H]^-$). These molecules accounting one-third of all Se species detected are presumed Se-containing sugars. Selenosugars in plants was first presented by Aureli *et al.* (2012). The species at *m/z* 407.04510 has been detected in several samples including crops and vegetables (Aureli *et al.* 2012, Ruszcynska *et al.* 2017) and may

be considered as ubiquitous Se species, still without structural elucidation. The structural identification of selenosugars generally requires NMR studies, however some properties can be noted on the basis of their MS/MS spectra.

The species at *m/z* 419 and *m/z* 581 share the selenium containing fragments at *m/z* 401.04, 257.00, and 167.95, and non-selenised fragments at *m/z* 214.07 and 232.08. The first fragment appears as an in-source fragment as well. The MS/MS spectra of both species show a series of -18 Da losses that is also characteristic to hexoses (sugars). The presence of the *m/z* 167.95 fragment is a reference to a selenocysteinyl moiety, which – together with the *m/z* 257.00 fragment – indicates that these molecules can be assigned as the mono or di-*N*-glycosides of selenolanthionine (Figure 28, A7, 29). The putative structures presented here are meant to present the origin of the fragments in the molecule, and they are not intended to show the actually formed fragment structure. Selenoamino acids and carbohydrates can form *N*-glycosyl conjugates by their direct reactions, or at alkaline pH, and through condensation in the Maillard reaction scheme when exposed to elevated temperature (Danehy and Pigman 1951). As selenium species are highly unstable under alkaline conditions (pH > 9.5), this way of *N*-glycoside formation can be excluded in this actual case. To the best of my knowledge, *N*-glycosylated selenoamino acids have never been reported in any natural sample. However, it is unclear whether these species were formed *in vivo* spontaneously or *ex vivo* during the freeze-drying process.

The presumable mono- and di-glycosylated lanthionines (S analogues) could be also detected in the high resolution spectra at *m/z* 371.11250 ($C_{12}H_{23}N_2O_9S^+$, Δppm=1.67) and at *m/z* 533.16335 ($C_{18}H_{33}N_2O_{14}S^+$, Δppm=-2.53), shown in appendix (Figure A8). The MS/MS fragmentation enabled the matching of several Se/S or non Se/S containing fragments of the analogues (Figure A8, Table 10, Table 11).

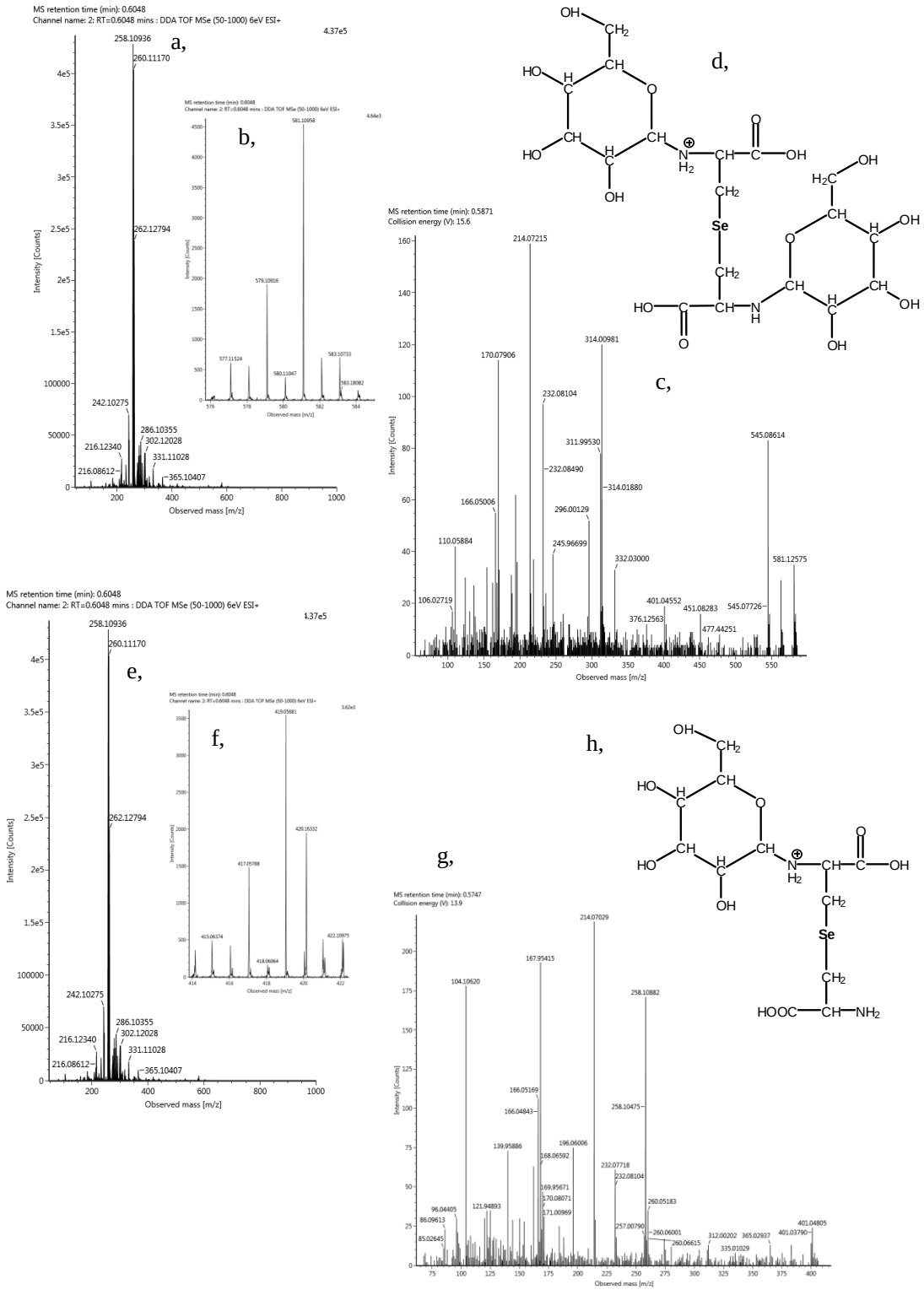

Figure 28. Putative mono- and di-*N*-glycosides of selenolanthionine.
(a) Full scan spectrum, (b) zoomed full scan spectrum, (c) MS/MS spectrum,
(d) structure of selenolanthionine-di-*N*-glycoside.
(e) Full scan spectrum, (f) zoomed full scan spectrum, (g) MS/MS spectrum
(h) structure of selenolanthionine-*N*-glycoside.
Additional MS/MS spectrum of selenolanthionine-di-*N*-glycoside can be found in appendix (Figure A7).

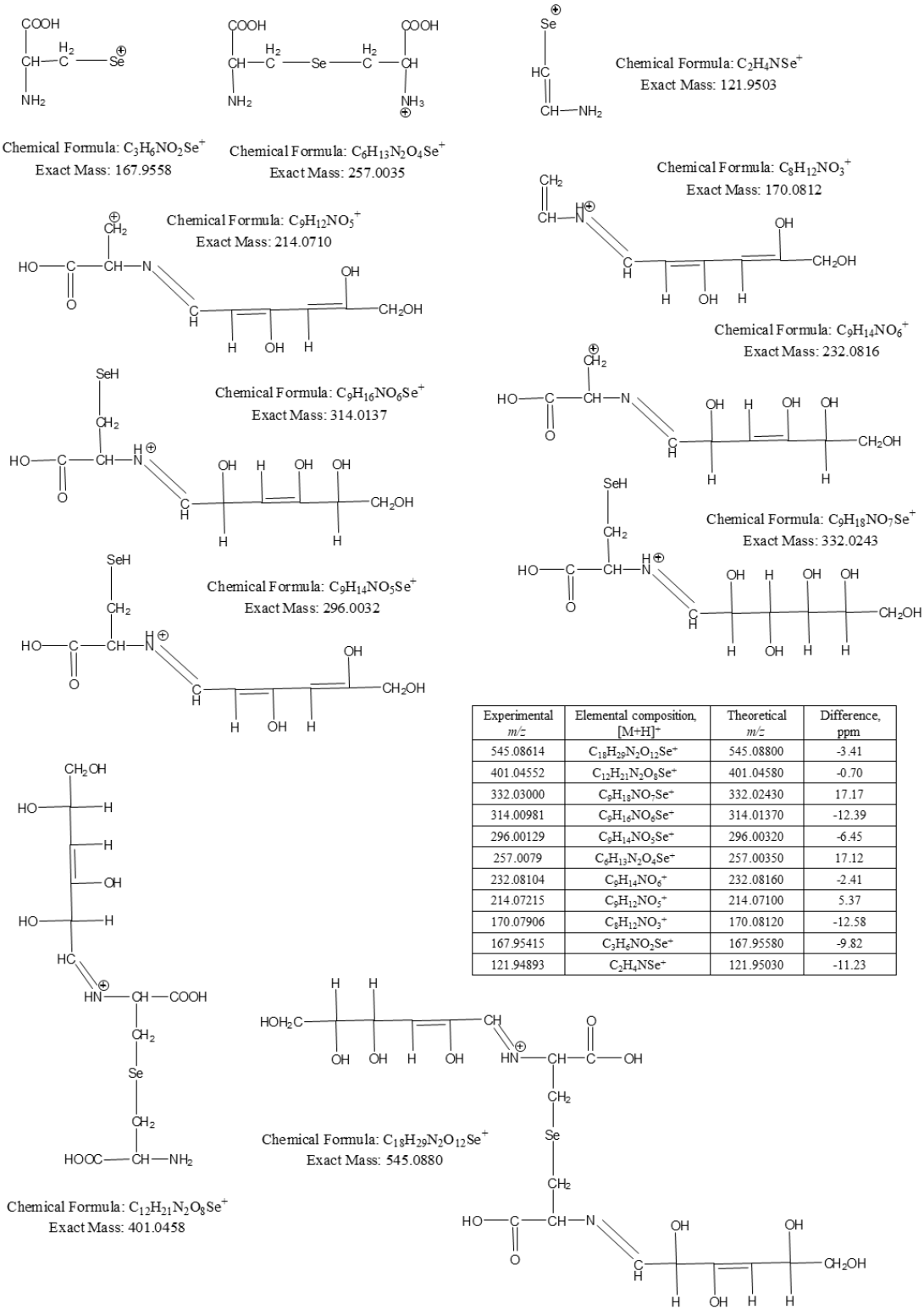

Experimental *m/z*	Elemental composition, $[M+H]^+$	Theoretical *m/z*	Difference, ppm
545.08614	$C_{18}H_{29}N_2O_{12}Se^+$	545.08800	-3.41
401.04552	$C_{12}H_{21}N_2O_8Se^+$	401.04580	-0.70
332.03000	$C_9H_{18}NO_7Se^+$	332.02430	17.17
314.00981	$C_9H_{16}NO_6Se^+$	314.01370	-12.39
296.00129	$C_9H_{14}NO_5Se^+$	296.00320	-6.45
257.0079	$C_6H_{13}N_2O_4Se^+$	257.00350	17.12
232.08104	$C_9H_{14}NO_6^+$	232.08160	-2.41
214.07215	$C_9H_{12}NO_5^+$	214.07100	5.37
170.07906	$C_8H_{12}NO_3^+$	170.08120	-12.58
167.95415	$C_3H_6NO_2Se^+$	167.95580	-9.82
121.94893	$C_2H_4NSe^+$	121.95030	-11.23

Figure 29. Proposed structures of the MS/MS fragments of the *m/z* 419.0568 and 581.1092 compounds, together with mass accuracy data of the fragments.

Table 10. MS/MS fragment matching of di-*N*-glycoside selenolanthionine and lanthionine.

Experimental *m/z* of detected fragment in the ***m/z* 581 Se-analogue** (elemental composition)	Experimental *m/z* of detected fragment in the ***m/z* 533 S-analogue** (elemental composition)
545.08614 ($C_{18}H_{29}N_2O_{12}Se^+$)	497.13639 ($C_{18}H_{29}N_2O_{12}S^+$)
401.04552 ($C_{12}H_{21}N_2O_8Se^+$)	353.10216 ($C_{12}H_{21}N_2O_8S^+$)
314.00981 ($C_9H_{16}NO_6Se^+$)	266.06981($C_9H_{16}NO_6S^+$)
296.00129 ($C_9H_{14}NO_5Se^+$)	248.06214 ($C_9H_{14}NO_5S^+$)
214.07215 ($C_9H_{12}NO_5^+$)	214.06937 ($C_9H_{12}NO_5^+$)
170.07906 ($C_8H_{12}NO_3^+$)	170.08195 ($C_8H_{12}NO_3^+$)
167.95580 ($C_3H_6NO_2Se^+$)	119.18535 ($C_3H_6NO_2S^+$)

Table 11. MS/MS fragment matching of *N*-glycoside selenolanthionine and lanthionine.

Experimental *m/z* of detected fragment in the ***m/z* 419 Se-analogue** (elemental composition)	Experimental *m/z* of detected fragment in the ***m/z* 371 S-analogue** (elemental composition)
401.04805 ($C_{12}H_{21}N_2O_8Se^+$)	353.10454 ($C_{12}H_{21}N_2O_8S^+$)
257.00790 ($C_6H_{13}N_2O_4Se^+$)	209.05841 ($C_6H_{13}N_2O_4S^+$)
232.08104($C_9H_{14}NO_6^+$)	232.08568($C_9H_{14}NO_6^+$)
214.07029 ($C_9H_{12}NO_5^+$)	214.07122 ($C_9H_{12}NO_5^+$)
170.08071 ($C_8H_{12}NO_3^+$)	170.07865 ($C_8H_{12}NO_3^+$)
167.95415 ($C_3H_6NO_2Se^+$)	120.01044 ($C_3H_6NO_2S^+$)

The loss of a deoxyhexose moiety (146.06 Da) is also a specific event in the fragmentation of oligosaccharides. There are two unknown selenohexoses at *m/z* 391.09 and 377.07 (Table 9) which can be associated to a couple of molecules sharing the core molecules together with an additional +146.06 Da sized moiety (at *m/z* 537.15 and 523.13, respectively). The detection of isomers also support the affiliation of selenohexoses and selenohexose-deoxyhexose molecules. The discovery of selenium containing disaccharides opens a new class of molecules that can deposit Se even though their structure cannot be unambiguously assigned on the basis of MS and MS/MS data.

5.1.7. Quantification of selenolanthionine in *C. violifolia* samples

5.1.7.1. Quantification of lanthionine and selenolanthionine with HILIC-QQQ-MS

The ratio of sulphur and selenium analogue compounds together with total S and Se concentration can provide useful information on the accumulation process (Németh and Dernovics 2015). As lanthionine standard is commercially available and SeLan has been in-house synthesised, their quantification could be carried out with HPLC electrospray ionisation – triple quadrupole – mass spectrometry (ESI-QQQ-MS). Hydrophilic interaction chromatography has been chosen as the cationic amino acids show retention on HILIC and the eluents applied are compatible with the ESI ion source. No considerable interferences could be observed at the monitored MRM transitions of the two analytes (Figure 30). The concentration of SeLan was found 4.8 mg g^{-1} DW sample (equal to 1.5 mg Se g^{-1}) while Lan was quantified to be 0.5 mg g^{-1} DW. Accordingly, the molar ratio of Lan:SeLan is about 1:8, which exceeds by far the substitution rate for SeMet in the hyperaccumulator plant *Lecythis minor* seeds where this ratio for Met:SeMet was found to be 1:2 (Németh and Dernovics 2015). Also, the Lan:SeLan molar ratio highly exceeds the quantified total S: total Se molar ratio of 10:1.

Based on this result selenolanthionine accounts for approximately 68% of Se of the water-soluble fraction and about 40% of total selenium in the highly selenised (3.7 g kg^{-1} DW) stem + leaves sample of *C. violifola*; however, the quantification might be biased due to the use of a non-commercial standard.

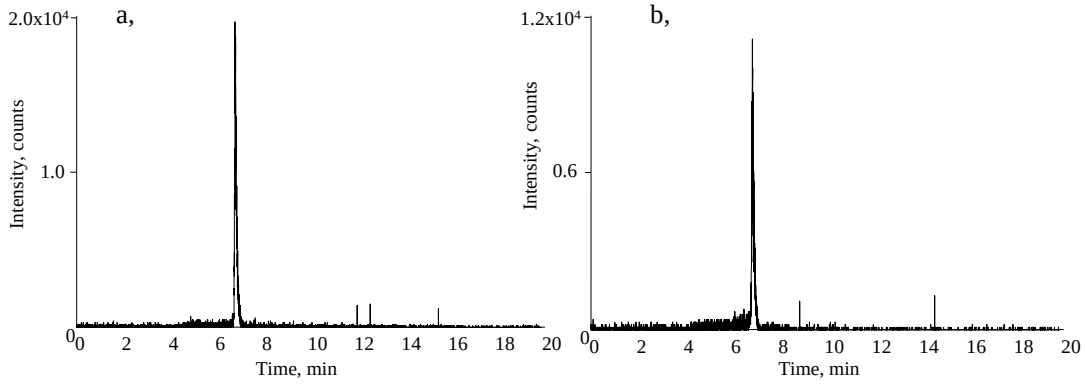

Figure 30. (a) HILIC-ESI-QQQ-MS chromatogram of selenolanthionine from the *C. violifolia* water extract (MRM transition 257→168; retention time: 6.77 min); (b) HILIC-ESI-QQQ-MS chromatogram of lanthionine from the *C. violifolia* water extract (MRM transition 209→120; retention time: 6.83 min).

5.1.7.2. Quantification of selenolanthionine with isotope dilution analysis (IDA)

The final dilution ratio of the water extract of lyophilised leaf sample of *C. violifolia* (261 mg total Se kg^{-1} DW; see Chapters 4.1.3.1 and 5.1.6.1) was 300 mL for 1.0 g lyophilised sample to achieve adequate resolution on the IP-RP setup for quantification through post-column IDA (Figure 31). The SeLan peak eluting at 6.8 min was evaluated and found at the concentration of 77.6 mg Se kg^{-1}, accounting for approximately 30% of the total selenium content of the leaf. Minor selenium species could remained unresolved/undiscovered in the chromatographic peak which could slightly bias the actual value. This case the percentage contribution of SeLan to total Se content is 10% less than the value determined in the highly selenised (3.7 g total Se kg^{-1} DW) pooled (stem + leaves) *C. violifolia* biomass, which might indicate that the relative concentration of this non-proteinaceous selenoamino acid increases by the higher selenium accumulation rate. According to scientific databases (that is, Scopus and Web of Knowledge), this has been the first successful application of the post column isotope dilution LC-ICP-MS technique in Hungary.

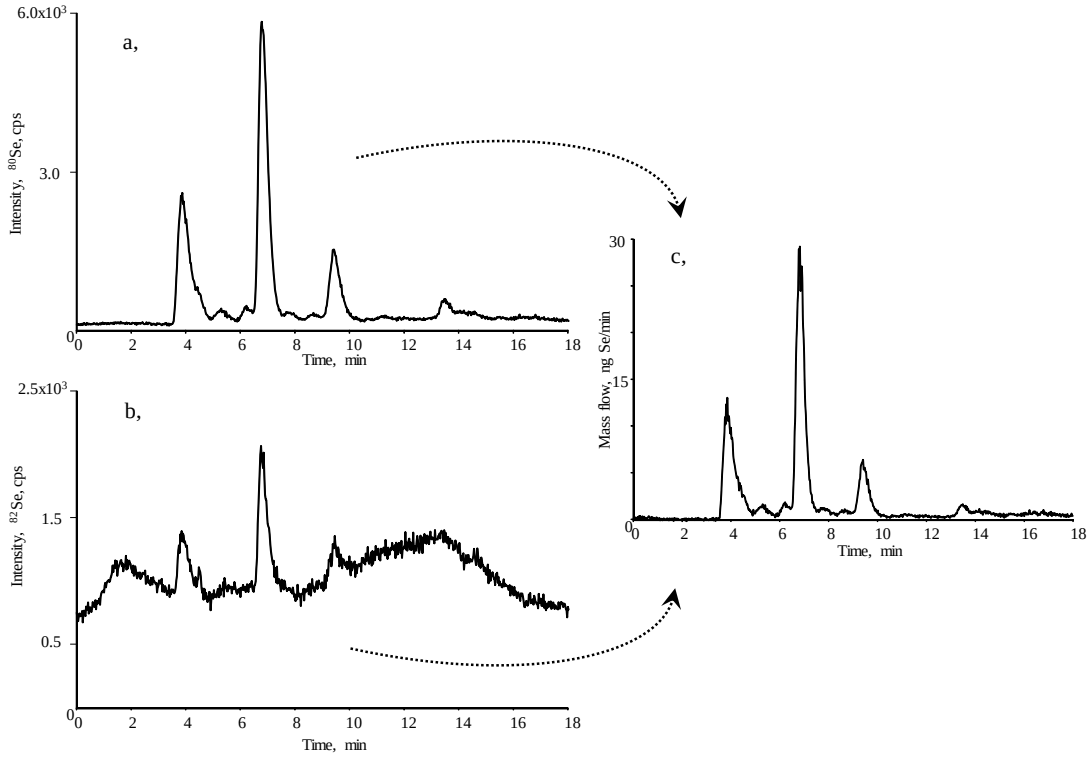

Figure 31. IP-RP-IDA-ICP-MS based quantification of selenolanthionine (eluting at 6.8 min) extracted from *C. violifolia* leaves. (a) LC-ICP-MS chromatogram recorded on ^{80}Se; (b) LC-ICP-MS chromatogram recorded on ^{82}Se used for isotope dilution; (c) selenium mass flow calculated from the $^{80}Se/^{82}Se$ data.

5.2. SELENIUM METABOLISM STUDIES OF *C. VIOLIFOLIA* IN COMPARISON WITH *C. PRATENSIS*

5.2.1. Selenium tolerance and accumulation

Shoot dry weight and root length parameters were chosen for characterising Se tolerance of the plant species at different selenate concentration present in the agar media. *C. violifolia* hyperaccumulator (HA) and the non-HA *C. pratensis* showed similar root lengths (Figure 32a) grown on agar medium without selenate supply but *C. pratensis* shoot dry weight (DW) was 3.5-fold smaller (Figure 32b) likely reflecting different plant species characteristics. Clear differences in Se tolerance was detectable between the two species: the 50% inhibition point on root growth was below 50 µM selenate for *C. pratensis* and 100 µM selenate was its highest tolerated Se concentration where *C. violifolia* was still unaffected (Figure 32a). Root length of *C. violifolia* was 50% inhibited between 200 and 400 µM. Shoot dry weight was not significantly inhibited by Se in either species. Overall, *C. violifolia* is relatively more tolerant to selenate than *C. pratensis*.

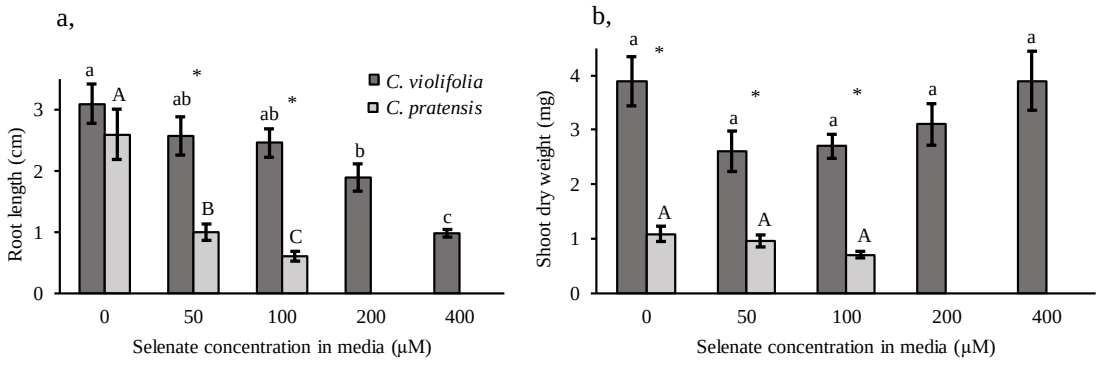

Figure 32. (a) Root length and (b) shoot biomass of *C. violifolia* (Se hyperaccumulator) and *C. pratensis* (control) grown on agar media supplied with different concentrations of Na_2SeO_4. Values shown are the means ± SEM. Different letters indicate statistically different means among treatments within species ($P < 0.05$). Asterisks indicate statistically different means between species within treatments ($P < 0.05$). Note: there was no germination for *C. pratensis* on 200 and 400 µM Se.

Total selenium, sulphur content determined by ICP-OES and the Se:S molar ratio in seedlings at different selenate treatments are shown in Figure 33. Seedlings of both species accumulated ~ 1000 mg Se kg^{-1} DW in shoots at 50 µM selenate supply. *C. pratensis* accumulation decreased to about 50% at 100 µM Se supply and could not survive at higher Se treatments. Se levels in *C. violifolia* shoots increased to 2000 mg kg^{-1} DW and 2700 mg kg^{-1} DW in case of 100 µM and 200 µM Se supply,

respectively, without showing any sign of toxicity while at 400 µM it decreased to a level of 1000 mg kg^{-1} DW similarly to the 50 µM supply. At the highest selenate concentration tested (400 µM) *C. violifolia* was still unaffected in terms of biomass but roots were significantly shorter than the control treatment indicating a Se tolerance ceiling for the HA.

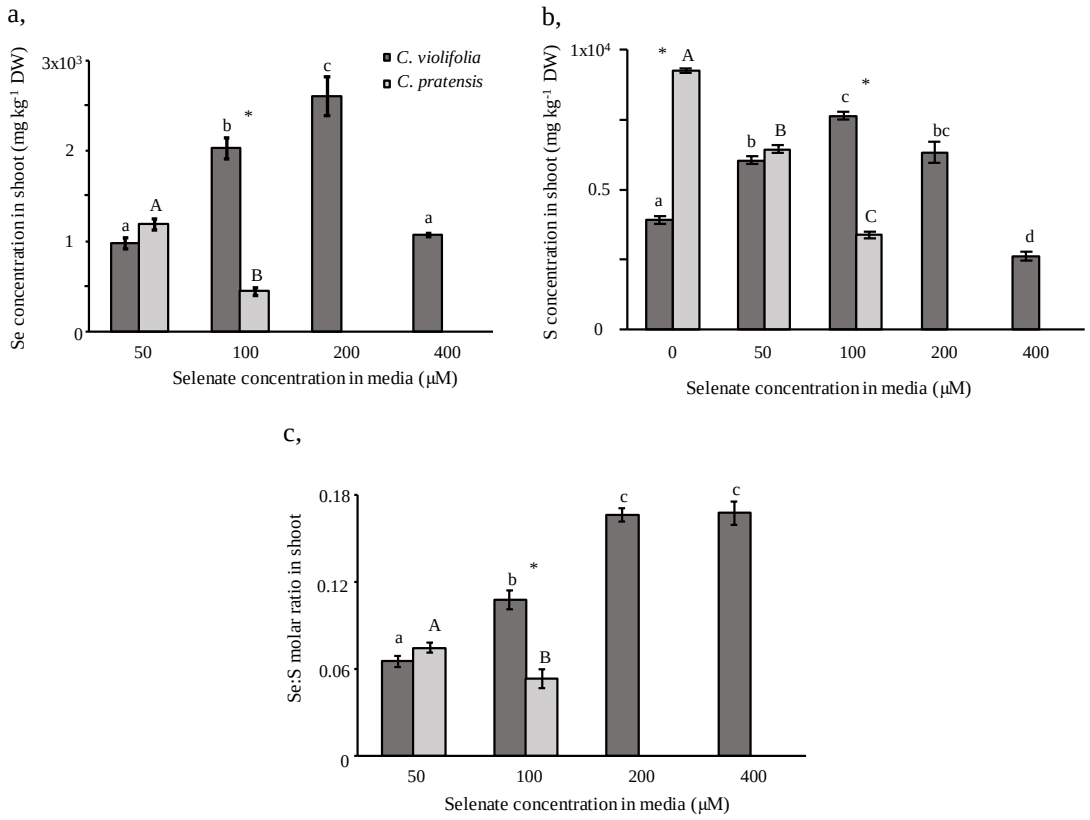

Figure 33. (a) Selenium (b) Sulphur concentration and (c) Se:S molar ratio in shoots of *C. violifolia* and *C. pratensis* grown on agar media supplied with different concentrations of Na_2SeO_4.. Note: In the case of the control treatment, Se concentrations were below the quantification limit. Values shown are the means ± SEM. Different letters indicate statistically different means among treatments within species, and asterisks indicate statistically different means between species within treatment ($P < 0.05$).

The shorter roots at 400 µM may in part explain the decreased shoot Se accumulation at that level as well. It can be concluded that *C. violifolia* is capable of higher Se accumulation than *C. pratensis* however *C. pratensis* can also reach significant tissue Se levels but its accumulation breaks down at elevated selenate concentrations which is an indicative of a lack of Se tolerance. Neither species showed evidence of growth stimulation by Se at the levels supplied, which is in contrast to several Se HA species, *e.g.*, *Symphyotrichum ericoides*, *Astragalus bisulcatus* and *Stanleya pinnata* (El Mehdawi *et al.* 2012, El Mehdawi *et al.* 2014). The Se:S molar

ratio in *C. violifolia* shoot increased with increasing selenate supply. At 400 µM Se treatment the ratio remained the same compared to 200 µM despite the lower Se concentration. With increasing Se uptake, *C. violifolia* showed increasing S uptake until 100 µM similarly to other Se HA *Astragalus bisulcatus* (El Mehdawi *et al.* 2014) and to secondary Se accumulator *Brassica juncea* (Harris *et al.* 2014). Opposite pattern was shown by *C. pratensis*: the S concentration decreased with higher selenate supply indicating different Se-S interactions between the HA and non-HA species.

The uptake capacity of different forms of Se (selenate, selenite) and the interactions of sulphate and phosphate were studied on mature plants grown in gravel, total Se and S concentrations in shoots and roots and their molar ratios were determined as shown in Figure 34.

Concerning the plants supplied with 20 µM selenate in gravel until the 4-week stage, both *Cardamine* species accumulated Se around 400 mg kg^{-1} DW in their shoot. However, in case of selenite treatment (20 µM) Se accumulation was significantly (~2-fold) higher for HA *C. violifolia* in compared to the non-HA species. In both species shoot Se accumulation was higher from selenate than from selenite (~10-fold) which is consistent with earlier studies and reflects the different transport mechanisms (de Souza *et al.* 1998). The two *Cardamine* species did not show any difference in terms of the sulphate ion effect on selenate uptake. The raised sulphate ion concentration inhibited selenate uptake (~5-fold) as both are taken up by the same group of sulphate transporters (Schiavon and Pilon-Smits 2017). The behaviour of HA *C. violifolia* in this respect is in contrast to other Se HA plants such as *S. pinnata* which have a more selenate-specific uptake that is less inhibited by sulphate (El Mehdawi *et al.* 2018, Harris *et al.* 2014, White *et al.* 2007). The Se:S molar ratio was ~1.5-fold and ~2-fold higher in *C. pratensis* and in *C. violifolia* shoots, respectively, compared to that in the medium, when treated with 20 µM selenate (0.08 Se:S molar ratio in the treatment solution: 1/4th Hoagland's solution contains 250 µM sulphate). The Se:S ratio in the shoot was ~ 70% compared to the ratio in the medium when the plants were supplied with 20 µM selenate + 5 mM sulphate (20-fold lower Se:S ratio in the treatment solution).

Phosphate did not inhibit selenite uptake in either species contrary to expectations and thus it seems that this process is not mediated by phosphate transporters in these plants and may involve anion channels as reported for some species (Schiavon and Pilon-Smits 2017).

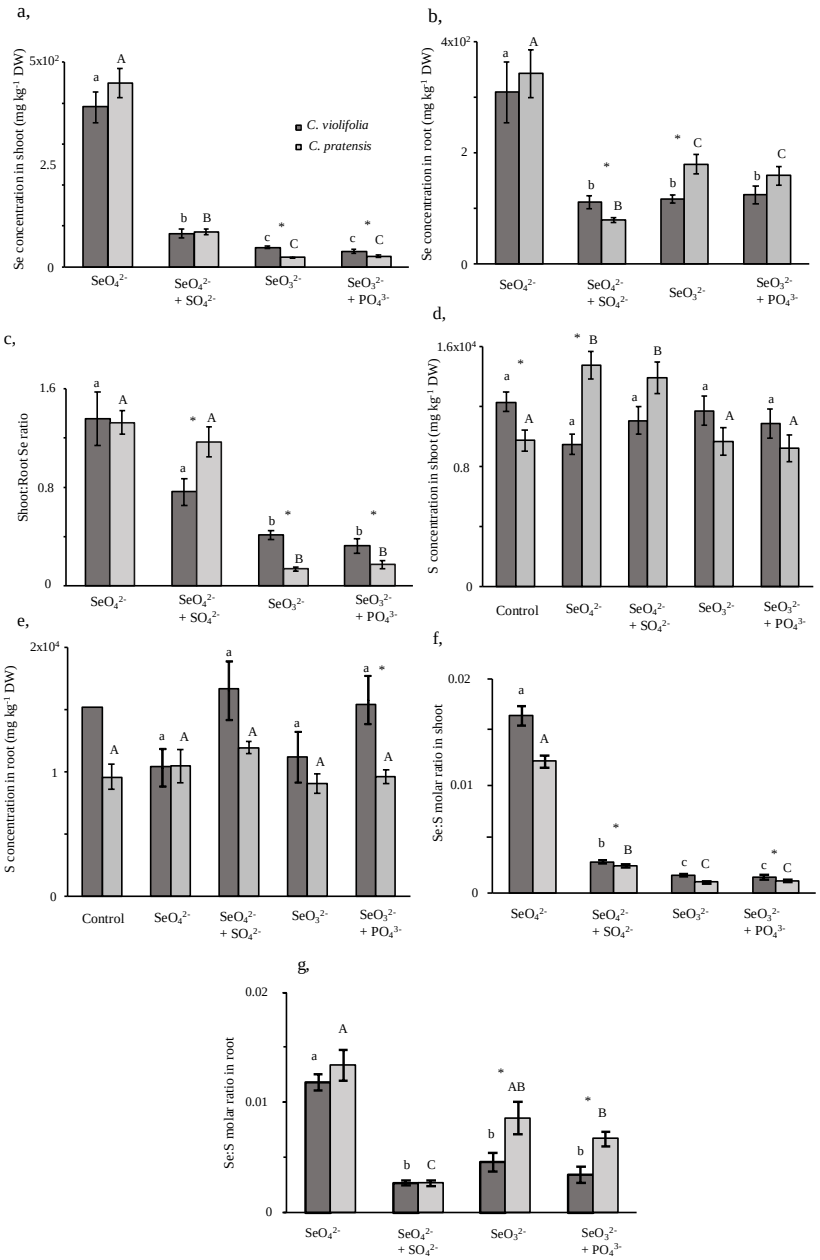

Figure 34. (a) Selenium concentration in shoots (b) in roots, (c) the shoot:root Se ratio, (d) S concentration in shoots, (e) in roots, (f) Se:S molar ratio in shoots and (g) in roots of *C. violifolia* and *C. pratensis* grown on Turface® gravel media subjected to different treatments. Note: In the case of the control treatment, Se concentrations were below the quantification limit and in case of *C. violifolia* the root dry material was not enough for more replicates and was excluded from statistical evaluation. Values shown are the means ± SEM. Different letters indicate statistically different means among treatments within species, and asterisks indicate statistically different means between species within treatment ($P < 0.05$).

The shoot:root Se ratio differed between the two species in some respects. The ratio was higher for *C. pratensis* than for *C. violifolia* in case selenate plus sulphate treatment because of higher root Se level in the HA; no such difference was observed

when only selenate was supplied. In case both selenite treatments (with or without phosphate) the shoot:root Se concentration ratio was 2-3 fold higher in the HA species.

C. violifolia generally showed higher Se:S molar ratio in their shoots than *C. pratensis* while *C. pratensis* had higher Se:S ratio in roots however it should be noted that the differences were not found significant in all cases at the statistical evaluation (Figure 34). The difference in translocation between Se and S in HA may be caused by a Se-specific root-to-shoot transporter, or may point to the translocation of Se and S in different chemical forms that use different transporters (*e.g.*, organic Se *vs.* inorganic Se).

5.2.2. Chlorophyll fluorescence, antioxidant capacity and total phenolic content

Assessing the physiological conditions of the plants under Se treatment was carried out by measuring Chl fluorescence, antioxidant capacity and total phenolic content.

Chlorophyll fluorescence parameters were measured on 4-week old mature plants after 10 days of treatments and are shown in Figure 35. Only one parameter of the Chl fluorescence data differed significantly among the two plant species: *C. violifolia* had lower relative Chl content for the selenate treatment compared to *C. pratensis. C. violifolia* appeared to have overall lower relativ Chl content and higher non-photochemical quenching (NPQt), but this was not significant except for the above mentioned case. It may be interpreted to be indicative of less well functioning light reactions however no sign of enhanced stress is apparent from the other physiological measurements. Among treatments and within species the selenite plus phosphate treatment had a significant effect only for *C. violifolia*, causing higher NPQt and photochemical quenching (Phi2) compared to either selenite alone or control treatments. Similar but non-significant pattern could be seen for *C. pratensis*. It is possible that the high phosphate concentration caused salinity stress. The observed effects do not seem to be Se-related because the selenite-only treatment did not show a similar effect. Zhou *et al.* (2018) found that high selenite concentration suppressed the expression of photosynthetic genes is *C. hupingshanensis*; however in that study 50-fold higher selenite concentration was used than in our case.

25 µM selenate supply did not have any significant effect on total phenolic content or on total antioxidant activity of seedlings grown on agar media (Table 12). The two species showed a difference in total phenolic content for *C. pratensis* having ~30 % higher levels.

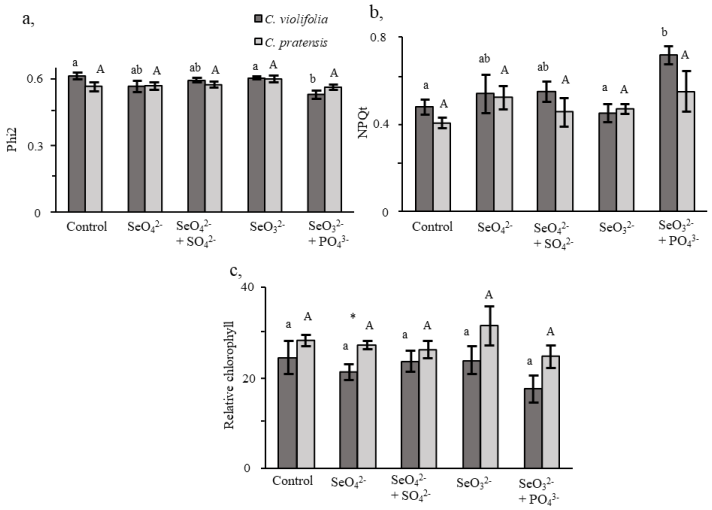

Figure 35. Chlorophyll fluorescence parameters of *C. violifolia* and *C. pratensis* grown on gravel media with different treatments. (a) Phi2, the fraction of light energy quenched photochemically due to electron transport through photosystem 2; (b) NPQt, fraction of light energy quenched via non-photochemical processes; (c) relative chlorophyll content (all parameters are unitless). Values shown are the means ± SEM. Different letters indicate statistically different means among treatments within species, and asterisk indicates statistically different means between species within treatment ($P < 0.05$).

Table 12. Total phenolic content and antioxidant activity of *C. violifolia* and *C. pratensis* grown on agar media supplied with or without 25 µM Na_2SeO_4. Total phenolic content is expressed in Gallic Acid Equivalents. Antioxidant activity is expressed as Trolox Equivalent Antioxidant Capacity. Different uppercase letters indicate statistically different means ($P < 0.05$).

Species	Se in media	Total phenolic content (mg GAE g^{-1} DW)	Antioxidant activity (µmol TEAC g^{-1} DW)
C. violifolia	+	18 ± 1^{a}	168 ± 12^{a}
C. violifolia	-	17 ± 2^{a}	179 ± 19^{a}
C. pratensis	+	26 ± 5^{b}	213 ± 24^{a}
C. pratensis	-	24 ± 8^{b}	197 ± 42^{a}

5.2.3. Selenium localisation and speciation based on X-ray microprobe analysis

X-ray microprobe analysis was carried out on seedlings grown on agar media supplied with selenate and on leaves of selenate/selenite treated mature plants grown on gravel media. Besides, the XANES spectra of the synthesised selenolanthionine was also recorded.

Selenate supplied seedlings of the two species showed some differences in terms of Se localisation (Figure 36). The HA *C. violifolia* showed pronounced concentration of Se in the tips of the shoot and roots, at the apical meristems, while the non-HA *C. pratensis* tended to concentrate Se in its vasculature.

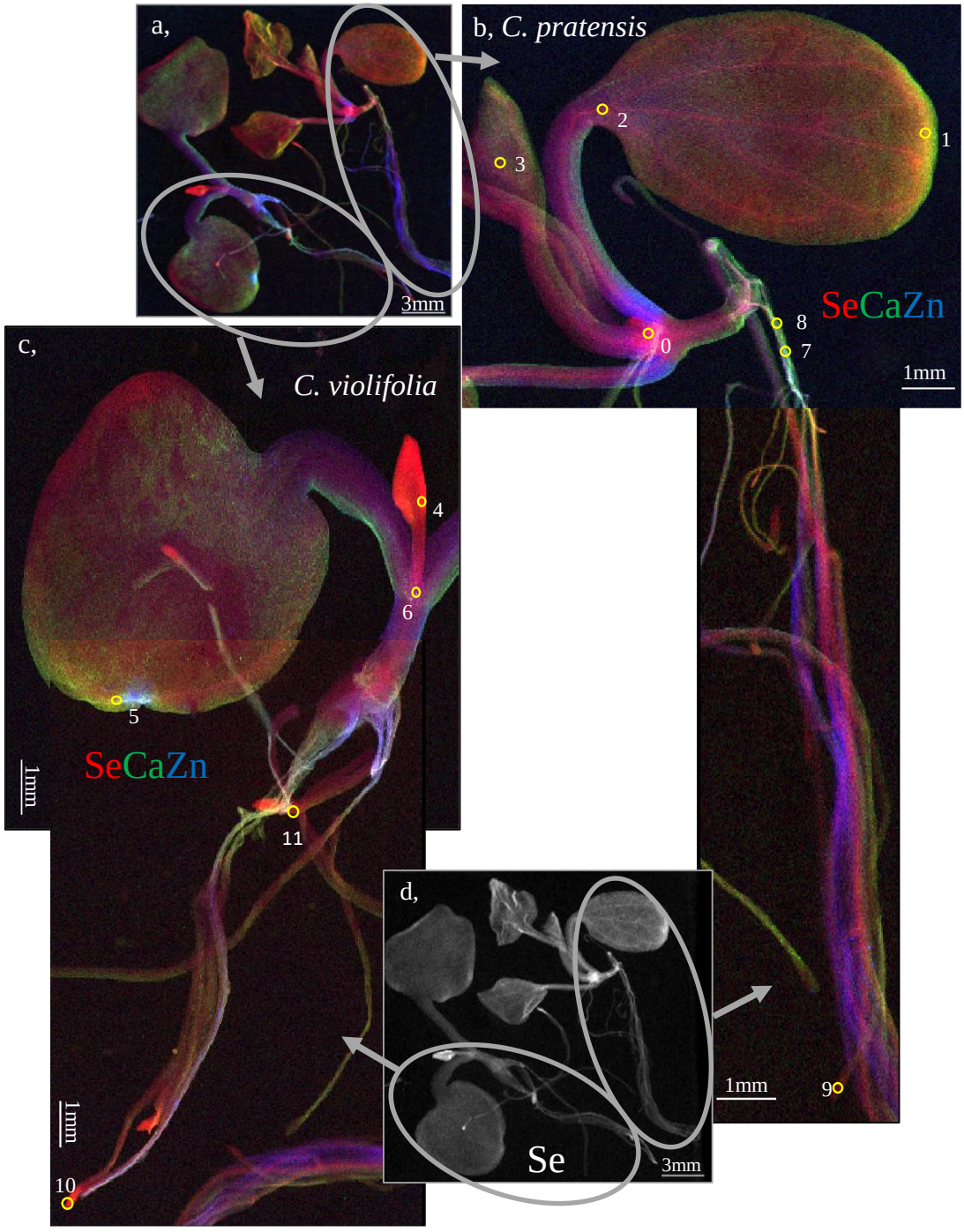

Figure 36. Micro focused X-ray fluorescence (µXRF) elemental maps of seedlings from *C. violifolia* (a, c, d) and *C. pratensis* (a, b, d) grown on agar media supplied with 25 µM selenate. Selenium is shown in red (or in white, b), calcium in green, zinc in blue. Yellow circles denote locations where XANES spectra were collected to determine Se speciation.

In case of the leaves from selenate treated 4-week old plants *C. violifolia* showed a more pronounced Se signal along the leaf edges and in undefined discrete locations along the outside of the petiole (Figure 37). Both species also showed relatively low concentration of Se in the vasculature. Leaf curling cannot be excluded as a reason for the higher Se signal in the leaf periphery, but it was detected only in the HA.

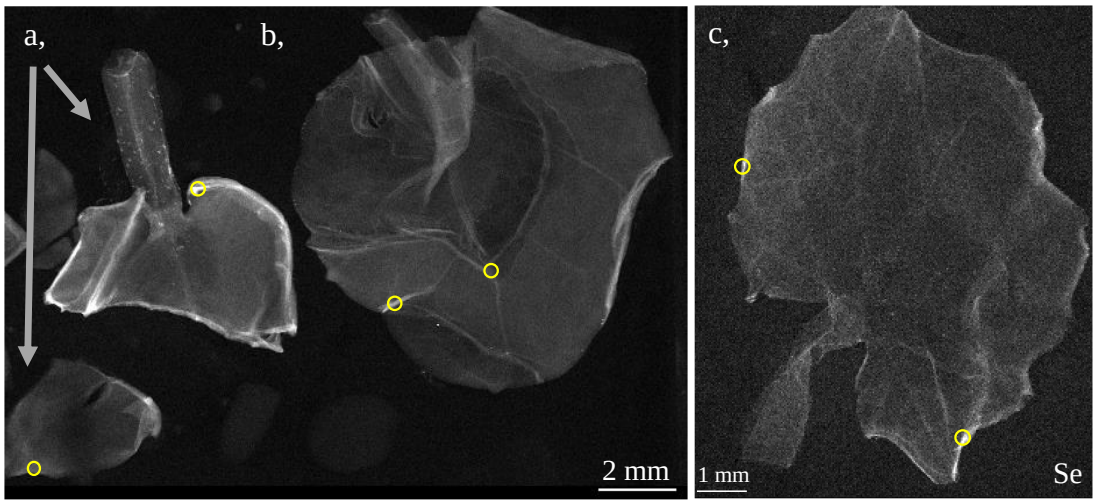

Figure 37. Micro focused X-ray fluorescence (XRF) elemental maps of leaves from 4-week old *C. violifolia (*a,c) and *C. pratensis* (b) grown on Turface® media supplied with 20 µM selenate (a,b) or selenite (c) for 10 days. Selenium is shown in white. Yellow circles denote locations where XANES spectra were collected to determine Se speciation. Note: *C. pratensis* treated with selenite is not shown because of lack of sufficient Se signal. Leaf a) broke during transfer of frozen leaf to the XRF cryostage.

Cui *et al.* (2018) concluded in an earlier µXRF study that in HA *Cardamine* species Se was primarily located in the cortex, endodermis and vascular cylinder in roots, while in the epidermis, the cortex and vascular bundle of stems; also, Se was concentrated in the leaf veins and the peripheral parts of leaves. These results are in agreement with our leaf data of *C. violifolia.* Other HA species also showed Se sequestration along the leaf periphery, *e.g.*, *Astragalus bisulcatus* and *Stanleya pinnata* (Freeman *et al.* 2006a). The concentration of Se in the leaf periphery of the HA may be indicative of specialised Se sequestration mechanisms in areas where Se can be tolerated to the highest extent and where it may offer the most ecological benefits via herbivore or pathogen protection. Concentration of Se in the leaf vasculature, as seen particularly in non-HA *C. pratensis*, is similar to what was found in other non-HA Brassicaceae such as *Brassica juncea* (Freeman *et al.* 2006a); it may reflect a more limiting uptake rate from the xylem into the mesophyll cell.

The µXANES based Se speciation of the seedlings were similar for both species. Yellow circles on Figures 36 and 37 denote the locations where XANES spectra were collected. Both species accumulated predominantly (~85%) organic Se with a "C-Se-C" configuration (Table 13). As selenolanthionine showed similar XANES spectra compared to other organic Se compounds containing "C-Se-C" configuration such as selenomethionine or *Se*-(methyl)selenocysteine, it cannot be determined which compound(s) is/are responsible for the signal (Figure 38). In the root of *C. violifolia* almost all Se was in the same form; unfortunately XANES spectra of *C. pratensis* root were of insufficient quality for fitting, because of lower Se signal intensity.

Table 13. Selenium speciation in *C. violifolia* (*C. v.*) and *C. pratensis* (*C. p.*) as determined by XANES LSQ fitting. Values show the average of the XANES spectra within species and organ, for each of the two experimental setups. Corresponding XRF images for agar-grown plants are shown in Fig. 36; gravel-grown XRF images are shown in Fig. 37. Numbers for each form of Se represent the percentage of total Se. ND: not detected. C-Se-C may include SeMet, MeSeCys, SeLan, etc.

Species	Growth media	Supplied Se form	Organ	Se (VI) (%)	Se(IV) (%)	C-Se-C (%)	Se(0) (%)	$Se(GSH)_2$ (%)	$SeCys_2$ (%)
C. v.	gravel	SeO_3	leaf	ND	6	91	ND	4	ND
C. v.	gravel	SeO_4	leaf	1	ND	87	ND	4.5	12
C. p.	gravel	SeO_4	leaf	44	ND	59	ND	0	ND
C. v.	agar	SeO_4	shoot	2	4	86	5	4	ND
C. p.	agar	SeO_4	shoot	8	6	84	ND	2	ND
C. v.	agar	SeO_4	root	2	ND	96	ND	1	ND

Se speciation showed differences between the two *Cardamine* species when sampled at the 4-week old stage. In case of selenate treatment the leaf of *C. violifolia* contained ~ 90% "C-Se-C" compounds while *C. pratensis* only contained ~56% and ~44% selenate, the form of Se supplied. Selenite supplied *C. violifolia* accumulated about 90% of Se in organic "C-Se-C" compounds and no adequate signal could be obtained from *C. pratensis*. The speciation differences between the mature stages can be possibly caused by different relative enzyme activities at developmental stages; it is also possible that the differences in selenate supply affected the speciation outcome.

The finding that at the mature plant stage the main form(s) of Se in the HA *C. violifolia* had "C-Se-C" configuration and the non-HA had relatively more selenate shows similarities to former studies where *S. pinnata* and *A. bisulcatus* had been compared with non-HA relatives (Alford *et al.* 2014, Freeman *et al.* 2006a).

The accumulation of relatively more organic Se indicates that the HA posses a more active sulphate/selenate assimilation pathway, converting selenate to organic "C-Se-C" forms; however the "C-Se-C" form of Se in the different HA species covers different Se species and their identification is highly required. *A. bisulcatus* and *S. pinnata* were found to contain mostly *Se*-(methyl)selenocysteine according to LC-MS based data and it was shown that *S. pinnata* also contains selenocystathionine.

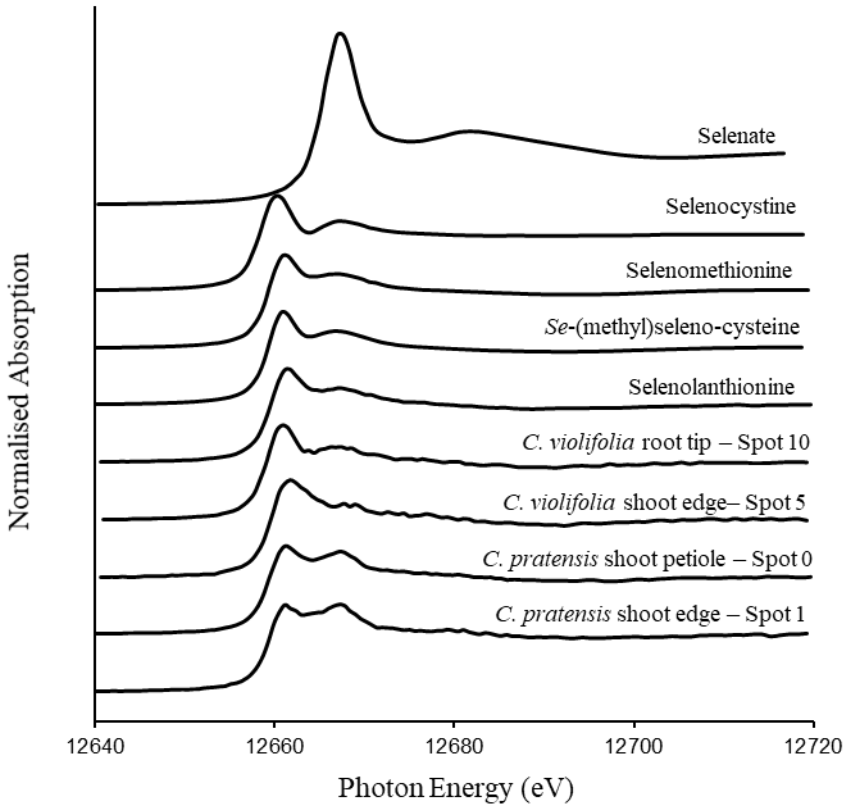

Figure 38. µXANES spectra of selenium standards (sodium selenate, selenocystine, selenomethionine, *Se*-(methyl)selenocysteine, selenolanthionine) and *C. violifolia* and *C. pratensis* seedlings (spots denoted in Figure 36).

The collected XANES data regarding *C. violifolia* contains mainly organic Se in "C-Se-C" form; this is in agreement with the above described selenolanthionine identification by LC-ICP-MS, LC-ESI-MS and chemical synthesis. Cui *et al.* (2018) investigated Se species in HA *Cardamine* by µXANES and found the majority of Se in the form of "C-Se-C" in roots and stems, but of "C-Se-" in leaves using selenocystine as model compound. According to Table 13, LSQ fitting indicated 12% of Se in the form of "C-Se-Se-C" in the leaf of selenate supplied *C. violifolia* grown on gravel media. Therefore, SCX-ICP-MS analyis was found to be necessary to determine whether selenocystine might be responsible for this signal. It should be

noted that the lack of $SeCys_2$ in the water extracts doesn't exclude the possible presence of minor water soluble "C-Se-Se-C" species such as selenohomocystine and its derivatives (Németh *et al.* 2013) or even some plant proteins (Cheajesadagul *et al.* 2014) where inherent "S(e)-S(e)" bonds can be present (*e.g.*, like in the granule bound starch synthase in rice; Uniprot entry Q0DEV5).

5.2.4. Investigation of the presence of selenocystine by SCX-ICP-MS in *Cardamine* samples

As selenocystine is a commercially available standard, its presence or absence in a sample can be determined with LC-ICP-MS on the basis of retention time matching. Strong cation exchange chromatography of the water extract of *C. violifolia* root (157 mg total Se kg^{-1} DW) and leaf samples (261 mg total Se kg^{-1} DW) collected in the Yutangba region are shown in Figures 39a and c, respectively. The highest peaks eluting at ~3 min correspond to the previously identified selenolanthionine. Both leaf and root extracts were spiked to 200 ng mL^{-1} selenocystine concentration, calculated for Se (Figures 39b and d). The peak of selenocystine eluted at 3.5 min between two peaks originating from the samples, which indicated that no selenocystine was present in considerable amount in the water extracts of the leaf and of the root. SCX chromatogram of the water extract of cultivated *C. pratensis* leaf sample (324 mg total Se kg^{-1} DW) is shown in Figure 40. Inorganic and other anionic Se species eluted in the void volume at the retention time of 1.1 min while several low intensity Se compounds eluted later. The peaks eluting at 4.6 min and 7.2 min matched the retention times of *Se*-(methyl)selenocysteine and SeLan, respectively, however their intensity was too low for reliable identification. In order to check whether the most abundant organic Se compound eluting at 12.1 min might be selenocystine, the extract was spiked to 500 ng mL^{-1} $SeCys_2$ (calculated for Se). The spiking procedure indicated no selenocystine was present in the leaf water extract in considerable amounts as a separate peak appeared at 11.9 min on the chromatogram.

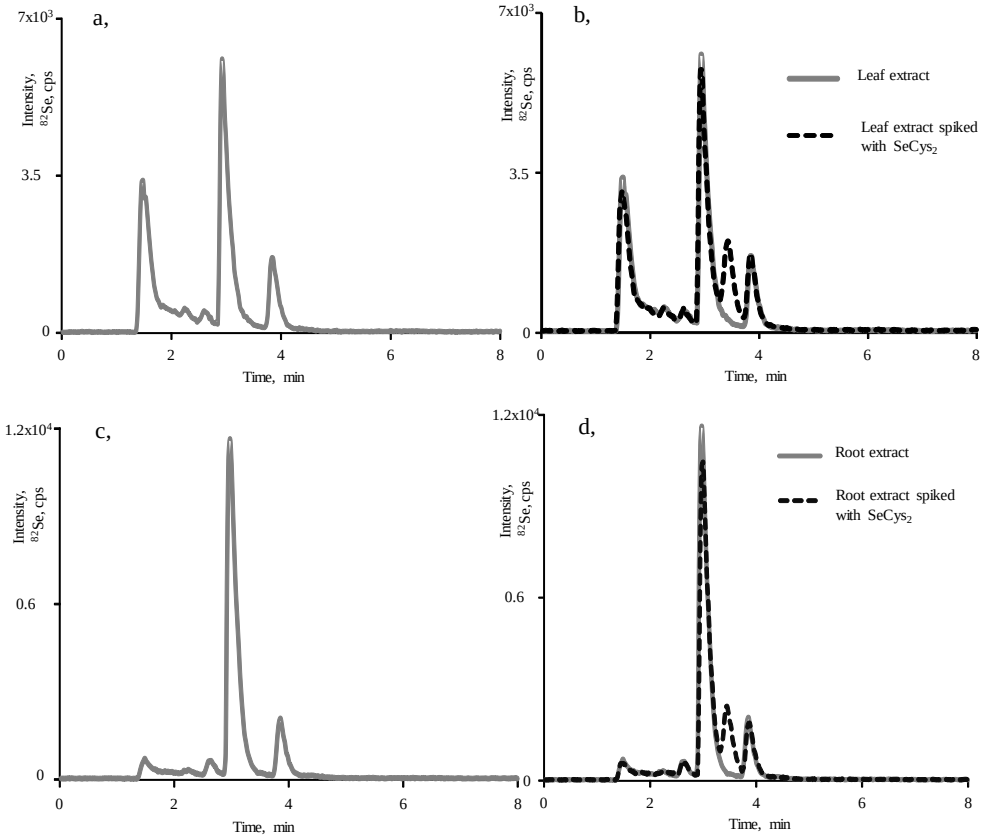

Figure 39. Strong cation exchange (SCX)-ICP-MS chromatogram of *C. violifolia* (a) leaf, (c) root water extract and (b, d) each spiked to 200 ng mL^{-1} selenocystine (dashed line).

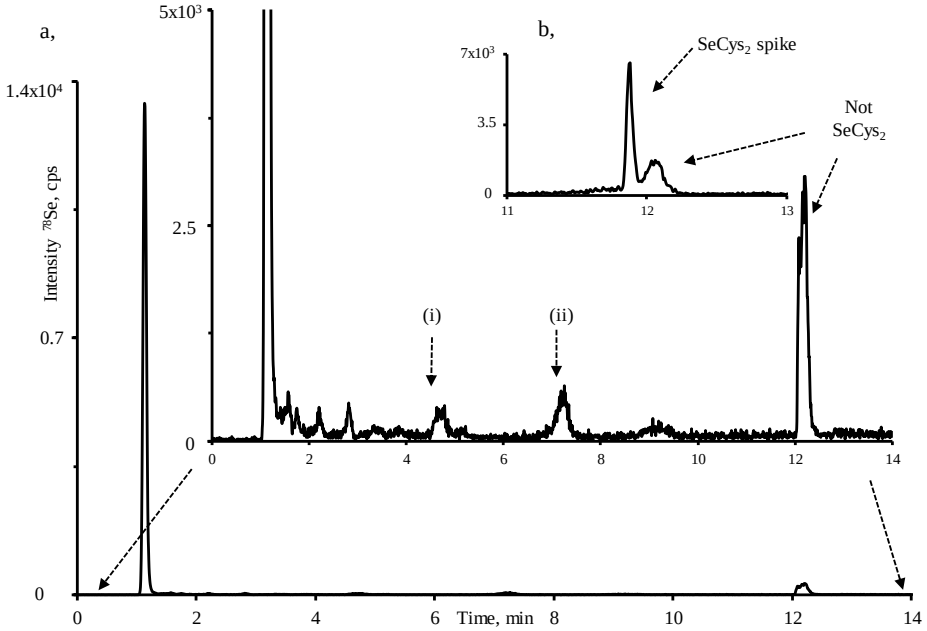

Figure 40. (a)Strong cation exchange (SCX)-ICP-MS chromatogram of selenium enriched non-HA *C. pratensis* leaf water extract and its spike to 500 ng mL^{-1} selenocystine (see the inset (b)). Signs of (i) and (ii) refer to the retention time of *Se*-(methyl)selenocysteine and selenolanthionine, respectively.

6. CONCLUSIONS AND SUGGESTIONS

Cardamine violifolia is a species from the genus *Cardamine*, which is one of the less studied genera of the Brassicaceae family. This latter has been in the focus of selenium speciation for decades due to the highly intense sulphur and selenium metabolism and to its evident importance in food industry. The basic instrumental approaches usually addressed for the selenium speciation of Brassicaceae plants, that is, one dimensional (mostly strong anion exchange) chromatographic purification followed by ICP-MS based identification has been referred / cited by so many research groups that analysts might believe it is not only a common but analytically well-established method.

This PhD thesis proves that such a general approach shouldn't be followed without a critical assessment, even in the case of samples arriving from the same plant family. One dimensional anion exchange purification has been unable to provide an adequate basis for the direct identification of even an extremely abundant selenium species, selenolanthionine. Taking into account that XRF and XANES cannot distinguish this "C-Se-C" type species from well-known selenium species such as selenomethionine and *Se*-(methyl)selenocysteine, it might be assumed that this non-proteinaceous selenoamino acid (maybe not alone…) has already escaped several identification trials in laboratories dealing with plant selenium accumulation before it could be clearly assigned in our studies. Without identification, no conclusion can be drawn about any concerned plant metabolic pathway in any plant, therefore the responsibility of the analysts providing such data is crucial and definitely influences all the upcoming research strategies.

Clearly, numerous papers published in the 2000's and 2010's should be carefully re-evaluated in this term, as seemingly "closed" and "completely described" metabol(om)ic information might derail future efforts and studies in this field. Indeed, the complexity of selenium metabolism (as evidenced by the 35 water soluble selenium species that were extracted from naturally selenium enriched, wild-grown plant biomass) should indicate that no scientist should stop after spotting a few selenium compounds in the actual sample and claim that all the compounds required for the unambiguous description of a metabolomic pathway are reported.

Accordingly, selenium speciation oriented studies should follow a workflow that ensures a reliable identification strategy, possessing access to LC-ICP-MS and LC-

ESI-HR-MS facilities, under a strict – and sometimes quite basic – quality assurance control: well, the fact that no direct identification can be done for any compound in the chromatographic void volume cannot be regarded as a novel requirement. XRF and XANES studies (especially if feed or food industry related experiments are running) must be accompanied with comprehensive (sometimes ultimate) ESI-MS based identification processes to support/decline XRF / XANES derived hypotheses. Taking into account that IDA experiments can provide the quantification of species without commercially available standards, limits are more and more pushed apart in selenium speciation.

The identification of the main selenium species in the water extract of *Cardamine violifolia* as selenolanthionine, a non-protein building amino acid which has never been identified in any Se containing sample before, the detection of numerous unknown Se species (including several selenosugars) and the physiological differences in contrast to other hyperaccunulators indicate the function of a unique, still non-elucidated metabolic pathway for Se detoxification in *C. violifolia*.

Concerning the limits and future goals, three aspects must be listed. First, the successful spotting/seeking of selenium metabolites in ESI-MS data has still been a challenging task for almost a decade on, calling for a straightforward bioinformatic tool. Second, the ultimate identification of selenium species definitely demands NMR applications, which in turn, requires highly efficient and non-invasive sample preparation protocols. The identification of new Se species (such as selenoamino acids, their derivatives or selenosugars) reaching significant concentration in plants calls the attention to the need of their nutritional physiological evaluation.

7. THESIS STATEMENTS

1) I identified the main selenometabolite, selenolanthionine, in the water extract of selenised *Cardamine violifolia* with the help of high resolution mass spectrometry that was assisted with the in-house chemical synthesis of the selenolanthionine standard. This selenium species has never been unambiguously identified before in any selenium containing sample.
2) I quantified selenolanthonine (accounting for ~30% of the total Se) from *Cardamine violifolia* derived samples with the help of a post-column isotope dilution LC-ICP-MS analysis. This was the first successful application of this technique in Hungary.
3) I revealed the complexity of the water soluble selenometabolome of naturally grown and naturally selenium enriched *Cardamine violifolia* leaf sample. Besides the presentation of 35 selenium species (apart from selenolanthionine) I reported for the first time the presence of an *N*-glycosylated selenoamino acid, *i.e.*, mono- and di-*N*-glycosylated selenolanthionines in a natural sample.
4) By conducting a comprehensive experiment regarding selenium-related physiological and biochemical properties of *C. violifolia* in comparison with related species *C. pratensis*, I presented that *C. violifolia* shows clear selenium-related physiological and biochemical differences compared to *C. pratensis* and other Se hyperaccumulators: *C. violifolia* is capable of higher Se accumulation and more tolerant to Se than *C. pratensis* however its growth is not stimulated by Se.
5) I recorded for the first time the μXANES spectra of a synthesised selenolanthionine standard which showed identical spectra with other "C-Se-C" bond containing compounds. I analysed for the first time the selenium localisation and speciation in intact tissues of *C. violifolia* and *C. pratensis* by X-ray microprobe analysis. I concluded that the results show similarities to other hyperaccumulator and related non-accumulator species: *C. violifolia* concentrated Se along the leaf periphery while *C. pratensis* in the vasculature. Mainly organic Se in the "C-Se-C" bond was found in mature *C. violifolia* plant, according to μXANES results, while selenate-supplied mature *C. pratensis* contained approximately half selenate and half "C-Se-C" bond containing compounds.

8. SUMMARY

Cardamine violifolia (family Brassicaceae) is the first discovered selenium (Se) hyperaccumulator species from the genus *Cardamine*, originating from the naturally seleniferous region Yutangba, Enshi, China. The plant is cultivated for phytoremediation purposes, soil reclamation and food/feed supplement production.

In my study I intended to investigate the selenium related characteristics of *C. violifola* including selenium speciation and physiological experiments.

The identification of selenometabolites was addressed by different extraction procedures and the complementary use of liquid chromatography inductively coupled plasma (inorganic) and high resolution organic mass spectrometry setups. No considerable amount was found of the "usual" organic species (that is, selenomethionine and *Se*-(methyl)selenocysteine) that are often formed in hyperaccumulator plants; moreover, the inorganic selenium content including elemental Se accounted only for less than 20% of the total Se. In our study the application of an orthogonal chromatographic purification allowed for the identification of the main selenometabolite, selenolanthionine, in the water extract of *C. violifolia* selenium hyperaccumulator plant species. This non-protein building amino acid has never been identified before in any selenium containing sample unambigously. It is of note that several conflicting LC-based chemical speciation reports have been published on the putatively same selenium compound from the putatively same *Cardamine* species (Yuan *et al.* 2013, Cui *et al.* 2018), but the identification of selenolanthionine was confirmed in our case with high resolution MS data and chemical synthesis as well. Our results warn that the application of at least two orthogonal separation mechanisms and the combination of inorganic (LC-ICP-MS) with high resolution organic mass spectrometry (ESI-MS) are usually required for adequate species assignment.

Species-unspecific (post-column) isotope dilution analysis was addressed for the quantification of selenolanthionine that accounted for ~ 30% of total Se in the *C. violifolia* sample. Apart from selenolanthionine, four previously known (*e.g.*, selenocystathionine, selenohomocystine) and 31 unknown selenium containing molecules were additionally detected in the water extract including derivatives of selenohomocysteine and selenosugars.

A comprehensive experiment about the Se related physiological characteristics of *C. violifolia* was conducted with the comparison of the related non-hyperaccumulator *Cardamine pratensis* species covering Se tolerance and accumulation, chlorophyll fluorescence, spatial selenium/sulphur distribution patterns through synchrotron-based X-ray fluorescence (µXRF) and ICP-OES, speciation analysis through selenium K-edge micro X-ray absorption near-edge structure analysis (µXANES). The physiological study revealed clear differences between the hyperaccumulator *C. violifolia* and the related non-accumulator *C. pratensis* plant species; on the other hand, *C. violifolia* showed contrasting properties with other hyperaccumulator species even within the *Brassicaceae* family, compared to, *e.g.*, *S. pinnata*, like missing growth stimulation by Se. The hyperaccumulator and non-hyperaccumulator *Cardamine* species did not show any difference in terms that sulphate inhibited selenate uptake but selenite uptake was not inhibited by phosphate.

µXRF derived distribution maps and selenium/sulphur uptake characteristics showed similarities to other formerly reported hyperaccumulator and non-hyperaccumulator Brassicaceae species. Mainly organic Se in "C-Se-C" bond was found in the seedlings of both species and in mature *C. violifolia* plant analysed by µXANES while selenate-supplied mature *C. pratensis* contained approximately half selenate and half "C-Se-C" bond containing selenocompounds. The lack of selenocystine was proved by strong cation exchange chromatography-ICP-MS in the water extract of both species.

All the speciation and selenium-related physiological properties refer to the function of a unique, still unelucidated biochemical pathway for Se detoxification in this hyperaccumulator plant.

9. ÖSSZEFOGLALÁS

A *Cardamine* nemzetség (Brassicaceae család) első szelén hiperakkumulálóként azonosított faja a *Cardamine violifolia*, mely Kína természetesen szelénben dús régiójából, Enshiből (Yutangba övezet, Hubei tartomány) származik. Ezen a területen a növényt fitoremediációs célokra, talajjavításra, valamint takarmány / táplálékkiegészítő gyártásban való felhasználásra termesztik ill. gyűjtik.

Kutatásom során a *C. violifolia* növény szelénnel kapcsolatos jellemzőit vizsgáltam, beleértve szelénspeciációs analízist és fiziológiai kísérleteket.

A szelénmetabolitok azonosításához különböző extrakciós eljárásokat, valamint folyadékkromatográfiával kapcsolt induktív csatolású plazma (szervetlen) és nagy felbontású szerves tömegspektrometriás rendszereket alkalmaztam. A növény nem tartalmazott számottevő mennyiségben a hiperakkumulálókban gyakran azonosított szerves komponenseket (mint pl. szelenometionin, *Se*-(metil)szelenocisztein), valamint a szervetlen és elemi szelén tartalom együtt is kevesebb, mint 20%-ot tett ki az összes szeléntartalomból. Ortogonális kromatográfiás tisztítás alkalmazása tette lehetővé a fő szelénmetabolit, a szelenolantionin azonosítását a *C. violifolia* vizes extraktumában. Ez a nem fehérjeépítő aminosav korábban még sosem került egyértelmű azonosításra szelén tartalmú mintában. Bár több ellentmondó, LC alapú speciációs eredmény került publikásra a feltehetően azonos szelénkomponens és *Cardamine* faj kapcsán (Yuan *et al.* 2013, Cui *et al.* 2018), azonban esetünkben a szelenolantionin azonosítása nagy felbontású MS adatok és kémiai szintézis útján is megerősítésre került. Az eredmények felhívják a figyelmet arra, hogy a megfelelő komponens azonosításhoz legalább két ortogonális elválasztási technika és szervetlen (LC-ICP-MS) valamint nagy felbontású szerves tömegspektrometria (ESI-MS) együttes alkalmazása szükséges.

Nem módosulat-specifikus (oszlop utáni) izotóphígítással került sor a szelenolantionin mennyiségi meghatározására, mely körülbelül az összes szeléntartalom 30%-át tette ki a *C. violifolia* mintában. A vizes extraktumban a szelenolantioninon túl négy korábban azonosított (pl.: szelenocisztationin, szelenohomocisztein) és 31 ismeretlen szeléntartalmú komponenst detektáltunk, többek között szelenohomocisztein származékokat és szelenocukrokat.

Széleskörű kísérletet végeztem a *C. violifolia* szelénnel kapcsolatos fiziológiai tulajdonságainak vizsgálatára, összehasonlítva a rokon, nem hiperakkumuláló

Cardamine pratensis fajjal, a következő szempontok/célok szerint: szelén tolerancia és akkumuláció, klorofill fluoreszcencia meghatározás, térbeli szelén/kén eloszlás vizsgálata szinkrotron alapú röntgen fluoreszcencia (µXRF) és induktív csatolású plazma optikai emissziós spektrometria (ICP-OES) révén, ill. speciációs analízis röntgen abszorpciós módszerrel (µXANES). A fiziológiai vizsgálatok egyértelmű különbségeket tártak fel a hiperakkumuláló *C. violifolia* és rokon nem hiperakkumuláló *C. pratensis* fajok között, valamint *C. violifolia* különbségeket mutatott más hiperakkumuláló fajokkal szemben, még a Brassicaceae családon belül is (pl. *Stanleya pinnata*), hiszen például a szelén jelenléte nem eredményezett növekedés stimulációt. A hiperakkumuláló és nem hiperakkumuláló *Cardamine* fajok nem különböztek abban a tekintetben, hogy szulfát jelenléte gátolta a szelenát felvételt, míg foszfátnak nem volt gátló hatása a szelenit felvételre.

A röntgen alapú méréstechnikával rögzített szelén eloszlás és a szelén/kén felvétel jellemzői hasonlóságot mutattak más, korábban jellemzett hiperakkumuláló és nem hiperakkumuláló Brassicaceae fajokkal. Főként szerves „C-Se-C” kötést tartalmazó szelénkomponensek jellemezték mindkét *Cardamine* fajta hajtásait és az érett *C. violifolia* növényt, míg a szelenáttal kezelt érett *C. pratensis* mintát körülbelül 50-50%-ban szelenát, ill. „C-Se-C” kötésű szelén jellemzi. Kationcserés-ICP-MS technikával igazoltam mindkét faj esetén, hogy a növények vizes extraktuma nem tartalmaz szelenocisztint.

Mind a speciációs, mind a szelénnel kapcsolatos fiziológiai tulajdonságok egy egyedi, eddig fel nem tárt szelén detoxifikációs útvonal működésére utalnak a *C. violifolia* növényben.

10. APPENDIX I: REFERENCES

ABORODE, F. A., RAAB, A., FOSTER, S., LOMBI, E., MAHER, W., KRUPP, E. M., FELDMANN, J. (2015): Selenopeptides and elemental selenium in *Thunbergia alata* after exposure to selenite: quantification method for elemental selenium. In: *Metallomics*, 7: 1056-1066. p.

ABRANKÓ, L., NAGY, Á., SZILVÁSSY, B., STEFANOVITS-BÁNYAI, É., HEGEDUS, A. (2015): Genistein isoflavone glycoconjugates in sour cherry (*Prunus cerasus* L.) cultivars. In: *Food Chemistry*, 166: 215-222. p.

ALFORD, É. R., LINDBLOM, S. D., PITTARELLO, M., FREEMAN, J. L., FAKRA, S. C., MARCUS, M. A., BROECKLING, C., PILON-SMITS, E. A. H., PASCHKE, M. W. (2014): Roles of rhizobial symbionts in selenium hyperaccumulation in *Astragalus* (Fabaceae). In: *American Journal of Botany*, 101 (11): 1895-1905. p.

ALFTHAN, G., EUROLA, M., EKHOLM, P., VENÄLÄINEN, E.-R., ROOT, T., KORKALAINEN, K., HARTIKAINEN, H., SALMINEN, P., HIETANIEMI, V., ASPILA, P., ARO, A. (2015): Effects of nationwide addition of selenium to fertilizers on foods, and animal and human health in Finland: From deficiency to optimal selenium status of the population. In: *Journal of Trace Elements in Medicine and Biology*, 31: 142-147. p.

ANDERSON, J. W. (1993): Selenium interactions in sulfur metabolism. In: de Kok L. J. (Ed): *Sulfur nutrition and assimilation in higher plants: regulatory, agricultural and environmental aspects*. The Hague: SPB Academic Publishing. 49-60. p.

ANDREOTE, F. D., GUMIERE, T., DURRER, A. (2014): Exploring interactions of plant microbiomes. In: *Scientia Agricola*, 71 (6): 528-539. p.

ARAIE, H., SHIRAIWA, Y. (2009): Selenium utilization strategy by microalgae. In: *Molecules*, 14(12): 4880-4891. p.

AURELI, F., OUERDANE, L, BIERLA, K., SZPUNAR, J., PRAKASH, N. T., CUBADDA, F. (2012): Identification of selenosugars and other low-molecular weight selenium metabolites in high-selenium cereal crops. In: *Metallomics*, 4: 968-978. p.

BANUELOS, G. S., ARROYO, I., PICKERING, I. J., YANG, S. I., FREEMAN, J. L. (2015): Selenium biofortification of broccoli and carrots grown in soil amended with Se-enriched hyperaccumulator *Stanleya pinnata*. In: *Food Chemistry*, 166: 603-608. p.

BARTHOLOMEES, U., STRUYF, T., LAUWERS, O., CEUNEN, S., GEUNS, J. M. C. (2016): Validation of an HPLC method for direct measurement of steviol equivalents in foods. In: *Food Chemistry*, 190: 270-275. p.

BEATH, O. A. (1943): Toxic vegetation growing on the salt wash sandstone member of the Morrison formation. In: *American Journal of Botany*, 30: 698-706. p.

BEATH, O. A., EPPSON, H. F., GILBERT, C. S. (1937): Selenium distribution in and seasonal variation of type vegetation occuring on seleniferous soils. In: *Journal of the American Pharmaceutical Association*. 26: 394-405. p.

BEATH, O. A., GILBERT, C. S., EPPSON, H. F. (1939a): The use of indicator plants in locating seleniferous areas in the Western United States. I. General. In: *American Journal of Botany*, 26: 257-269. p.

BEATH, O. A., GILBERT, C. S., EPPSON, H. F. (1939b): The use of indicator plants in locating seleniferous areas in the Western United States. II. Correlation studies by states. In: *American Journal of Botany*, 26: 394-405. p.

BEATH, O. A., GILBERT, C. S., EPPSON, H. F. (1940): The use of indicator plants in locating seleniferous areas in western United States. III. Further studies. In: *American Journal of Botany*, 27: 564-573. p.

BEATH, O. A., GILBERT, C. S., EPPSON, H. F. (1941): The use of indicator plants in locating seleniferous areas in western United States. IV. Progress report. In: *American Journal of Botany*, 28: 887-900. p.

BECKER, J. S., MATUSCH, A., DEPBOYLU, C., DOBROWOLSKA, J., ZORIY, M. V. (2007): Quantitative Imaging of Selenium, Copper, and Zinc in Thin Sections of Biological Tissues (Slugs – Genus Arion) Measured by Laser Ablation Inductively Coupled Plasma Mass Spectrometry. In: *Analytical Chemistry*, 79 (16): 6074-6080. p.

BERTELSEN, F., GISSEL-NIELSEN, G., KJAER, A., SKRYDSTRUP, T. (1988): Selenoglucosinolates in nature: Fact or myth? In: *Phytochemistry*, 27(12): 3743-3749. p.

BIANGA, J., GOVASMARK, E., SZPUNAR, J. (2013): Characterization of Selenium Incorporation into Wheat Proteins by Two-Dimensional Gel Electrophoresis-Laser Ablation ICP MS followed by capillary HPLC-ICP MS and Electrospray Linear Trap Quadrupole Orbitrap MS. In: *Analytical Chemistry*, 85: 2037-2043. p.

BLOCK, E., BIRRINGER, M., JIANG, W. Q., NAKAHODO, T., THOMPSON, H. J., TOSCANO, P. J., UZAR, H., ZHANG, X., ZHU, Z. J. (2001): Allium chemistry: synthesis, natural occurence, biological activity, and chemistry of Se-alk(en)ylselenocysteines and their gamma-glutamyl derivatives and oxidation products. In: *Journal of Agricultural and Food Chemistry*, 49: 458-470. p.

BROWN, T. A., SHRIFT, A. (1980): Identification of Selenocysteine in the Proteins of Selenate-grown *Vigna radiata*. In: *Plant Physiology*, 66: 758-761. p.

BYERS, H. G., (1935): Selenium occurence in certain soils in the United States with a discussion of related topics. In: *United States Department of Agriculture Technical Bulletin* 482. p.

BYERS, H. G., MILLER, T. J., WILLIAMS, K. T., LAKIN, H. W. (1938): Selenium occurence in certain soils in the United States with a discussion of related topics, third report. In: *United States Department of Agriculture Technical Bulletin.* 601. p.

CABANNES, E., BUCHNER, P., BROADLEY, M. R., HAWKESFORD, M. J. (2011): A comparison of sulfate and selenium accumulation in relation to the expression of sulfate transporter genes in *Astragalus* species. In: *Plant Physiology*, 157 (4): 2227-2239. p.

CAI, X-J., BLOCK, E., UDEN, P. C., ZHANG, X., QUIMBY, B. D., SULLIVAN, J. J. (1995): *Allium* Chemistry: Identification of Selenoamino Acids, in Ordinary and Selenium-Enriched Garlic, Onion, and Broccoli Using Gas Chromatography with Atomic Emission Detection. In: *Journal of Agriculture and Food Chemistry*, 43: 1754-1757. p.

CALDERÓN-CELIS, F., SANZ-MEDEL, A., ENCINAR, J. R. (2018): Universal Absolute Quantification of Biomolecules using Element Mass Spectrometry and Generic Standards. In: *Chemical Communications*, 54(8): 904-907. p.

CALDERÓN-CELIS, F., SUGIYAMA, N., YAMANAKA, M., SAKAI, T., DIEZ-FERNANDEZ, S., CALVETE, J. J., SANZ-MEDEL, A., ENCINAR, J. R. (2019): Enhanced universal quantification of biomolecules using element MS and generic standards: application to intact protein and phosphoprotein determination. In: *Analytical Chemistry*, 91(1): 1105-1112. p.

CANKUR, O., YATHAVAKILLA, S. K. V., CARUSO, J. A. (2006): Selenium speciation in dill (Anethum graveolens L.) by ion pairing reversed phase and cation exchange HPLC with ICP-MS detection. In: *Talanta*, 70(4): 784-790. p.

CAPPA, J. J., CAPPA, P. J., EL MEHDAWI, A. F., MCALEER, J. M., SIMMONS, M. P., PILON-SMITS, E. A. H. (2014): Characterization of selenium and sulfur accumulation across the genus *Stanleya* (Brassicaceae): A field survey and common-garden experiment. In: *American Journal of Botany*. 101 (5): 830-839. p.

CAPPA, J. J., YETTER, C., FAKRA, S., CAPPA, P. J., DETAR, R., LANDES, C., PILON-SMITS, E. A. H., SIMMONS, M. P. (2015): Evolution of selenium hyperaccumulation in *Stanleya* (Brassicaceae) as inferred from phylogeny, physiology and X-ray microprobe analysis. In: *New Phytologist*, 205: 583-595. p.

CASIOT, C., VACCHINA, V., CHASSAIGNE, H., SZPUNAR, J., POTIN-GAUTIER, M., LOBINSKI, R. (1999): An approach to the identification of selenium species in yeast extracts using pneumatically-assisted electrospray tandem mass spectrometry. In: *Analytical Communications*, 36: 77-80. p.

CASTILLO, Á., GRACIA-LOR, E., ROIG-NAVARRO, A. F., SANCHO, J. V., RODRÍGUEZ-GONZÁLEZ, P., ALONSO, J. I. G. (2013): Isotope pattern deconvolution-tandem mass spectrometry for the determination and confirmation of diclofenac in wastewaters. In: *Analytica Chimica Acta*, 765: 77-85. p.

CHANG, C., YIN, R., WANG, X., SHAO, S., CHEN, C., ZHANG, H. (2019): Selenium translocation in the soil-rice system in the Enshi seleniferous area, Central China. In: *Science of the Total Environment*. 669: 83-90. p.

CHAO, D-Y., BARANIECKA, P., DANKU, J., KOPRIVOVA, A., LAHNER, B., LUO, H., YAKUBOVA, E., DILKES, B., KOPRIVA, S., SALT, D. E. (2014): Variation in sulfur and selenium accumulation is controlled by naturally occurring isoforms of the key sulfur assimilation enzyme ADENOSINE 5'-PHOSPHOSULFATE REDUCTASE2 across the *Arabidopsis* species range. In: *Plant Physiology*, 166:1 593-1608. p.

CHEAJESADAGUL, P., BIANGA, J., ARNAUDGUILHEM, C., LOBINSKI, R., SZPUNAR, J. (2014): Large-scale speciation of selenium in rice proteins using ICP-MS assisted electrospray MS/MS proteomics. In: *Metallomics*, 6: 646-653. p.

CHEN, Y. W., LI, L., D'ULIVO, A., BELZILE, N. (2006): Extraction and determination of elemental selenium in sediments – a comparative study. In: *Analytica Chimica Acta*, 577: 126-133. p.

CHOI, H. G., MOON, B. Y., KANG, N. J. (2015): Effects of LED light on the production of strawberry during cultivation in a plastic greenhouse and in a growth chamber. In: *Scientia Horticulturae*, 189: 22-31. p.

CHU, J., YAO, X., ZHANG, Z. (2010): Responses of wheat seedlings to exogenous selenium supply under cold stress. In: *Biological Trace Element Research*, 136 (3): 355-363. p.

CLOUGH, R., HARRINGTON, C. F., HILL, S. J., MADRID, Y., TYSON, J. F. (2017): Atomic spectrometry update: review of advances in elemental speciation. In: *Journal of Analytical Atomic Spectrometry*, 32: 1239-1282. p.

COCHRAN, A. T. (2017): Selenium and the Plant Microbiome. In: PILON-SMITS, E. A. H., WINKEL, L. H. E., LIN, Z-Q. (Eds): *Selenium in plants* (Plant Ecophysiology 11) Springer International Publishing. 109-121. p.

COCHRAN, A. T., BAUER, J., METCALF, J. L., LOVECKA, P., SURA DE JONG, M., WARRIS, S., MOOIJMAN, P. J. W., VAN DER MEER, I., KNIGHT, R., PILON-SMITS, E. A. H. (2018): Plant Selenium Hyperaccumulation Affects Rhizosphere: Enhanced Species Richness and Altered Species Composition. In: *Phytobiomes Journal*, 2: 82-91. p.

COSSINS, E. A., CHEN, L. (1997): Folates and one-carbon metabolism in plants and fungi. In: *Phytochemistry*, 45: 437-452. p.

CRUZ, E. C. S., BECKER, J. S., BECKER, J. S., SUSSULINI, A. (2018): Imaging of Selenium by Laser Ablation Inductively Coupled Plasma Mass Spectrometry (LA-ICP-MS) in 2-D Electrophoresis Gels and Biological Tissues. In: CHAVATTE, L. (Ed.): *Selenoproteins: Methods and Protocols* (Methods in Molecular Biology 1661) Humana. 219-227. p.

CUI, L., ZHAO, J., CHEN, J., ZHANG, W., GAO, Y., LI, B., LI, Y-F. (2018): Translocation and transformation of selenium in hyperaccumulator plant *Cardmine enshiensis* from Enshi, Hubei, China. In: *Plant and Soil*, 425: 577-588. p.

DA SILVA, M. A. O., ARRUDA, M. A. Z. (2013): Laser ablation (imaging) for mapping and determining Se and S in sunflower leaves. In: *Metallomics*, 5: 62-67. p.

DANEHY, J. P., PIGMAN, W. W. (1951): Reactions between Sugars and Nitrogenous Compounds and Their Relationship to Certain Food Problems. In: *Advances in Food Research*, 3: 241-290. p.

DE SOUZA, M. P., CHU, D., ZHAO, M., ZAYED, A. M., RUZIN, S. E., SCHICHNES, D., TERRY, N. (1999): Rhizosphere Bacteria Enhance Selenium Accumulation and Volatilization by Indian Mustard. In: *Plant Physiology*, 119: 565-573. p.

DE SOUZA, M. P., PILON-SMITS, E. A. H., LYTLE, C. M., HWANG, S., TAI, J., HONMA, T. S. U. YEH, LL., TERRY, N. (1998): Rate-limiting steps in selenium assimilation and volatilization by Indian mustard. In: *Plant Physiology*, 117: 1487-1494. p.

DERNOVICS, M., FAR, J., LOBINSKI, R. (2009): Identification of anionic selenium species in Se-rich yeast by electrospray QTOF MS/MS and hybrid linear ion trap/orbitrap MS. In: *Metallomics*, 1: 317-329. p.

DERNOVICS, M., GARCÍA-BARRERA, T., BIERLA, K., PREUD'HOMME, H., LOBINSKI, R. (2007): Standardless identification of selenocystathionine and its γ-glutamyl derivatives in monkeypot nuts by 3D liquid chromatography with ICP-MS detection followed by nanoHPLC-Q-TOF-MS/MS. In: *The Analyst*, 132(5): 439-499. p.

DERNOVICS, M., LOBINSKI, R. (2008a): Speciation Analysis of Selenium Metabolites in Yeast-Based Food Supplements by ICPMS-Assisted Hydrophilic Interactin HPLC-Hybrid Linear Ion Trap/Orbitrap MS. In: *Analytical Chemistry*, 80: 3975-3984. p.

DERNOVICS, M., LOBINSKI, R. (2008b): Characterization of the selenocysteine-containing metabolome in selenium-rich yeast. Part I: Identification of new species by multi-dimensional liquid chromatography with parallel ICP-MS and electrospray Q-TOFMS/MS detection. In: *Journal of Analytical and Atomic Spectrometry*, 23: 72-83. p.

DERNOVICS, M., OUERDANE, L., TASTET, L., GIUSTI, P., PREUD'HOMME, H., LOBINSKI, R. (2006): Detection and characterization of artefact compounds during selenium speciation analysis in yeast by ICP-MS assisted MALDI MS, oMALDI MS/MS and LC-ES-MS/MS. In: *Journal of Analytical Atomic Spectrometry*, 21(7): 703-707. p.

DEY, S., STAFFORD, R., DEB ROY, M. K., BHATTACHARJEE, C. R., KHATHING, D. T., BHATTACHARJEE, P. C., DKHAR, P. S. (1999): Metal toxicity and trace element deficiency in some wild animals species from north-east India, as revealed by cellular, bio-inorganic and behavioural studies. In: *Current Science*, 77: 276-280. p

DHILLON, K. S., BAWA, S. S., DHILLON, S. K. (1992): Selenium Toxicity in Some Plants and Soils of Punjab. In: *Journal of the Indian Society of Soil Science*, 40: 132-136. p.

DHILLON, K. S., DHILLON, S. K. (2003): Distribution and management of seleniferous soils. In: *Advances in Agronomy*. 79: 119-184. p.

DJANAGUIRAMAN, M., PRASAD, P. V. V., SEPPANEN, M. (2010): Selenium protects sorghum leaves from oxidative damage under high temperature stress by enhancing antioxidant defense system. In: *Plant Physiology and Biochemistry*, 48 (12): 999-1007. p.

DOLGOVA, N. V., NEHZATI, S., CHOUDHURY, S., MACDONALD, T. C., REGNIER, N. R., CRAWFORD, A. M., PONOMARENKO, O., GEORGE, G. N., PICKERING, I. J. (2018): X-ray spectroscopy and imaging of selenium in living systems. In: *Biochimica et Biophysica Acta – General Subjects*, 1862: 2383-2392. p.

EFSA (2014): Scientific Opinion on Dietary Reference Values for selenium. In: *EFSA Journal*, 12(10): 3864. p.

EGRESSY-MOLNÁR, O., MAGYAR, A., GYEPES, A., DERNOVICS, M. (2014): Validation of the 2,3-dihydroxy-propionyl group in selenium speciation by chemical synthesis and LC-MS analyses. In: *RSC Advances*, 4: 27532-27540. p.

EGRESSY-MOLNÁR, O., OUERDANE, L., GYŐRFI, J., DERNOVICS, M. (2016): Analogy in selenium enrichment and selenium speciation between selenized yeast Saccharomyces cerevisiae and *Hericium erinaceus* (lion's mane mushroom). In: *LWT – Food Science and Technology*, 68: 306-312. p.

EICHE, E., BARDELLI, F., NOTHSTEIN, A. K., CHARLET, L., GÖTTLICHER, J., STEININGER, R., DHILLON, K. S., SADANA, U. S. (2015): Selenium distribution and speciation in plant parts of wheat (*Triticum aestivum*) and Indian mustard (*Brassica juncea*) from a seleniferous area of Punjab, India. In: *Science of the Total Environment*. 505: 952-961. p.

EL MEHDAWI A. F., REYNOLDS, R. J. B., PRINS, C. N., LINDBLOM, S. D., CAPPA, J. J., FAKRA, S. C., PILON-SMITS, E. A. H. (2014): Analysis of selenium accumulation, speciation and tolerance of potential selenium hyperaccumulator *Symphyotrichum ericoides*. In: *Physiologia Plantarum*. 152 (1): 70-83. p.

EL MEHDAWI, A. F., CAPPA, J., FAKRA, S., SELF, J., PILON-SMITS, E. A. H. (2012): Interactions of selenium hyperaccumulators and nonaccumulators during cocultivation on seleniferous or nonseleniferous soil – the importance of having good neighbors. In: *New Phytologist*, 194: 264-277. p.

EL MEHDAWI, A. F., JIANG, Y., GUIGNARDI, Z. S., ESMAT, A., PILON, M., PILON-SMITS, E. A. H. (2018): Influence of sulfate supply on selenium uptake dynamics and expression of sulfate/selenate transporters in selenium hyperaccumulator and nonhyperaccumulator Brassicaceae. In: *New Phytologist*, 217 (1): 194-205. p.

EL MEHDAWI, A. F., PASCHKE, M. W., PILON-SMITS, E. A. H. (2015): *Symphyotrichum ericoides* populations from seleniferous and nonseleniferous soil display striking variation in selenium accumulation. In: *New Phytologist*, 206: 231-242. p.

EL MEHDAWI, A. F., PILON-SMITS, E. A. H. (2012): Ecological aspects of plant selenium hyperaccumulation. In: *Plant Biology*, 14 (1): 1-10. p.

EL MEHDAWI, A. F., QUINN, C. F., PILON-SMITS, E. A. H. (2011): Effects of selenium hyperaccumulation on plant-plant interactions: evidence for elemental allelopathy? In: *New Phytologist*, 191: 120-131. p.

EN 14130:2003: Foodstuffs – Determination of Vitamin C by HPLC

ENCINAR, J. R., RUZIK, R., BUCHMANN, W., JEANINE, T., LOBINSKI, R., SZPUNAR, J. (2003b): Detection of selenocompounds in a tryptic digest of yeast selenoprotein by MALDI time-of-flight MS prior to their structural analysis by electrospray ionization triple quadrupole MS. In: *Analyst*. 128(3): 220-224. p.

ENCINAR, J. R., SCHAUMLÖFFEL, D., OGRA, Y., LOBINSKI, R. (2004): Determination of Selenomethionine and Selenocysteine in Human Serum Using Speciated Isotope Dilution-Capillary HPLC-Inductively Coupled Plasma Collision Cell Mass Spectrometry. In: *Analytical Chemistry*, 76(22): 6635-6642. p.

ENCINAR, J. R., SLIWKA-KASZYNSKA, M., POLATAJKO, A., VACCHINA, V., SZPUNAR, J. (2003a): Methodological advances for selenium speciation analysis in yeast. In: *Analytica Chimica Acta*, 500(1-2): 171-183. p.

EUSTICE, D. C., KULL, F. J., SHRIFT, A. (1981): Selenium toxicity: aminoacylation and peptide bond formation with selenomethionine. In: *Plant Physiology,* 67: 1054-1058. p.

EVANS, C. S., ASHER, C. J., JOHNSON, C. M. (1968): Isolation of dimethyl diselenide and other volatile selenium compounds from *Astragalus Racemosus* (Pursh). In: *Australian Journal of Biological Sciences*, 21: 13-20. p.

FAKRA, S. C., LUEF, B., CASTELLE, C. J., MULLIN, S. W., WILLIAMS, K. H., MARCUS, M. A., SCHICHNES, D., BANFIELD, J. F. (2018): Correlative cryogenic spectromicroscopy to investigate selenium bioreduction products. In: *Environmental Science & Technology*, 52: 503-512. p.

FAR, J., PREUD'HOMME, H., LOBINSKI, R. (2010): Detection and identification of hydrophilic selenium compounds in selenium-rich yeast by size exclusion-microbore normal-phase HPLC with the on-line ICP-MS and electrospray Q-TOF-MS detection. In: *Analytica Chimica Acta*, 657: 175-190. p.

FARGASOVÁ, A., PASTIEROVÁ, J., SVETKOVÁ, K. (2006): Effect of Se-metal pair combinations (Cd, Zn, Cu, Pb) on photosynthetic pigments production and metal accumulation in *Sinapsis alba* L. seedlings. In: *Plant, Soil and Environment,* 52 (1): 8-15. p.

FASSEL, V. A. (1978): Quantitative elemental analyses by plasma emission-spectroscopy. In: *Science*, 202: 183-191. p.

FASSETT, J. D., PAULSEN, P. J. (1989): Isotope Dilution Mass Spectrometry for Accurate Elemental Analysis. In: *Analytical Chemistry,* 61 (10): 643A-649A. p.

FENG, R., WEI, C., TU, S. (2013): The roles of selenium in protecting plants against abiotic stresses. In: *Environmental and Experimental Botany,* 87: 58-68. p.

FERRI, T., COCCIOLI, F., DE LUCA, C., CALLEGARI, C. V., MORABITO, R. (2004): Distribution and speciation of selenium in *Lecythis ollaria* plant. In: *Microchemical Journal*, 78: 195-203. p.

FINLEY, J. W., IP, C., LISK, D. J., DAVIS, C. D., HINTZE, K. J., WHANGER, P. D. (2001): Cancer-Protective Properties of High-Selenium Broccoli. In: *Journal of Agricultural and Food Chemistry*, 49: 2679-2683. p.

FLEMING, G. A. (1962): Selenium in Irish soils and plants. In: *Soil Science*, 94: 28-35. p.

FLEMING, G. A., WALSH, T. (1957): Selenium occurrence in certain Irish soils and its toxic effects on animal. In: *Proceedings of the Royal Irish Academy. Section B: Biological, Geological and Chemical Science*, 58: 151-166. p.

FORDYCE, F. M., GUANGDI, Z., GREEN, K., XINPING, L. (2000): Soil, grain and water chemistry in relation to human selenium-responsive diseases in Enshi District, China. In: *Applied Geochemistry*. 15 (1): 117-132. p.

FREEMAN, J. L., QUINN, C. F., MARCUS, M. A., FAKRA, S., PILON-SMITS, E. A. H. (2006b): Selenium-Tolerant Diamondback Moth Disarms Hyperaccumulator Plant Defense. In: *Current Biology*, 16: 2181-2192. p.

FREEMAN, J. L., TAMAOKI, M., STUSHNOFF, C., QUINN, C. F., CAPPA, J. J., DEVONSHIRE, J., FAKRA, S. C., MARCUS, M. A., MCGRATH, S. P., VAN HOEWYK, D., PILON-SMITS, E. A. H. (2010): Molecular mechanisms of selenium tolerance and hyperaccumulation in *Stanleya pinnata*. In: *Plant Physiology*. 153 (4): 1630-1652. p.

FREEMAN, J. L., ZHANG, L. H., MARCUS, M. A., FAKRA, S., MCGRATH, S. P., PILON-SMITS E. A. H. (2006a): Spatial Imaging, Speciation, and Quantification of Selenium in the Hyperaccumulator Plants *Astragalus bisulcatus* and *Stanleya pinnata*. In: *Plant Physiology*, 142: 124-134. p.

GALEAS, M. L, ZHANG, L. H., FREEMAN, J. L., WEGNER, M., PILON-SMITS, E. A. H. (2007): Seasonal fluctuations of selenium and sulfur accumulation in selenium hyperaccumulators and related nonaccumulators. In: *New Phytologist*, 173: 517-525. p.

GAMES, P. A., HOWELL, J. F. (1976): Pairwise multiple comparison procedures with uniqueal N's and/or variances: a Monte Carlo study. In: *Journal of Educational Statistics*, 1: 113-125. p.

GAO, S., TANJI, K. K., PETERS, D. W., HERBEL, M. J. (2000): Water selenium speciation and sediment fractionation in a California flow-through wetland system. In: *Journal of Environmental Quality*, 29: 1275-1283. p.

GARCÍA-REYES, J. F., DERNOVICS, M., ORTEGA-BARRALES, P., FERNÁNDEZ-ALBA, A. R., MOLINA-DÍAZ, A. (2007): Accurate mass analysis and structure elucidation of selenium metabolites by liquid chromatography electrospray time-of-flight mass spectrometry. In: *Journal of Analytical Atomic Spectrometry*, 22: 947-959. p.

GARCÍA-SEVILLANO, M. A., GARCÍA-BARRERA, T., GÓMEZ-ARIZA, J. L. (2014): Simultaneous speciation of selenoproteins and selenometabolites in plasma and serum by dual size exclusion-affinity chromatography with online isotope dilution inductively coupled plasma mass spectrometry. In: *Analytical and Bioanalytical Chemistry*, 406(11): 2719-2725. p.

GIL-CASAL, S., FAR, J., BIERLA, K., OUERDANE, L., SZPUNAR, J. (2010): Study of the Se-containing metabolomes in Se-rich yeast by size-exclusion – cation-exchange HPLC with the parallel ICP MS and electrospray orbital ion trap detection. In: *Metallomics*, 2: 535-548. p.

GRANT, T. D., MONTES-BAYÓN, M., LEDUC, D., FRICKE, M. W., TERRY, N., CARUSO, J. A. (2004): Identification and characterization of Se-methyl selenomethionine in *Brassica juncea* roots. In: *Journal of Chromatography A*, 1026: 159-166. p.

GUIGNARDI, Z., SCHIAVON, M. (2017): Biochemistry of Plant Selenium Uptake and Metabolism. In: PILON-SMITS, E. A. H., WINKEL, L. H. E., LIN, Z-Q. (Eds): *Selenium in plants* (Plant Ecophysiology 11) Springer International Publishing. 21-34. p.

HAMILTON, J. W. (1975): Chemical Examination of Seleniferous Cabbage *Brassica oleracea capitata*. In: *Journal of Agircultural and Food Chemistry*, 23(6): 1150-1152. p.

HANSON, B., LINDBLOM, S. D., LOEFFLER, M. L., PILON-SMITS, E. A. H. (2004): Selenium protects plants from phloem-feeding aphids due to both deterrence and toxicity. In: *New Phytologist*, 162 (3): 655-662. p.

HARNLY, J. M., BHAGWAT, S., LIN, L.-Z. (2007): Profiling methods for the determination of phenolic compounds in foods and dietary supplements. In: *Analytical and Bioanalytical Chemistry*, 389(1): 47-61. p.

HARRIS, J., SCHNEBERG, K. A., PILON-SMITS, E. A. (2014): Sulfur-selenium-molybdenum interactions distinguish selenium hyperaccumulator *Stanleya pinnata* from non-hyperaccumulator *Brassica juncea* (Brassicaceae). In: *Planta*, 239 (2): 479-491. p.

HARTIKAINEN, H. (2005): Biogeochemistry of selenium and its impact on food chain quality and human health. In: *Journal of Trace Elements in Medicine Biology*, 18 (4): 309-318. p.

HARTIKAINEN, H., XUE, T. (1999): The promotive effect of selenium on plant growth as triggered by ultraviolet irridiation. In: *Journal of Environmental Quality*, 28 (4): 1372-1375. p.

HAWKESFORD, M., DAVIDIAN, J. C., GRIGNON, C. (1993): Sulphate/proton cotransport in plasma-membrance vesicles isolated from roots of *Brassica napus* L.: increased transport in membranes isolated from Sulphur-starved plants. In: *Planta*, 190: 297-304. p.

HOAGLAND, D. R., ARNON, D. I. (1950): The water-culture method for growing plants without soil. In: *Circular California Agricultural Experiment Station* 347: 32. p.

HOPPER, J. L., PARKER, D. R. (1999): Plant availability of selenite and selenate as influenced by the competing ions phosphate and sulfate. In: *Plant and Soil*, 210: 199-207. p.

HUERTA, V. D., REYES, L. H., MARCHANTE-GAYÓN, J. M., SÁNCHEZ, M. L. F., SANZ-MENDEL, A. (2003): Total determination and quantitative speciation analysis of selenium in yeast and wheat flour by isotope dilution analysis ICP-MS. In: *Journal of Analytical Atomic Spectrometry*, 18: 1243-1247. p.

INFANTE, H. G., O'CONNOR, G., RAYMAN, M., HEARN, R., COOK, K. (2006): Simultaenous identification of selenium-containing glutathione species in selenised yeast by on-line HPLC with ICP-MS and electrospray ionisation quadrupole time of flight (QTOF)-MS/MS. In: *Journal of Analytical Atomic Spectrometry*, 21: 1256-1263. p.

INFANTE, H. G., OVEJERO BENDITO, M. C., CÁMARA, C., EVANS, L, HEARN, R., MOESGAARD, S. (2008): Isotope dilution quantification of ultratrace gamma-glutamyl-Se-methylselenocysteine species using HPLC with enhanced ICP-MS detection by ultrasonic nebulisation or carbon-loaded plasma. In: *Analytical and Bioanalytical Chemistry*, 390: 2099-2106. p.

JACCARD, J., BECKER, M. A., WOOD, G. (1984): Pairwise multiple comparison procedures – a review. In: *Psychological Bulletin*, 96: 589-596. p.

JECFA (2010): Steviol glycosides. FAO JECFA Monographs 10.

JIANG, Y., EL MEHDAWI, A. F., TRIPTI, LIMA, L.W., STONEHOUSE, G., FAKRA, S. C., HU, Y., QI, H., PILON-SMITS, E. A. H. (2018b): Characterization of selenium accumulation, localization and speciation in buckwheat-implications for biofortication. In: *Frontiers in Plant Science*, 9: 1583

JIANG, Y., SCHIAVON, M., LIMA, L. W., TRIPTI, JONES, R. R., EL MEHDAWI, A. F., ROYER, S., ZENG, Z., HU, Y., PILON-SMITS, E. A. H., PILON, M. (2018a): Comparison of ATP sulfurylase 2 from selenium hyperaccumulator *Stanleya pinnata* and non-accumulator *Stanleya elata* reveals differential intracellular localization and enzyme activity levels. In: *Biochimica et Biophysica Acta – General Subjects*. 1862 (11): 2363-2371. p.

KAHAKACHCHI, C., BOAKYE, H. T., UDEN, P. C., TYSON, J. F. (2004): Chromatographic speciation of anionic and neutral selenium compounds in Se-accumulating *Brassica juncea* (Indian mustard) and in selenized yeast. In: *Journal of Chromatography A*, 1054: 303-312. p.

KANEHISA, M., GOTO, S. (2000): KEGG: Kyoto encyclopedia of genes and genomes. In: *Nucleic Acids Research*. 28(1): 27-30.p. https://www.genome.jp/kegg-bin/show_pathway?org_name=boe&mapno=00450&mapscale=&show_description=show (accessed at 02/11/2020)

KIKKERT, J., BERKELAAR, E. (2013): Plant uptake and translocation of inorganic and organic forms of selenium. In: *Archives of Environmental Contamination Toxicology*, 65: 458-465. p.

KIRBY, J. K., LYONS, G. H., KARKKAINEN, M. P. (2008): Selenium Speciation and Bioavailability in Biofortified Products Using Species-Unspecific Isotope Dilution and Reverse Phase Ion Pairing-Inductively Coupled Plasma-Mass Spectrometry. In: *Journal of Agricultural and Food Chemistry*, 56(5): 1772-1779. p.

KNIGHT, S. H., BEATH, O. A. (1937): The occurnce of selenium and seleniferous vegetation in Wyoming. In: *University of Wyoming Agricultural Experiment Station Bulletin* 221. p.

KNOTT, S. G., MCCRAY, C. W. R. (1959): Two naturally occurring outbreaks of selenosis in Queensland. In: *The Australian Veterinary Journal*. 35: 161-165. p.

KOELLENSPERGER, G., HANN, S., NURMI, J., PROHASKA, T., STINGEDER, G. (2003): Uncertainty of species unspecific quantification strategies in hyphenated IPC-MS analysis. In: *Journal of Analytical Atomic Spectrometry*, 18: 1047-1055. p.

KOLBERT, Z., MOLNÁR, Á., FEIGL, G., VAN HOEWYK, D. (2019): Plant selenium toxicity: Proteome in the crosshairs. In: *Journal of Plant Physiology*, 232: 291-300. p.

KONG, L., WANG, M., BI, D. (2005): Selenium modulates the activities of antioxidant enzymes, osmotic homeostasis and promotes the growth of sorrel seedling under salt stress. In: *Plant Growth Regulation*, 45 (2): 155-163. p.

KOTREBAI, M., BIRRINGER, M., TYSON, J. F., BLOCK, E., UDEN, P. C. (2000): Selenium speciation in enriched and natural samples by HPLC-ICP-MS and HPLC-ESI-MS with perfluorinated carboxylic acid ion-pairing agents. In: *Analyst*, 125: 71-78. p.

KRATA, A. A., WOJCIECHOWSKI, M., KRASINSKI, J., BULSKA, E. (2008): Comparative study of high performance liquid chromatography species-specific and species-unspecific isotope dilution iductively coupled plasma mass spectrometry. A case study of selenomethionine and the origin of its oxidized form. In: *Microchemical Journal*, 143: 416-422. p.

KROUKAMP, E. M., WONDIMU, T., FORBES, P. B. C. (2016): Metal and metalloid speciation in plants: Overview, instrumentation, approaches and commonly assessed elements. In: *Trends in Analytical Chemistry*, 77: 87-99. p.

KUBACHKA, K. M., MEIJA, J., LEDUC, D. L., TERRY, N., CARUSO, J. A. (2007): Selenium volatiles as proxy to the metabolic pathways of selenium in genetically modified Brassica juncea. In: *Environmental Science and Technology*, 41(6): 1863-1869. p.

KUZNETSOV, V. V., KHOLODOVA, V. P., KUZNETSOV, V. V., YAGODIN, B. A. (2003): Selenium regulates water relations of plants under drought. In: *Doklady Akademii Nauk*, 390 (5): 713-716. p.

LAKIN, H. W., BYERS, H. G. (1941): Selenium occurence in certain soils in the United States with a discussion of related topics, sixth report. In: *United States Department of Agriculture Technical Bulletin*. 783. p.

LAKIN, H. W., BYERS, H. G. (1948): Selenium occurence in certain soils in the United States with a discussion of related topics, seventh report. In: *United States Department of Agriculture Technical Bulletin*. 950. p.

LARSEN, E. H., LOBINSKI, R., BURGER-MEŸER, K., HANSEN, M., RUZIK, R., MAZUROWSKA, L., RASMUSSEN, P. H., SLOTH, J. J., SCHOLTEN, O., KIK, C. (2006): Uptake and speciation of selenium in garlic cultivated in soil amended with symbiotic fungi (mycorrhiza) and selenate. In: *Analytical and Bioanalytical Chemistry*, 385(6):1098-1108. p.

LASS, B., ULLRICH-EBERIUS, C. I. (1984): Evidence for proton/sulfate cotransport and its kinetics in *Lemna gibba* G1. In: *Planta*, 161: 53-60. p.

LAUCHLI, A. (1993): Selenium in Plants: Uptake, Functions and Environmental Toxicity. In: *Botanica Acta*, 106 (6): 455-468. p.

LEDUC, D. L., ABDELSAMIE, M., MONTEY-BAYON, M., WU, C. P., REISINGER, S. J., TERRY, N. (2006): Overexpressing both ATP sulfurylase and selenocysteine methyltransferase enhances selenium phytoremediation traits in Indian mustard. In: *Environmental Pollution*, 144(1): 70-76. p.

LIMA, L. W., STONEHOUSE, G. C., WALTERS, C. EL MEHDAWI, A. F., FAKRA, S. C., PILON-SMITS, E. A. H. (2019): Selenium Accumulation, Speciation and Localization in Brazil Nuts (*Bertholletia excelsa* H.B.K.). In: *Plants*, 8: 289

LIN, L.-Z., MUKHOPADHYAY, S., ROBBINS, R. J., HARNLY, J. M. (2007): Identification and quantification of flavonoids of Mexican oregano (Lippia graveolens) by LC-DAD-ESI/MS analysis. In: *Journal of Food Composition and Analysis*, 20: 361-369. p.

LINDBLOM, S. D., FAKRA, S. C., LANDON, J., SCHULZ, P., TRACY, B., PILON-SMITS, E. A. H. (2014): Inoculation of selenium hyperaccumulator *Stanleya pinnata* and related non-accumulator *Stanleya elata* with

hyperaccumulator rhizosphere fungi – investigation of effects on Se accumulation and speciation. In: *Physiologia Plantarum*, 150: 107-118. p.

LINDBLOM, S. D., FAKRA, S. C., LANDON, J., SCHULZ, P., TRACY, B., PILON-SMITS, E. A. H. (2013a): Inoculation of *Astragalus racemosus* and *Astragalus convallarius* with selenium-hyperaccumulator rhizosphere fungi affects growth and selenium accumulation. In: *Planta*, 237: 717-729 p.

LINDBLOM, S. D., VALDEZ-BARILLAS, J. R., FAKRA, S. C., MARCUS, M. A., WANGELINE, A. L., PILON-SMITS, E. A. H. (2013b): Influence of microbial associations on selenium localization and speciation in roots of *Astragalus* and *Stanleya* hyperaccumulators. In: *Environmental and Experimental Botany*, 88: 33-42. p.

LOBINSKI, R., MOULIN, C., ORTEGA, R. (2006a): Imaging and speciation of trace elements in biological environment. In: *Biochimie*, 88: 1591-1604. p.

LOBINSKI, R., SHCAUMLÖFFEL, D., SZPUNAR, J (2006b): Mass spectrometry in bioinorganic analytical chemistry. In: *Mass Spectrometry Reviews*, 25: 255-289. p.

LYI, S. M., HELLER, L. I., RUTZKE, M., WELCH, R. M., KOCHIAN, L. V., LI, L. (2005): Molecular and Biochemical Characterization of the Selenocysteine Se-Methyltransferase Gene and Se-Methylselenocysteine Synthesis in Broccoli. In: *Plant Physiology*, 138: 409-420. p.

LYI, S. M., ZHOU, X., KOCHIAN, L. V., LI, L. (2007): Biochemical and molecular characterization of the homocysteine S-methyltransferase from broccoli (*Brassica oleracea* var. *italica*). In: *Phytochemistry*, 68: 1112-1119. p.

MATICH, A. J., MCKENZIE, M. J., LILL, R. E., BRUMMEL, D. A., MCGHIE, T. K., CHEN, R. K., ROWAN, D. D. (2012): Selenoglucosinolates and their metabolites produced in *Brassica* spp. fertilized with sodium selenate. In: *Phytochemistry*, 75: 140-152. p.

MCCRAY, C. W. R., HURWOOD, I. S. (1963): Selenosis in North-Western Queensland. In: *Journal of Agricultural Science*. 20: 475-498. p.

MCKENZIE, M., MATICH, A., HUNTER, D., ESFANDIARI, A., TROLOVE, S., CHEN, R., LILL, R. (2019): Selenium Application During Radish (*Raphanus sativus*) Plant Development Alters Glucosinolate Metabolic Gene Expression and Results in the Production of 4-(methylseleno)but-3-enyl glucosinolate. In: *Plants*, 8: 427

MCSHEEHY, S., KELLY, J., TESSIER, L., MESTER, Z. (2005): Identification of selenomethionine in selenized yeast using two-dimensional liquid chromatography-mass spectrometry based proteomic analysis. In: *The Analyst*, 130: 35-37. p.

MCSHEEHY, S., PANNIER, F., SZPUNAR, J., POTIN-GAUTIER, M., LOBINSKI, R. (2002): Speciation of seleno compounds in yeast aqueous extracts by three-dimensional liquid chromatography with inductively coupled plasma mass spectrometric and electrospray mass spectrometric detection. In: *The Analyst*, 127: 223-229. p.

MCSHEEHY, S., POHL, P., SZPUNAR, J., POTIN-GAUTIER, M., LOBINSKI, R. (2001): Analysis for selenium speciation in selenized yeast extracts by two

dimensional liquid chromatography with ICP-MS and electrospray MS-MS detection. In: *Journal of Analytical Atomic Spectrometry*, 16: 68-73. p.

MCSHEEHY, S., YANG, W., PANNIER, F., SZPUNAR, J., LOBINSKI, R., AUGER, J., POTIN-GAUTIER, M. (2000): Speciation analysis of selenium in garlic by two-dimensional high-performance liquid chromatography with parallel inductively coupled plasma mass spectrometric and electrospray tandem mass spectrometric detection. In: *Analytica Chimica Acta*, 421: 147-153. p.

MEIJA, J., MONTES-BAYÓN, M., LE DUC, D. L., TERRY, N. CARUSO, J. A. (2002): Simultaneous Monitoring of Volatile Selenium and Sulfur Species from Se Accumulating Plants (Wild Type and Genetically Modified) by GC/MS and GC/ICPMS Using Solid-Phase Microextraction for Sample Introduction. In: *Analytical Chemistry*, 74: 5837-5844. p.

MICHALSKA-KACMIROW, M., KUREK, E., SMOLIS, A., WIERZBICKA, M., BULSKA, E. (2014): Biological and chemical investigation of *Allium cepa* L. response to selenium inorganic compounds. In: *Analytical and Bioanalytical Chemistry*, 406: 3717-3722. p.

MILLER, N. J., RICE-EVANS, C. A. (1996): Spectrophotometric determination of antioxidant activity. In: *Redox Report*, 2: 161-171. p.

MOLLER, L. H., JENSEN, C. S., NGUYEN, T. T. T. N., STÜRUP, S., GAMMELGAARD, B. (2005): Evaluation of a membrane desolvator for LC-ICP-MS analysis of selenium and platinum species for application to peptides and proteins. In: *Journal of Analytical Atomic Spectrometry*, 30: 277-284. p.

MONTES-BAYÓN, M., YANES, E. G., DE LEÓN, C. P., JAYASIMHULU, K., STALCUP, A., SHANN, J., CARUSO, J. A. (2002): Initial Studies of Selenium Speciation in *Brassica juncea* by LC with ICPMS and ES-MS Detection: an Approach for Phytoremediation Studies. In: *Analytical Chemistry*, 74: 107-113. p.

MORENO RODRIGUEZ, M. J., CALA RIVERO, V., JIMÉNEZ BALLESTA, R. (2005): Selenium distribution in topsoils and plants of a semi-arid Mediterranean environment. In: *Environmental Geochemistry and Health*, 27: 513-519.p.

MOUNICOU, S., DERNOVICS, M., BIERLA, K., SZPUNAR, J. (2009): A sequential extraction procedure for an insight into selenium speciation in garlic. In: *Talanta*, 77: 1877-1882. p.

MOXTON, A. L., OLSON, O. E., SEARIGHT, W. V. (1939): Selenium in rocks, soils and plants. *South Dakota Agricultural Experimental Station Technical Bulletin* 2.

MURASHIGE, T., SKOOG, F. (1962): A Revised Medium for Rapid Growth and Bio Assays with Tobacco Tissue Cultures. In: *Physiologia Plantarum*, 15: 473-497. p.

NANCHARAIAH, Y. V., LENS, P. N. L. (2015): Ecology and Biotechnology of Selenium-Respiring Bacteria. In: *Microbiology and Molecular Biology Reviews*, 79: 61-80. p.

NÉMETH, A. (2015): Application of hyphenated analytical techniques in the investigation of selenium speciation of different plant. Doctoral Thesis. Corvinus University of Budapest. Doi: 10.14267/phd.2015054

NÉMETH, A., DERNOVICS, M. (2015): Effective selenium detoxification in the seed proteins of a hyperaccumulator plant: The analysis of selenium-containing proteins of monkeypot nut (*Lecythis minor*) seeds. In: *Journal of Biological Inorganic Chemistry*. 20(1):23-33. p.

NÉMETH, A., GARCÍA REYES, J. F., KOSÁRY, J., DERNOVICS, M. (2013): The relationship of selenium tolerance and speciation in Lecythidaceae species. In: *Metallomics*, 5:1663-1673.p.

NG, B. H., ANDERSON, J. W. (1979): Light-dependent incorporation of selenite and sulphite into selenocysteine and cysteine by isolated pea chloroplasts. In: *Phytochemistry*, 18: 573-580. p.

NIGAM, S. N., MCCONNELL, W. B. (1976): Isolation and identification of two isomeric glutamylselenocystathionines from the seeds of *Astragalus pectinatus*. In: *Biochimica et Biophysica Acta*, 437: 116-121. p.

OGRA, Y., ANAN, Y. (2009): Selenometabolomics: Identification of selenometabolites and specification of their biological significance by complementary use of elemental and molecular mass spectrometry. In: *Journal of Analytical Atomic Spectrometry*, 24 (11): 1477-1488. p.

OGRA, Y., KITAGUCHI, T., ISHIWATA, K., SUZUKI, N., IWASHITA, Y, SUZUKI, K. T. (2007): Identification of selenohomolanthionine in selenium-enriched Japanese pungent radish. In: *Journal of Analytical Atomic Spectrometry*, 22: 1390-1396. p.

OGRA, Y., OGIHARA, Y., ANAN, Y. (2017): Comparison of the metabolism of inorganic and organic selenium species between two selenium accumulator plants, garlic and Indian mustard. In: *Metallomics*, 9 (1): 61-68. p.

OROZCO, D., SKAMARACK, J., REINS, K., TITLOW, K., LUNETTA, S., LI, F., ROMAN, M. (2007): Determination of Ubidecarenone (Coenzyme Q10, Ubiquinol-10) in Raw Materials and Dietary Supplements by High-Performance Liquid Chromatography with Ultraviolet Detection: Single-Laboratory Validation. In: *Journal of AOAC International*, 90(5): 1227-1236. p.

OUERDANE, L., AURELI, F., FLIS, PL, BIERLA, K., PREUD'HOMME, H., CUBADDA, F., SZPUNAR, J. (2013): Comprehensive speciation of low-molecular weight selenium metabolites in mustard seeds using HPLC-electrospray lineart rap/orbitrap tandem mass spectrometry. In: *Metallomics*, 5(9): 1294-1304. p.

PEDRERO, Z, MADRID, Y. (2009): Novel approaches for selenium speciation in foodstuffs and biological specimens: A review. In: *Analytica Chimica Acta*, 634: 135-152. p.

PEDRERO, Z., MADRID, Y., CÁMARA, C. (2006): Selenium Species Bioaccessibility in Enriched Radish (*Raphanus sativus*): A Potential Dietary Source of Selenium. In: *Journal of Agricultural and Food Chemistry*, 54: 2412-2417. p.

PFISTER, J. A., DAVID, T. Z., HALL, J. O. (2013): Effect of selenium concentration on feed preferences by cattle and sheep. In: *Journal of Animal Science*. 91: 5970-5980. p.

PILON-SMITS, E. A. H. (2012): Plant selenium metabolism – genetic manipulation, phytotechnological applications, and ecological implications. In: WONG, M. H. (Ed): *Environmental contamination: health risks and ecological restoration*. Boca Raton: CRC Press. 293-311. p.

PILON-SMITS, E. A. H. (2017): Mechanisms of Plant Selenium Hyperaccumulation. In: PILON-SMITS, E. A. H., WINKEL, L. H. E., LIN, Z-Q. (Eds): *Selenium in plants* (Plant Ecophysiology 11) Springer International Publishing. 53-66. p.

PILON-SMITS, E. A. H. (2019): On the ecology of selenium accumulation in plants. In: *Plants*, 8 (7): 197

PILON-SMITS, E. A. H., DE SOUZA, M. P., HONG, G., AMINI, A., BRAVO, R. C., PAYABYAB, S. B., TERRY, N. (1999): Selenium volatilization and accumulation by twenty aquatic plant species. In: *Journal of Environmental Quality*, 28: 1011-1018. p.

PILON-SMITS, E. A. H., LE DUC, D. L. (2009): Phytoremediation of selenium using transgenic plants. In: *Current Opinion in Biotechnology*, 20: 207-212. p.

PILON-SMITS, E. A., QUINN, C. F., TAPKEN, W., MALAGOLI, M., SCHIAVON, M. (2009): Physiological functions of beneficial elements. In: *Current Opinion in Plant Biology*, 12 (3): 267-274. p.

PIRJO, S. (2005): Increasing the selenium content of agricultural crops: decisions and monitoring. In: EUROLA, M. (Ed.): *Proceedings - Twenty Years of Selenium Fertilization*. MTT Agrifood Research Reports 69: 14-15. p.

PREUD'HOMME, H., FAR, J., GIL-CASAL, S., LOBINSKI, R. (2012): Large-scale identification of selenium metabolites by online size-exclusion-reversed phase liquid chromatography with combined inductively coupled plasma (ICP-MS) and electrospray ionization linear trap-Orbitrap mass spectrometry (ESI-MS^n). In: *Metallomics*, 4: 422-432. p.

PRÖFROCK, D., PRANGE, A. (2009): Compensation of gradient related effects when using capillary liquid chromatography and inductively coupled plasma mass spectrometry for the absolute quantification of phosphorylated peptides. In: *Journal of Chromatography A*, 1216: 6706-6715. p.

PUSHIE, M. J., PICKERING, I. J., KORBAS, M., HACKETT, M. J., GEORGE, G. N. (2014): Elemental and Chemically Specific X-ray Fluorescence Imaging of Biological Systems. In: *Chemical Reviews*. 114: 8499-8541. p.

PYRZYNSKA, K., SENTKOWSKA, A. (2019): Liquid chromatographic analysis of selenium species in plant materials. In: *Trends in Analytical Chemistry*, 111: 128-138. p.

QIN, H., ZHU, J., SU, H. (2012): Selenium fractions in organic matter from Se-rich soils and weathered stone coal in selenosis areas of China. In: *Chemosphere*, 86: 626-633. p.

QUINLIVAN, E. P., DANSON, A. D., GREGORY, J. F. (2006): The analysis of folate and its metabolic precursors in biological samples. In: *Analytical Biochemistry*, 348: 163-184. p.

QUINN, C. F., PRINS, C. N., FREEMAN, J. L., GROSS, A. M., HANTZIS, L. J., REYNOLDS, R. J. B., IN YANG, S., COVEY, P. A., BANUELOS, G. S., PICKERING, I. J., FAKRA, S. C., MARCUS, M. A., ARATHI, H. S., PILON-SMITS, E. A. H. (2011): Selenium accumulation in flowers and its effects on pollination. In: *New Phytologist*. 192 (3): 727-737 p.

RAYMAN, M. P., INFANTE, H. G., SARGENT, M. (2008): Food-chain selenium and human health: Spotlight on speciation. In: *British Journal of Nutrition*, 100 (2): 238-253. p.

REYES, L. H., GAYÓN, J. M. M., ALONSO, J. I. G., SANZ-MENDEL, A. (2003a): Determination of selenium in biological materials by isotope dilution analysis with an octapole reaction system ICP-MS. In: *Journal of Analytical Atomic Spectrometry*, 18: 11-16. p.

REYES, L. H., MARCHANTE-GAYÓN, J. M., ALONSO, J. I. G., SANZ-MENDEL, A. (2003b): Quantitative speciation of selenium in human serum by affinity chromatography coupled to post-column isotope dilution analysis ICP-MS. In: *Journal of Analytical Atomic Spectrometry*, 18: 1210-1216. p.

REYNOLDS, R. J. B., CAPPA, J. J., PILON-SMITS, E. A. H. (2017): Evolutionary Aspects of Plant Selenium Accumulation. In: PILON-SMITS, E. A. H., WINKEL, L. H. E., LIN, Z-Q. (Eds): *Selenium in plants* (Plant Ecophysiology 11) Springer International Publishing. 189-205. p.

REYNOLDS, R. J. B., JONES, R. R., STONEHOUSE, G. C., EL MEHDAWI, A. F., LIMA, L. W., FAKRA, S. C., PILON-SMITS, E. A. H. (2020): Identification and physiological comparison of plant species that show positive or negative co-occurrence with selenium hyperaccumulators. In: *Metallomics*, 12: 133-143. p.

RODRÍGUEZ-CASTRILLÓN, J. Á, ReyES, L. H., MARCHATEN-GAYÓN, J. M., MOLDOVAN, M., ALONSO, J. I. G. (2008): Internal correction of spectral interferences and mass bias in ICP-MS using isotope pattern deconvolution: Application to the determination of selenium in biological samples by isotope dilution analysis. In: *Journal of Analytical Atomic Spectrometry*, 23: 579-582. p.

RODRIGUEZ-GONZÁLEZ, P., MARCHANTE-GAYÓN, J. M., ALONSO, J. I. G., SANZ-MENDEL, A. (2005): Isotope dilution analysis for elemental speciation: A tutorial review. In: *Spectrochimica Acta Part B*, 60: 151-207. p.

ROGERS, P. A., ARORA, S. P., FLEMING, G. A., CRINION, R. A. P., MCLAUGHLIN, J. G. (1990): Selenium toxicity in farm animals: treatment and prevention. In: *Irish Veterinary Journal*, 43: 151-153. p.

ROSENFELD, I., BEATH, O. A. (1964): Selenium: geobotany, biochemistry, toxicity and nutrition. New York: Academic Press. 411 p.

ROTTMAN, L., HEUMANN, K. G. (1994): Determination of Heavy Metal Interactions with Dissolved Organic Materials in Natural Aquatic Systems by Coupling a High-Performance Liquid Chromatography System with an Inductively Coupled Plasma Mass Spectrometer. In: *Analytical Chemistry*, 66(21): 3709-3715. p.

RUEDEN, C. T., SCHINDELIN, J., HINER, M. C., DEZONIA, B. E., WALTER, A. E., ARENA, E. T., ELICEIRI, K. W. (2017): Image J2: ImageJ for the next generation of scientific image data. In: *BMC Bioinformatics*, 18: 529

RUSZCZYNSKA, A., KONOPKA, A., KUREK, E., ELGUERA, J. C. T., BULSKA, E. (2017): Investigation of biotransformation of selenium in plants using spectrometric methods. In: *Spectrochimica Acta Part B*, 130: 7-16. p.

SARRET, G., PILON-SMITS, E. A. H., MICHEL, H. C., ISAURE, M. P., ZHAO, F. J., TAPPERO, R. (2013): Use of Synchrotron-Based Techniques to Elucidate Metal Uptake and Metabolism in Plants. In: SPARKS, D. L. (Ed.): *Advances in Agronomy*. Academic Press. 119: 1-82. p.

SCHIAVON, M., PILON, M., MALAGOLI, M., PILON-SMITS, E. A. H. (2015): Exploring the importance of sulfate transporters and ATP sulphurylases for selenium hyperaccumulation – a comparison of *Stanleya pinnata* and *Brassica juncea* (Brassicaceae). In: *Frontiers in Plant Science*. 6: 2

SCHIAVON, M., PILON-SMITS, E. A. H. (2017): The fascinating facets of plant selenium accumulation – biochemistry, physiology, evolution and ecology. In: *New Phytologist*, 213: 1582-1596. p.

SENTKOWSKA, A., PYRZYNSKA, K. (2018): Hydrophilic interaction liquid chromatography in the speciation analysis of selenium. In: *Journal of Chromatography B*, 1074-1075: 8-15. p.

SEPPANEN, M. M., EBRAHIMI, N., KONTTURI, J., HARTIKAINEN, H., HERAS, I. L., CÁMARA, C., MADRID, Y. (2018): Dynamics of selenium uptake and metabolism of organic selenium species in the leaves and seeds of *Brassica napus* L. In: *Agricultural and Food Science*, 27: 38-49. p.

SEPPANEN, M. M., KONTTURI, J., HERAS, I. L., MADRID, Y., CÁMARA, C., HARTIKAINEN, H. (2010): Agronomic biofortification of *Brassica* with selenium – enrichment of SeMet and its identification in *Brassica* seeds and meal. In: *Plant and Soil*, 337: 273-283. p.

SHAH, M., KANNAMKUMARATH, S. S., WUILLOUD, C. A., WUILLOUD, R. G., CARUSO, J. A. (2004): Identification and characterization of selenium species in enriched green onion (*Allium fistulosum*) by HPLC-ICP-MS and ESI-ITMS. In: *Journal of Analytical Atomic Spectrometry*, 19: 381-386. p.

SHALTOUT, A. A., CASTILHO, I. N. B., WELZ, B., CARASEK, E., MARTENS, I. B. G., MARTENS, A., COZZOLINO, S. M. F. (2011): Method development and optimization for the determination of selenium in beand and soil samples using hydride generation electrothermal atomic absportion spectrometry. In: *Talanta*, 85: 1350-1356. p.

SHAO, S., DENG, G., MI, X., LONG, S., ZHANG, J., TANG, J. (2014): Accumulation and speciation of selenium in *Cardamine* sp. In Yutanga Se mining field, Enshi, China. In: *Chinese Journal of Geochemistry*, 33: 357-364. p.

SHAO, S., MI, X., OUERDANE, L., LOBINSKI, R., GARCÍA-REYES, J. F., MOLINA-DÍAZ, A., VASS, A., DERNOVICS, M. (2014): Quantification of Se-methylselenocysteine and its γ-glutamyl derivative from naturally Se-enriched green bean (Phaseolus vulgaris vulgaris) after HPLC-ESI-TOF-MS and orbitrap MS^n-based identification. In: *Food Analytical Methods*, 7: 1147-1157. p.

SHIBAGAKI, N., ROSE, A., MCDERMOTT, J. P., FUJIWARA, T., HAYASHI, H., YONEYAMA, T., DAVIES, J. P. (2002): Selenate resistant mutants of *Arabidopsis thaliana* identify sultr1;2 a sulfate transporter required for efficient transport of sulfate into root. In: *The Plant Journal*, 29: 475-486. p.

SHING, N. K., RAGHUBANSHI, A. S., UPADHYAY, A. K., RAI, U. N. (2016): Arsenic and other heavy metal accumulation in plants and algae growing naturally in contaminated area of West Bengal, India. In: *Ecotoxicology and Environmental Safety*. 130: 224-233. p.

SILVA JUNIOR, E. C., WADT, L. H. O. SILVA, K. E., LIMA, R. M. B., BATISTA, K. D., GUEDES, M. C., CARVALHO, G. S., CARVALHO, T. S., REIS, A. R., LOPES, G., GUILHERME, L. R. G. (2017): Natural variation of selenium in Brazil nuts and soils from the Amazon region. In: *Chemosphere*, 188: 650-658. p.

SINGLETON, V. L., ROSSI, J. A. (1965): Colorimetry of total phenolics with phosphomolybdic-phosphotungstic acid reagents. In: *American Journal of Enology and Viticulture*, 16: 144-158. p.

SLOTH, J. J., LARSEN, E. H., JULSHAMN, K. (2004): Selective arsenic speciation analysis of human urine reference materials using gradient elution ion-exchange HPLC-ICP-MS. In: *Journal of Analytical Atomic Spectrometry*. 19: 973-978. p.

SORS, T. G., ELLIS, D. R., NAM NA, G., LAHNER, B., LEE, S., LEUSTEK, T., PICKERING, I. J., SALT, D. E. (2005b): Analysis of sulfur and selenium assimilation in *Astragalus* plants with varying capacities to accumulate selenium. In: *The Plant Journal*, 42: 785-797. p.

SORS, T. G., ELLIS, D. R., SALT, D. E. (2005a): Selenium uptake, translocation, assimilation and metabolic fate in plants. In: *Photosynthesis Research*, 86: 373-389. p.

SORS, T. G., MARTIN, C. P., SALT, D. E. (2009): Characterization of selenocysteine methyltransferases from *Astragalus* species with contrasting selenium accumulation capacity. In: *The Plant Journal*, 59: 110-122. p.

STAICU, L. C., OREMLAND, R. S., TOBE, R., MIHARA, H. (2017b): Bacteria Versus Selenium: A View from the Inside Out. In: PILON-SMITS, E. A. H., WINKEL, L. H. E., LIN, Z-Q. (Eds): *Selenium in plants* (Plant Ecophysiology 11) Springer International Publishing. 79-108. p.

STAICU, L. C., VAN HULLEBUSCH, E. D., RITTMANN, B. E., LENS, P. N. L. (2017a): Industrial Selenium Pollution: Sources and Biological Treatment Technologies. In: VAN HULLEBUSCH, E. D. (Ed.): *Bioremediation of Selenium Contaminated Wastewater*. Springer International Publishing. 75-101. p.

SUGIHARA, S., KONDO, M., CHIHARA, Y., YUJI, M., HATTORI, H., YOSHIDA, M. (2004): Preparation of Selenium-enriched Sprouts and Identification of Their Selenium Species by High-performance Liquid Chromatography-Inductively Coupled Plasma Mass Spectrometry. In: *Bioscience, Biotechnology, and Biochemistry*, 68: 193-199. p.

SURA-DE JONG, M., REYNOLDS, R. J. B., RICHTEROVA, K., MUSILOVA, L., STAICU, L. C., CHOCHOLATA, I., CAPPA, J. J., TAGHAVI, S., VAN DER LELIE, D., FRANTIK, T., DOLINOVA, IL, STREJCEK, M., COCHRAN, A. T., LOVECKA, P., PILON-SMITS, E. A. (2015): Selenium hyperaccumulators harbor a diverse endophytic bacterial community characterized by high selenium resistance and plant growth promoting properties. In: *Frontiers in Plant Science*. 6: 113. p.

SYKORA, J. (1984): Selenolanthionine analysis by ion-exchange chromatography. In: *Chemicke Zvesti*, 38: 419-423. p.

SZPUNAR, J., LOBINSKI, R. (2002): Multidimensional approaches in biochemical speciation analysis. In: *Analytical and Bioanalytical Chemistry*, 373: 404-411. p.

SZPUNAR, J., LOBINSKI, R. (2003): Hyphenated Techniques in Speciation Analysis. (RSC Chromatography Monographs) The Royal Society of Chemistry.

SZPUNAR, J., LOBINSKI, R., PRANGE, A. (2003): Hyphenated techniques for elemental speciation in biological systems. In: *Applied Spectroscopy*, 57 (3): 102A-112A. p.

TAGMOUNT, A., BERKEN, A., TERRY, N. (2002): An essential role of S-adenosyl-L-methionine:L-methionine S-methyltransferase in selenium volatilization by plant. Methylation of selenomethionine to selenium-methyl-L-seleniummethionine, the precursor of volatile seleniuim. In: *Plant Physiology*, 130: 847-856. p.

TEMPLETON, D. M., ARIESE, F., CORNELIS, R., DANIELSSON, L.-G., MUNTAU, H., VAN LEEUWEN, H. P., LOBINSKI, R. (2000): Guidelines for terms related to chemical speciation and fractionation of elements. Definitions, structural aspects, and methological approaches. In: *Pure and Applied Chemistry*, 72 (8): 1453-1470. p.

TERRY, N., ZAYED, A. M., DE SOUZA, M. P., TARUN, A. S. (2000): Selenium in Higher Plants. In: *Annual Review of Plant Physiology and Plant Molecular Biology*, 51: 401-432. p.

TONG, X., YUAN, L., LUO, L., YIN, X. (2014): Characterization of a Selenium-Tolerant Rhizosphere Strain from a Novel Se-Hyperaccumulating Plant *Cardamine hupinshanesis*. In: *The Scientific World Journal*, 2014: 108562

TUKEY, J. W. (1977): Exploratory Data Analysis. Addison-Wesley Publishing Company, Reading, MA.

TURAKAINEN, M., HARTIKAINEN, H., SEPPANEN, M. M. (2004): Effects of selenium treatments on potato (*Solanum tuberosum* L.) growth and concentrations of soluble sugars and starch. In: *Journal of Agricultural and Food Chemistry*, 52 (17): 5378-5382. p.

TURNER, T. R., JAMES, E. K., POOLE, P. S. (2013): The plant microbiome. In: *Genome Biology*, 14: 209

UDEN, P. C., BOAKYE, H. T., KAHAKACHICHI, C., HAFEZI, R., NOLIBOS, P., BLOCK, E., JOHNSON, S., TYSON, J. F. (2004): Element selective characterization of stability and reactivity of selenium species in selenized yeast. In: *Journal of Analytical Atomic Spectrometry*, 19: 65-73. p.

VAN HOEWYK, D. (2013): A tale of two toxicities: malformed selenoproteins and oxidative stress both contribute to selenium stress in plants. In: *Annals of Botany*, 112: 965-972. p.

VAN HOEWYK, D., GARIFULLINA, G. F., ACKLEY, A. R., ABDEL-GHANY, S. E., MARCUS, M. A., FAKRA, S., ISHIYAMA, K., INOUE E., PILON, M., TAKAHASHI, H., PILON-SMITS, E. A. H. (2005): Overexpression of At CpNifS enhances selenium tolerance and accumulation in *Arabidopsis*. In: *Plant Physiology*, 139: 1518-1528. p.

VAN HUYSEN, T., ABDEL—GHANY, S., HALE, K. L., LEDUC, D., TERRY, N., PILON-SMITS, E. A. H. (2003): Overexpression of cystathionine-g-synthase in Indian mustard enhances selenium volatilization. In: *Planta*, 218: 71-78. p.

VELINSKY, D. J., CUTTER, G. A. (1990): Determination of elemental selenium and pyrite-selenium in sediments. In: *Analytical Chimica Acta*, 235: 419-425. p.

VIRUPAKSHA, T. K., SHRIFT, A. (1963): Biosynthesis of selenocystathionine from selenate in Stanleya pinnata. In: *Biochmica et Biophysica Acta*. 74:791-793. p.

WACH, A., PYRZYNSKA, K., BIESAGE, M. (2007): Quercetin content in some food and herbal samples. In: *Food Chemistry*, 100: 699-704. p.

WANG, X. (2010): Selenium Speciation in *Arabidopsis Thaliana*. Master Thesis. Department of Plant and Environmental Sciences, Norwegian University of Life Sciences. Available at: https://nmbu.brage.unit.no/nmbu-xmlui/handle/11250/189372 (accessed at 30/01/2020)

WHITE, P. J. (2016): Selenium accumualtion by plants. In: *Annals of Botany*, 117 (2): 217-235. p.

WHITE, P. J. (2017): The Genetics of Selenium Accumulation by Plants. In: PILON-SMITS, E. A. H., WINKEL, L. H. E., LIN, Z-Q. (Eds): *Selenium in plants* (Plant Ecophysiology 11) Springer International Publishing. 143-163. p.

WHITE, P. J., BOWEN, H. C., MARSHALL, B., BROADLEY, M. R. (2007): Extraordinarily high leaf selenium to sulfur ratios define 'Se-accumulator' plants. In: *Annals of Botany*, 100 (1): 111-118. p.

WHITE, P. J., BROADLEY, M. R. (2009): Biofortification of crops with seven mineral elements often lacking in human diets – iron, zinc, copper, calcium, magnesium, selenium and iodine. In: *New Phytologist*, 182: 49-84. p.

WIESNER-REINHOLD, M., SCHREINER, M., BALDERMANN, S., SCHWARZ, D., HANSCHEN, F. S., KIPP, A. P., ROWAN, D. D., BENTLEY-HEWITT, K. L., MCKENZIE, M. J. (2017): Mechanisms of Selenium Enrichment and Measurement in Brassicaceous Vegetables, and Their Application to Human Health. In: *Frontiers in Plant Science*. 8: 1365

WILBER, C. G. (1980): Toxicology of selenium: a review. In: *Clinical Toxicology*, 17: 171-230. p.

WILLIAMS, K. T., LAKIN, H. W., BYERS, H. G. (1940): Selenium occurence in certain soils in the United States with a discussion of related topics, fourth report. In: *United States Department of Agriculture Technical Bulletin*. 702. p.

WROBEL, K., WROBEL, K., CARUSO, J. A. (2002): Selenium speciation in low molecular weight fraction of Se-enriched yeasts by HPLC-ICP-MS: detection of selenoadenosylmethionine. In: *Journal of Analytical Atomic Spectrometry*, 17: 1048-1054. p.

XANTHAKIS, E., GOGOU, E., TAOUKIS, P., AHRNÉ, L. (2018): Effect of microwave assisted blanching ont he ascorbic acid oxidae inactivation and vitamin C degradation in frozen mangoes. In: *Innovative Food Science and Emerging Technologies*, 48: 248-257. p.

XUE, T., HARTIKAINEN, H., PIIRONEN, V. (2001): Antioxidative and growth-promoting effect of selenium on senescing lettuce. In: *Plant and Soil*, 237 (1): 55-61. p.

YASIN, M., EL MEHDAWI, A. F., ANWAR, A., PILON-SMITS, E. A. H., FAISAL, M. (2015): Microbial-enhanced Selenium and Iron Biofortification of Wheat (*Triticum aestivum* L.) – Applications in Phytoremediation and Biofortification. In: *International Journal of Phytoremediation*. 17: 341-347. p.

YAWATA, A., OISHI, Y., ANAN, Y., OGRA, Y. (2010): Comparison of Selenium Metabolism in Three Brassicaceae Plants. In: *Journal of Health Science*, 56 (6): 699-704. p.

YUAN, L., ZHU, Y., LIN, Z.-Q., BANUELOS, G., LI, W., YIN, X. (2013): A Novel Selenocystine-Accumulating Plant in Selenium-Mine Drainage Area in Enshi, China. In: *Plos One*, 8 (6): 1-9. p.

ZAYED, A. M., TERRY, N. (1994): Selenium Volatilization in Roots and Shoots: Effects of Shoot Removal and Sulfate Level. In: *Journal of Plant Physiology*, 143: 8-14. p.

ZHANG, L., HU, B., LI, W., CHE, R., DENG, K., LI, H., YU, F., LING, Y., CHU, C. (2014): OsPT2, a phosphate transporter, is involve in the active uptake of selenite in rice. In: *New Phytologist*, 201: 1183-1191. p.

ZHAO, C., REN, J., XUE, C., LIN, E. (2005): Study on the relationship between soil selenium and plant selenium uptake. In: *Plant and Soil*, 277: 197-206. p.

ZHAO, X. Q., MITANI, N., YAMAJI, N., SHEN, R. F., MA, J. F. (2010): Involvement of silicon influx transporter OsNIP2;1 in selenite uptake in rice. In: *Plant Physiology*, 153: 1871-1877. p.

ZHOU, X., YUAN, Y., YANG, Y., RUTZKE, M., THANNHAUSER, T. W., KOCHIAN, L. V., LI, L. (2009): Involvement of a broccolis COQ5 methyltransferase in the production of volatile selenium comopunds. In: *Plant Physiology*, 151: 528-540. p.

ZHOU, Y. F., TANG, Q. Y., WU, M. R., MOU, D., LIU, H., WANG, S. C., ZHANG, C., DING, L., LUO, J. (2018): Comparative transcriptomics provides novel insights into the mechanisms of selenium tolerace in the hyperaccumulator plant *Cardamine hupingshanensis*. In: *Scientific Reports*, 8: 2789

ZHU, J., WANG, N., LI, S., LI, L., SU, H., LIU, C. (2008): Distribution and transport of selenium in Yutangba, China: Impact of human activities. In: *Science of The Total Environment*. 392: 252-261. p.

ZHU, J., ZUO, W., LIANG, X., LI, S., ZHENG, B. (2004): Occurence of native selenium in Yutangba and its environmental implications. In: *Applied Geochemistry*, 19: 461-467. p.

11. APPENDIX II: TABLES AND FIGURES

Table A1. Instrumental parameters of the HPLC-ESI-QTOF-MS set-up.

6530 Accurate Mass QTOF LC-MS (Agilent)

ESI source	Dual ESI (Agilent)
Precursor ion selection in MS/MS mode	low (1.7 m/z)
Mass accuracy	< 2 ppm
Mass resolution	>10000
Detection frequency	4 GHz
Curtain voltage	65 V
Drying gas	13 L min^{-1}
Capillary voltage	800 V
Nebuliser pressure	40 psig
Gas temperature	325°C
Data analysis software	Mass Hunter Acquisition B. 02.01 with SP3

Table A2. UPLC-Unispray-QTOFMS instrumental setup parameters.

Acquity I-Class UPLC		**Vion IMS Unispray (+/-) -QTOF-MS**	
UPLC column	Acquity BEH C_{18}, 2.1*100 mm; 1.7 µm	Source temperature	120°C
Eluent "A"	water with 0.1 v/v% formic acid	Desolvation temperature	550°C
Eluent "B"	acetonitrile with 0.1 v/v% formic acid	Capillary voltage	300 V
Flow rate	0.4 mL min^{-1}	Desolvation gas	1000 L h^{-1}
Column temperature	25°C	Cone gas	100 L h^{-1}
Gradient	0 – 1.0 min 10% „B" 1.0 – 4.0 min ↑ 80% „B" 4.0 – 4.5 min 80% „B" 4.5 – 5.0 min ↓ 10% „B" 5.0 – 7.0 min 10% „B"	IMS MS scan MS scan time Lock mass MS/MS scan	OFF 100 – 1000 m/z 0.2 s ON 50 – 1000 m/z
Injection volume	3.0 µL	Low mass ramp	20 – 30 eV
Sample temperature	8°C	High mass ramp	30 – 80 eV

Table A3. Optimal parameters and instrumental data for the LC-MS quantification of selenolanthionine and lanthionine.

Compound	Retention time (min)	Precursor (m/z)	Declustering potential (V)	Quantification peak (m/z)	Collision Energy (V)	Confirmation peak No. 1 (m/z)	Collision Energy (V)	Confirmation peak No. 2 (m/z)	Collision Energy (V)
Lanthionine	6.83	209.1	36	120.2	19	74.0	37	146.0	17
Selenolanthionine	6.77	256.9	31	167.9	19	140.2	27	74.2	37

Ion spray voltage: 5500 V; curtain gas (N_2): 10 psi; ion source gas: 40 psi; desolvation temperature: 350 °C; collision activated dissociation gas: 5 arbitrary units.

Table A4. Calculation settings for the elemental calculator tool.

Element	Min.	Max.
C	3	20
H	5	50
O	0	10
S	0	2
P	0	1
N	0	4
Se	1	1

Table A5. Efficiency of automatic selenium pattern recognition. It is to note that the compounds with detected theoretical selenium mass defect include false positive hits and the different isotopologues of the same compound as well.

Fraction	Number of compounds detected	Number of compounds with detected theoretical selenium mass defect	Relative amount of compounds detected with theoretical selenium mass defect	Number of compounds with detected theoretical selenium mass defect	Relative amount of compounds detected with theoretical selenium mass defect
		Settings: defect paddig, 60 mDa; mass padding, 200 Da; minimum intensity, 2000 cps		Settings: defect paddig, 80 mDa; mass padding, 200 Da; minimum intensity, 2000 cps	
#1	7293	350	4.8%	457	6.3%
#2	5062	227	4.5%	277	5.5%
#3	4838	229	4.7%	269	5.6%
#4	4572	178	3.9%	206	4.5%

Table A6. Effect of defect padding settings on the efficiency of automatic selenium pattern recognition.

Fraction	m/z	Minimally required mass padding (Da) for successful detection			
		at 20 mDa defect padding	at 40 mDa defect padding	at 60 mDa defect padding	at 80 mDa defect padding
#1	282	>1000	17	11	10
	284	89	12	11	11
	407	>1000	121	106	71
	242	27	21	21	21
	391	>1000	>1000	191	116
	391	>1000	>1000	190	116
#2	419	>1000	130	115	86
	581	>1000	>1000	>1000	437
	419	>1000	173	125	115
	401	>1000	120	103	67
	285	>1000	21	13	12
	405	106	98	85	41
	285	>1000	21	13	12
#3	441	391	138	128	100
	419	>1000	175	125	115
	446	>1000	>1000	457	180
	268	>1000	2	2	2
	197	53	52	52	52
	215	40	40	40	39
#4	254	15	12	12	12
	312	53	33	31	31
	271	1	1	1	1
	282	>1000	17	11	10
	284	89	12	11	11

Table A7. Efficiency of automatic selenium pattern recognition at optimised settings (mass padding: 200 Da, defect padding: 80 mDa). Values in bold indicate successful detection.

FR1		FR2		FR3	FR4	
m/z	background of unsuccessful automatic detection	*m/z*	background of unsuccessful automatic detection	*m/z*	*m/z*	background of unsuccessful automatic detection
241.99302	-	**285.05998**	-	**197.00725**	**254.02883**	-
377.07037	isobaric interference	301.09063	isobaric interference	**241.99302**	**271.02005**	-
391.08672	isobaric interference	405.06603	low intensity	**268.04482**	**282.06027**	-
407.04499	-	416.08220	low intensity	**270.02341**	**284.03997**	-
435.04004	low intensity	**419.05681**	-	**446.09233**	**312.03454**	-
447.11604	low intensity	434.09228	low intensity	**463.02100**	313.02949	low intensity
448.10670	low intensity	537.14451	low intensity		**364.95162**	-
460.10880	low intensity	581.10958	low mass padding		444.86739	low intensity + triple selenium
482.99120	low intensity				489.05794	low intensity
523.12784	low intensity					
552.06109	low intensity					
614.14680	low intensity					

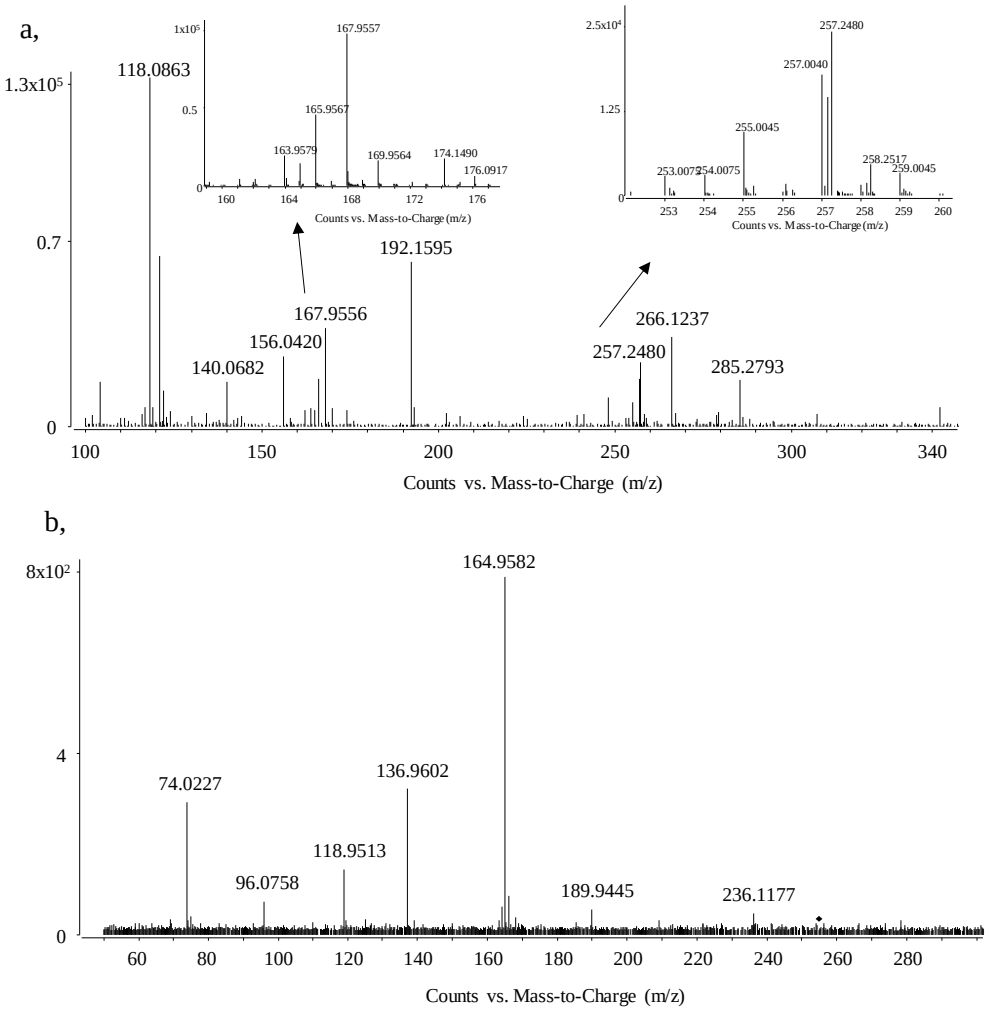

Figure A1. (a) HPLC-ESI-QTOF-MS full scan spectrum of the *C. violifolia* selenolanthionine fraction spiked with synthesised selenolanthionine prior to MS/MS analysis. (b) HPLC-ESI-QTOF-MS/MS collision induced dissociation (CID) spectrum of the *C. violifolia* selenolanthionine fraction spiked with synthesised selenolanthionine fragmented on the ^{77}Se isotopologue.

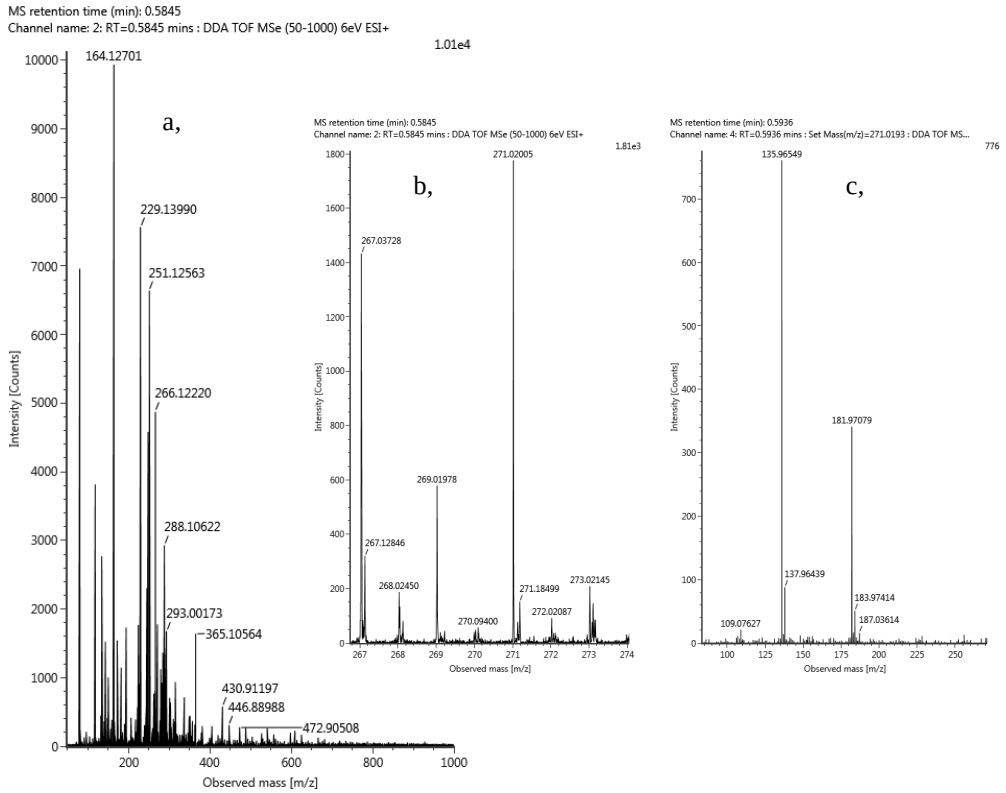

Figure A2. Selenocystathionine (for details, see Table 9); (a) full scan spectrum; (b) full scan spectrum /zoomed/; (c) MS/MS spectrum.

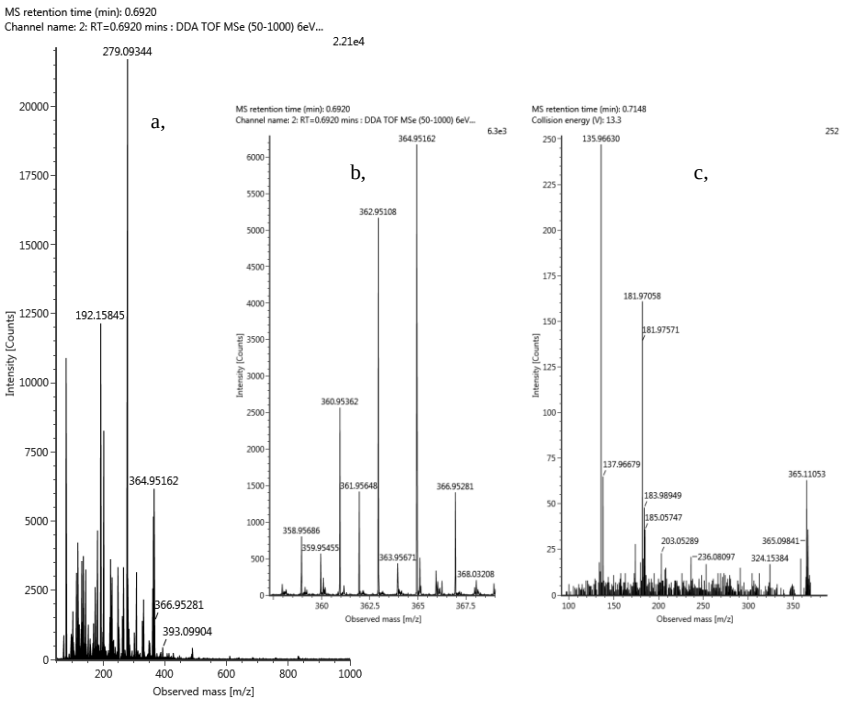

Figure A3. Selenohomocystine (for details, see Table 9); (a) full scan spectrum; (b) full scan spectrum /zoomed/; (c) MS/MS spectrum.

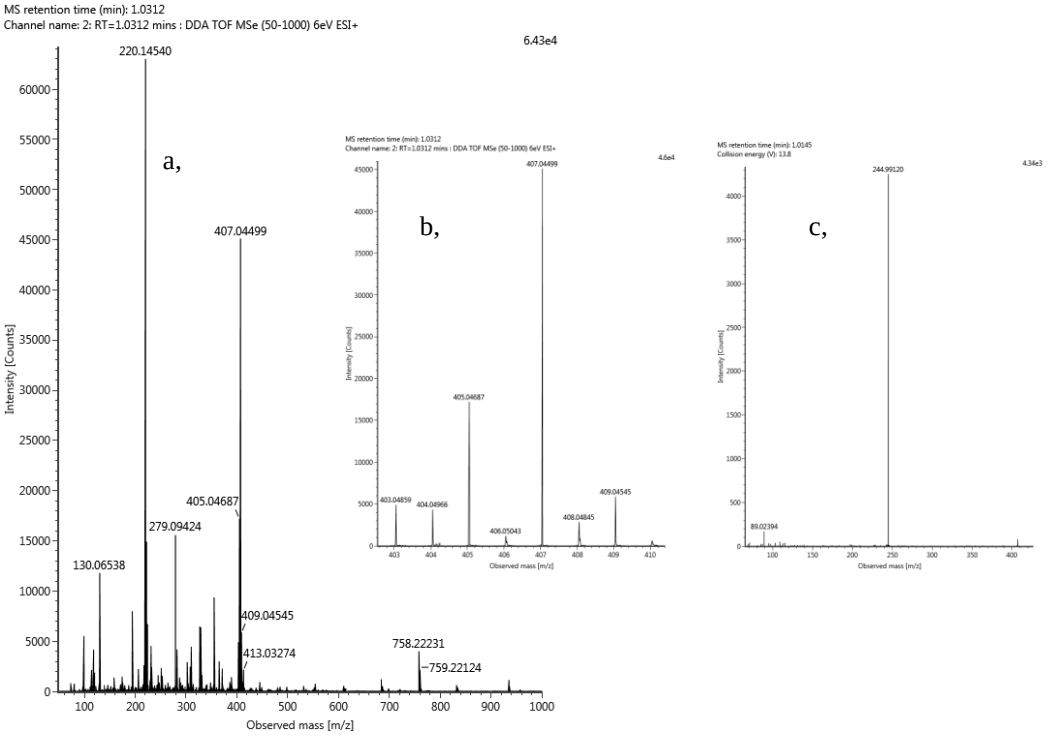

Figure A4. Selenosugar at *m/z* 407 (for details, see Table 9); (a) full scan spectrum; (b) full scan spectrum /zoomed/; (c) MS/MS spectrum.

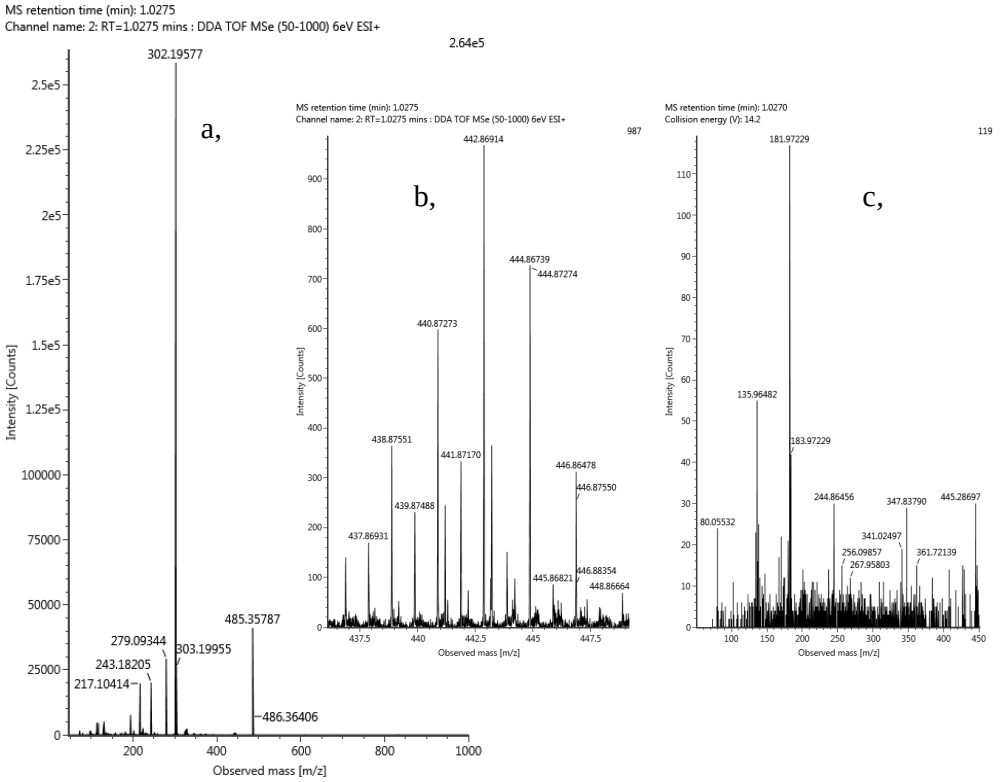

Figure A5. Se-selenohomocysteinyl-diseleno-homocysteine (for details, see Table 9); (a) full scan spectrum; (b) full scan spectrum /zoomed/; (c) MS/MS spectrum.

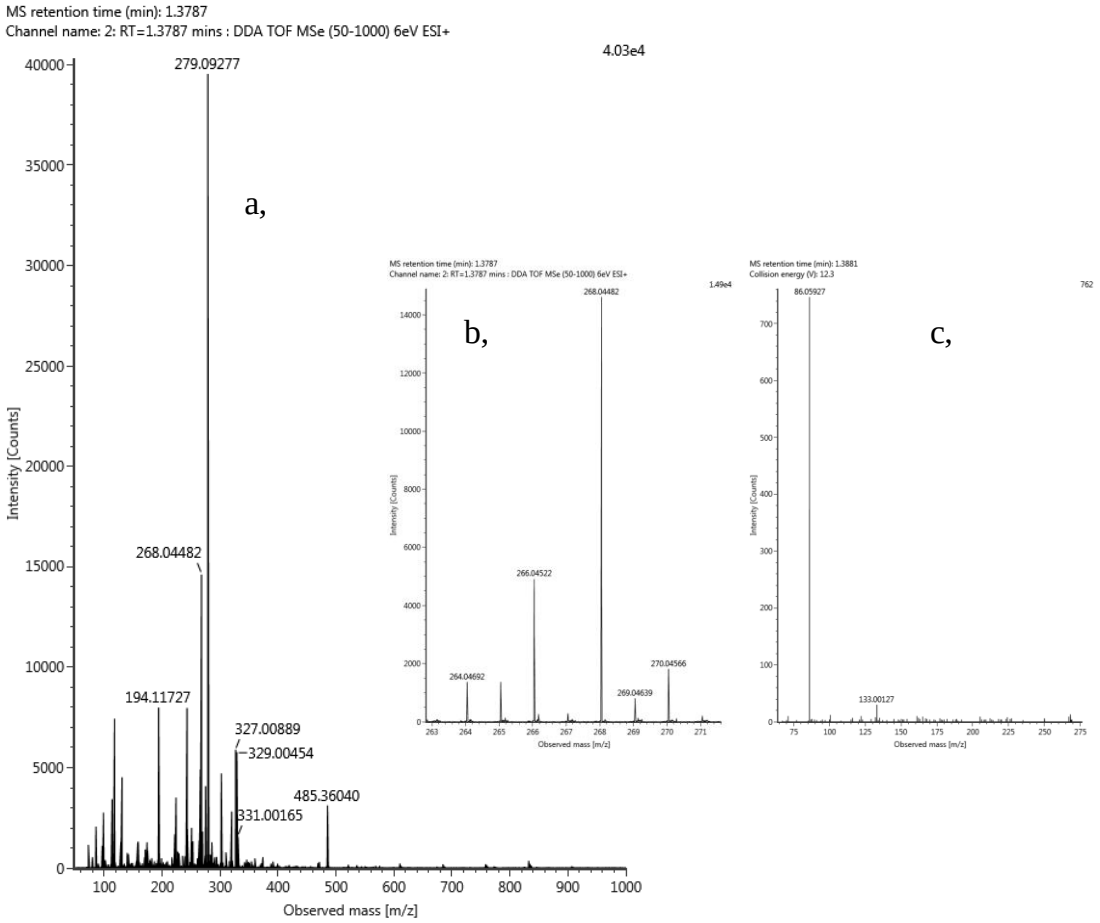

Figure A6. Compound at the experimental *m/z* 268.04482 (for details, see Table 9); (a) full scan spectrum; (b) full scan spectrum /zoomed/; (c) MS/MS spectrum.

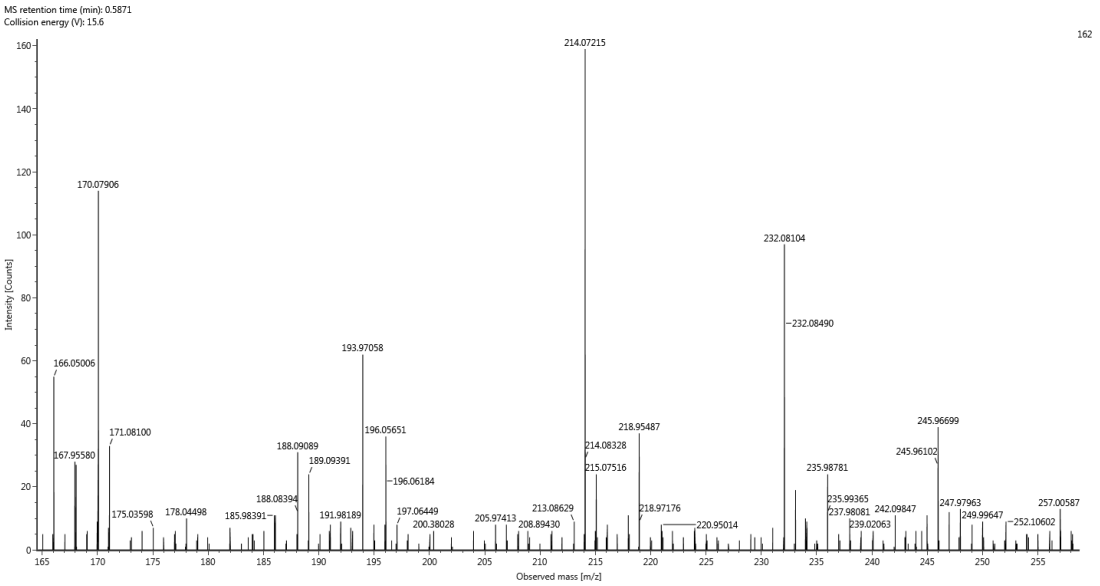

Figure A7. Additional (zoomed) MS/MS spectrum of the *m/z* 581.1092 compound.

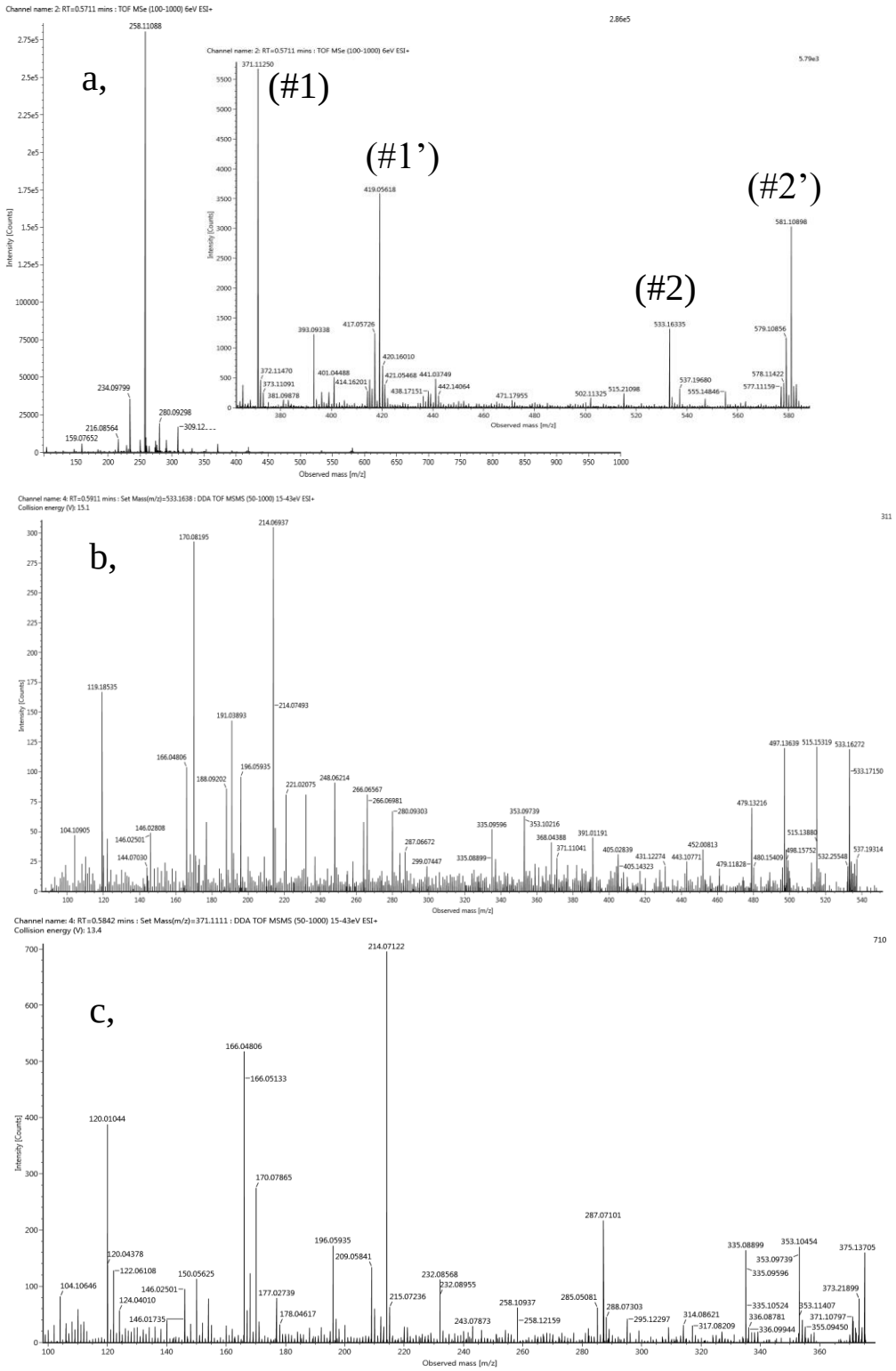

Figure A8. Full scan with zoomed view in the inset (a) and MS/MS (b, c) spectra of the sulphur analogues (#1, #2) of the putative N-glycosides of selenolanthionine (#1', #2'). (b) presents the MS/MS spectrum of the molecule *m/z* 533.163 ($C_{18}H_{33}N_2O_{14}S^+$), while (c) shows the MS/MS spectrum of the molecule *m/z* 371.112 ($C_{12}H_{23}N_2O_9S^+$).

ACKNOWLEDGEMENTS

First and foremost I would like to thank my parents whose unconditional love and support accompany me throughout my entire life.

I would like to express my gratitude to my supervisors Dr. Mihály Dernovics and Dr. Zsuzsanna Szatura for their professional guidance and continuous support during the years of my Ph.D. studies.

I thank Zsuzsanna Firisz, Erzsébet Lippai and all my colleagues from the department for their help in everyday laboratory work.

The support of Pharma Nord Kft. (Budapest) is highly acknowledged.

I am grateful to Prof. Elizabeth Pilon-Smits and Prof. Bernhard Michalke for the possibility to work in their laboratory. This research used resources of the Advanced Light Source, a U.S. DOE Office of Science User Facility under contract no. DE-AC02-05CH11231. I thank Prof. Anna Magyar for her help in chemical synthesis. I thank the Academy of Agricultural Sciences of Enshi Tujia and Miao Autonomous Prefecture (Wuhan, China) for the plant tissue and seed samples.

I am thankful to my colleagues at Soft Flow Kft. for their support during dissertation writing.

Last but not least I would like to thank my Love for his patience and encouragement in the hardest times.